UNIVERSITAT DE BARCELONA

Final Degree Project

**Biomedical Engineering Degree**

# “Pilot Study of Leg Muscle Activity During Treadmill Running at Different Speeds and Inclines”

# “Estudi Pilot de l'Activitat Muscular de la Cama Durant la Cursa en Cinta a Diferents Velocitats i Pendents”

Barcelona, 10th June 2026

Author: Max van der Aa

Director: Ricardo Marco

Tutora: Roser Sala

# Abstract

Running overuse injuries are common in recreational runners, and predicting them requires understanding how muscle load is distributed across the lower limb at different speeds and inclines. This pilot study characterises leg muscle activation, lower limb kinematics, and running dynamics across a systematic grid of treadmill conditions in 4 recreational runners aged 21 to 54.

Each participant completed 10 treadmill conditions: a fixed walking baseline at 5 km/h and 0% incline, followed by 9 running conditions covering 3 speeds (8, 10, 12 km/h) and 3 inclines (0%, 5%, 10%) in randomised order. Data were recorded simultaneously using 16-channel surface EMG across 8 leg muscles per side, full-body kinematics via an Xsens MVN Awinda inertial measurement suit, and stride and cardiovascular metrics from a Garmin Forerunner 255. EMG was normalised to the walking baseline. Statistical analysis used the Friedman test with Kendall's W as effect size.

Speed increased neuromuscular and biomechanical load consistently across all participants. Muscle activation rose across most channels, hip and knee flexion range of motion increased, and ground contact time shortened. The incline response was more selective: heart rate and hip flexion ROM increased consistently with grade, but EMG responses varied between participants. Joint kinematics showed higher statistical consistency than EMG, with hip flexion ROM reaching $W = 0.971$. Cross-modal associations were identified between ground contact time and tibialis anterior activation (mean Spearman $\rho = -0.613$), and between hamstring activation and knee flexion ROM (mean $\rho = +0.683$). Persistent bilateral asymmetries were found in two participants and were stable across all conditions.

The results provide a condition-mapped multimodal dataset linking muscle activation, joint kinematics, and consumer wearable metrics across a systematic speed and incline grid. This is a first step toward the Myalbatross goal of estimating muscle load from watch data alone.

**Keywords:** surface electromyography, running biomechanics, treadmill running, inertial measurement units, wearable sensors, muscle activation, range of motion, bilateral asymmetry, recreational runners, injury prevention, pilot study, Myalbatross.

# Resum

Les lesions per sobrecàrrega en corredors recreatius són freqüents, i predir-les requereix entendre com es distribueix la càrrega muscular a les extremitats inferiors a diferents velocitats i pendents. Aquest estudi pilot descriu l'activació muscular de la cama, la cinemàtica de l'extremitat inferior i la dinàmica de la cursa en una graella sistemàtica de condicions en cinta de córrer en 4 corredors recreatius d'entre 21 i 54 anys.

Cada participant ha completat 10 condicions en cinta: una baseline de caminar a 5 km/h i 0% de pendent, seguida de 9 condicions de cursa que combinaven 3 velocitats (8, 10, 12 km/h) i 3 pendents (0%, 5%, 10%) en ordre aleatoritzat. Les dades s'han registrat simultàniament amb EMG de superfície de 16 canals en 8 músculs per cama, cinemàtica corporal completa mitjançant un vestit d'unitats de mesura inercial Xsens MVN Awinda, i mètriques de cursa i cardiovasculars amb un Garmin Forerunner 255. L'EMG s'ha normalitzat al baseline de caminar. L'anàlisi estadística ha utilitzat el test de Friedman amb la W de Kendall com a mesura de l'efecte.

La velocitat ha augmentat la càrrega neuromuscular i biomecànica de forma consistent en tots els participants. L'activació muscular ha augmentat en la majoria dels canals, el rang de moviment de maluc i genoll ha crescut i el temps de contacte amb el terra ha disminuït. La resposta al pendent ha estat més selectiva: la freqüència cardíaca i el ROM de flexió de maluc han augmentat de forma consistent amb el pendent, però les respostes EMG han variat entre participants. La cinemàtica articular ha mostrat una consistència estadística superior a l'EMG, amb la flexió de maluc assolint $W = 0.971$. S'han identificat associacions entre el temps de contacte i l'activació del tibial anterior ($\rho$ de Spearman mitjà = $-0.613$), i entre l'activació dels isquiotibials i el ROM de flexió de genoll ($\rho$ mitjà = $+0.683$). S'han observat asimetries bilaterals persistents en dos participants, estables en totes les condicions.

Els resultats proporcionen un conjunt de dades multimodals lligades a condicions concretes, que relacionen l'activació muscular, la cinemàtica articular i les mètriques de rellotge de consum en una graella sistemàtica de velocitat i pendent. Això és un primer pas cap a l'objectiu de Myalbatross d'estimar la càrrega muscular a partir de les dades del rellotge.

**Paraules clau:** electromiografia de superfície, biomecànica de la cursa, cursa en cinta, unitats de mesura inercial, sensors vestibles, activació muscular, rang de moviment, asimetria bilateral, corredors recreatius, prevenció de lesions, estudi pilot, Myalbatross.

# Acknowledgements

This project was carried out with the support of many people, and I want to thank them all here.

I want to thank Ricardo Marco and the Myalbatross team for the collaboration that motivated this project. Their applied goal gave the study a clear direction and made every design decision easier to justify.

Roser Sala supervised this TFG from the Universitat de Barcelona. Her feedback throughout the process was direct and useful, and I am grateful for her guidance.

This study would not have been possible without Míriam Febrer, who gave me access to the Biomechanical Engineering Laboratory at CREB (ETSEIB, UPC) and provided the equipment and infrastructure needed for data collection. Henri de Jonghe assisted during the recording sessions, and his help with electrode placement and session logistics made the protocol run smoothly.

I also want to thank Michel Evrard from INEFC, who met with me early in the project and shared data from a previous treadmill EMG study. That preliminary dataset was essential for validating the pipeline before the main data collection began.

Finally, I want to thank the four participants who volunteered their time. Each session lasted up to two hours, and their patience made this study possible.

# Glossary

***AI:*** *Artificial Intelligence*

***ASIS:*** *Anterior Superior Iliac Spine*

***BF:*** *Biceps femoris*

***CREB:*** *Centre de Recerca en Enginyeria Biomèdica*

***EMG:*** *Electromyography*

***ETSEIB:*** *Escola Tècnica Superior d'Enginyeria Industrial de Barcelona*

***GCT:*** *Ground Contact Time*

***GDPR:*** *General Data Protection Regulation*

***GM:*** *Gluteus medius*

***GRF:*** *Ground Reaction Force*

***HRmax:*** *Maximum heart rate (estimated as 220 – age)*

***ICC:*** *Intraclass Correlation Coefficient*

***IEG:*** *Índice de Estrés Global (Global Stress Index)*

***IMU:*** *Inertial Measurement Unit*

***INEFC:*** *Institut Nacional d'Educació Física de Catalunya*

***MAD:*** *Median Absolute Deviation*

***MG:*** *Medial gastrocnemius*

***MVC:*** *Maximum Voluntary Contraction*

***MVN:*** *Moven. The Xsens full-body inertial motion capture product line used in this study*

***PERT:*** *Program Evaluation and Review Technique*

***RF:*** *Rectus femoris*

***RMS:*** *Root Mean Square*

***ROM:*** *Range of Motion*

***SENIAM:*** *Surface EMG for Non-Invasive Assessment of Muscles*

***SI:*** *Symmetry Index*

***SO:*** *Soleus*

***spm:*** *steps per minute*

***ST:*** *Semitendinosus*

***SWOT:*** *Strengths, Weaknesses, Opportunities, Threats*

***TA:*** *Tibialis anterior*

***TFG:*** *Treball de Fi de Grau (Final Degree Project)*

***UB:*** *Universitat de Barcelona*

***UPC:*** *Universitat Politècnica de Catalunya*

***VL:*** *Vastus lateralis*

***VO:*** *Vertical Oscillation*

***WBS:*** *Work Breakdown Structure*

# List of Figures

# List of Tables

# Table of Contents

# 1. Introduction

This TFG was developed in collaboration with Myalbatross [1], a Barcelona-based startup working on running injury prediction. Their goal is to estimate injury risk from wearable sensor data collected during training, before an injury happens. The study presented in this report is a direct contribution to that goal.

The study was conducted at the Biomechanical Engineering Laboratory of the CREB (Centre de Recerca en Enginyeria Biomèdica), at ETSEIB (UPC, Barcelona). The lab provided the instrumentation and infrastructure for simultaneous multi-modal data collection across all participants.

Running has a high injury rate. Between 19% and 79% of recreational runners sustain at least one injury per year [2]. Almost all are overuse injuries: not a single traumatic event, but load accumulating over time until the tissue fails. That pattern should be, in principle, detectable before it causes damage.

Predicting overuse injuries requires understanding how mechanical load is distributed across individual muscles during running, and how that distribution shifts with speed and incline. That relationship is not yet well characterised in the literature. Direct measurement is what makes the characterisation possible: which muscles work harder at 10% incline compared to flat ground, by how much, and whether the pattern holds across individuals. Without that baseline, any model trying to connect running load to injury risk is working without the underlying data it needs.

Surface electromyography (EMG), inertial measurement units (IMUs), and running watches can provide that information. EMG records the electrical activity of individual muscles, giving a direct measure of activation level per stride. IMUs track joint angles and segmental motion throughout the gait cycle. A running watch adds physiological and stride metrics, including heart rate, ground contact time, vertical oscillation, and cadence, from the same session. Previous studies have characterised lower limb EMG across varying speeds and incline [3], [4], and others have combined EMG with lab-based kinematics [5]. The simultaneous combination of surface EMG, a full-body inertial suit, and a consumer running watch across a systematic speed and incline grid has not been reported.

This study addresses that gap. Four participants completed ten treadmill conditions: a walking baseline at 5 km/h and 0% incline, followed by nine combinations of three speeds (8, 10, 12 km/h) and three inclines (0%, 5%, 10%) in randomised order. Each session was recorded simultaneously with 16-channel surface EMG across 8 leg muscles per side, full-body kinematics via an XSENS inertial suit, and running metrics from a Garmin watch.

## 1.1 Objectives

The overall objective of this study is to characterise how muscular load is distributed across the lower limb during treadmill running at different speeds and inclines, as a foundation for understanding injury patterns in recreational runners.

The specific aims are:

1. To quantify how leg muscle activation changes with speed and incline across 9 running conditions, using surface EMG normalised to a walking baseline.

2. To describe the associated changes in lower limb joint kinematics, including range of motion and bilateral symmetry, using a full-body inertial measurement suit.

3. To describe changes in physiological and stride metrics across the same conditions using a consumer running watch.

4. To identify cross-modal associations between EMG, IMU, and Garmin variables that could inform load estimation from wearable data alone.

5. To validate the full multi-modal recording pipeline as a foundation dataset for Myalbatross's injury prediction work.

## 1.2 Scope and Limitations

This study is a pilot. The sample consists of 4 recreational runners, which is sufficient to test the methodology and identify preliminary trends, but not to draw population-level conclusions. All conditions were performed on a motorised treadmill, which allows precise control of speed and incline but does not replicate the variability of outdoor running. Only positive inclines were tested. Each condition lasted one minute, and fatigue effects were not measured. The results should be interpreted as descriptive and hypothesis-generating rather than confirmatory.

# 2. Background and State of the Art

Analyzing leg muscle activity and running mechanics across conditions requires grounding in four areas: running biomechanics, surface electromyography, inertial sensor kinematics, and wearable running metrics. This section reviews what each area has established and identifies the gap this study is designed to fill.

## 2.1 Running Biomechanics

Running alternates between stance and swing. Stance begins at foot contact and ends at toe-off; swing carries the limb to the next contact. During stance, ground reaction forces are transmitted through the lower limb to the pelvis, and muscles first absorb impact energy and then generate propulsion. During swing, the limb accelerates and decelerates to position the foot for the next contact.

Speed reorganizes this cycle. As pace increases, both stride length and step frequency increase, ground contact time (GCT) decreases, and sagittal-plane joint angles and angular velocities at the ankle and knee increase, with the hip following the same trend [6], [7]. The contribution of stride length versus step frequency shifts with speed: at lower paces, runners primarily lengthen their stride; at higher paces, step frequency plays a larger role [6].

Incline changes which joints carry the load. On uphill grades, the hip and ankle extensors generate more positive work. Both joints show greater flexion at foot contact than on level ground, which helps raise the center of mass against gravity and maintain forward propulsion. Swanson and Caldwell [5] ran participants at 4.5 m/s on a 30% treadmill grade and found substantial changes in sagittal-plane joint kinematics and lower-limb EMG compared to level running at the same speed, confirming that steep uphill grades redistribute muscular work across the lower limb. Downhill running reverses the pattern: eccentric braking demands increase at the knee, while hip extensor loading decreases relative to level grade [7].

A consistent finding in the graded running literature is that joint moments and powers respond to grade more strongly than joint angles do. Khassetarash et al. [7] measured 19 runners at five grades (0°, ±5°, ±10°) and three speeds (2.50, 3.33, 4.17 m/s). Ankle and hip kinetics changed substantially with grade while sagittal-plane ROM changes were smaller. This dissociation suggests that muscles increase activation to maintain similar joint kinematics under greater gravitational demand. Measuring both EMG and kinematics is therefore necessary: kinematics alone would underestimate the neuromuscular changes accompanying graded running. Pelvic kinematics also adapt to combinations of speed and incline, with pelvic tilt and rotation modulating ankle and knee motion downstream [8].

The eight muscles recorded in this study each have a distinct role in the running gait cycle. Tibialis anterior dorsiflexes the foot during swing for toe clearance and decelerates plantarflexion eccentrically at foot contact; as speed increases, this repositioning must occur faster, which raises tibialis anterior activation. Medial gastrocnemius and soleus are the primary plantarflexors during push-off and together generate most of the propulsive impulse per stride. Their contribution increases with both speed and uphill grade, since faster running and positive incline both demand more positive ankle work [6], [7]. Vastus lateralis and rectus femoris extend the knee during early stance to absorb impact and maintain limb support. Rectus femoris also flexes the hip during late swing, giving it a phase-dependent role that shifts between swing initiation and propulsion support within a single stride. Semitendinosus and biceps femoris extend the hip during late swing and early stance and decelerate the swinging limb before foot contact. Their activation increases with speed as leg swing velocity rises, and with uphill grade as the hip extension demand per step grows [5]. Gluteus medius stabilizes the pelvis in the frontal plane during single-leg support. Without adequate activation, the contralateral pelvis drops, which propagates to increased knee valgus and altered ankle loading downstream.

Bilateral asymmetry is a final dimension relevant to this study. Most healthy runners show small asymmetries in spatiotemporal variables but larger asymmetries in kinetic parameters. Vertical average loading rate and peak vertical ground reaction force can differ by 15–20% between limbs even in uninjured runners [9]. Mo et al. [9] examined runners at 8–12 km/h across different experience levels. Competitive runners became more symmetrical as speed increased. Recreational runners showed a U-shaped speed dependence, with asymmetry first decreasing and then increasing again at higher speeds. A study of 800 m track running [10] found persistent low-to-moderate mechanical asymmetries that did not increase over the race duration, suggesting that some degree of asymmetry is normal in healthy runners. Whether moderate asymmetry predicts injury remains debated [11].

## 2.2 Surface Electromyography in Running Research

Surface EMG records the electrical activity of active motor units through electrodes placed on the skin over a muscle. The raw signal is the superimposed action potentials of all motor units firing within the electrode detection volume. In running research, EMG quantifies how activation amplitude and timing change across conditions.

Standard acquisition follows SENIAM recommendations [12]: abrasion and skin cleaning before electrode placement, bipolar electrodes aligned with the muscle fiber direction, and a minimum interelectrode distance of 20 mm. In running, electrode fixation is critical. Cable movement and skin deformation at high cadence generate motion artifacts that contaminate the signal, and poor fixation is one of the main sources of data loss in treadmill EMG studies.

The signal is band-pass filtered (20–450 Hz) and rectified. A linear envelope is then computed via moving RMS or low-pass filtering. Normalization is required to compare activation levels across muscles, conditions, and participants. The standard reference is a maximal voluntary contraction (MVC). In protocols where obtaining valid MVCs during high-speed treadmill running is impractical, normalization to a dynamic baseline condition is an established alternative [13]. This study normalizes all running conditions to a 5 km/h walking trial, expressing EMG amplitude as a percentage of that reference.

The most directly relevant prior study is Whiteley et al. [3], who measured 11 lower-limb muscles across five speeds (12–24 km/h) and three inclines (−15% to +15%) on an Alter-G treadmill at indicated bodyweights of 60% and 100%. Speed produced the largest and most consistent increases in EMG amplitude across all muscles. Incline had smaller and less predictable effects. This is the only published study with a factorial speed × incline EMG design covering multiple muscles bilaterally, but partial bodyweight support limits its comparability to normal-weight treadmill running.

Vernillo et al. [6] measured stride parameters and muscle activations on a full-bodyweight treadmill at five grades and three speeds in 19 runners. Hip and ankle extensor EMG increased on uphill grades, consistent with the greater positive work demand at those joints described in Section 2.1. Saito et al. [4] examined muscle synergy structure during level and uphill running and found that the same underlying coordination patterns explained activation at both grades. The nervous system adapts to incline by scaling existing synergies rather than recruiting new ones. Swanson and Caldwell [5] confirmed this picture at steeper gradients: at 30% incline and 4.5 m/s, lower-limb EMG amplitudes changed substantially relative to level running, with the largest differences in the calf and hip extensors.

Biceps femoris loading during incline running is particularly relevant to injury risk. One study found peak biceps femoris activation of approximately 49% MVC during running at 10% grade at 3.6–4.2 m/s [14], a level approaching that reported for targeted hamstring exercises. A thesis comparing high-incline walking to level jogging at the same metabolic cost found higher peak EMG in tibialis anterior and vastus lateralis during jogging [15], reinforcing that speed drives neuromuscular demand more than incline does even when metabolic cost is held constant.

Quality control matters more in pilot work than in large studies. Losing one channel from one participant has a larger effect on results when the total sample is four. Standard mitigation includes Hampel filtering for transient artifact spikes, visual inspection of every channel before analysis, and exclusion of windows where signal quality is insufficient. Channels with confirmed electrode contact loss are excluded rather than interpolated.

The remaining gap in the EMG literature is the absence of a factorial speed × incline design at normal bodyweight that combines multi-channel bilateral EMG with both full-body inertial kinematics and synchronized wearable running metrics. That combination is what this study contributes.

## 2.3 Inertial Measurement Units in Running

An inertial measurement unit (IMU) is a small sensor that measures how a body segment moves and rotates in space. It does this by combining two types of sensors: accelerometers, which detect linear acceleration, and gyroscopes, which detect rotational velocity. A software algorithm fuses these two signals continuously to estimate the orientation of the sensor at any moment in time. The key advantage over traditional optical motion capture is that IMUs do not require a fixed camera setup or a dedicated laboratory space. A participant can wear them and move freely.

Xsens MVN uses 17 of these sensors, placed on segments across the whole body. Joint angles are calculated from the difference in orientation between two adjacent sensors. A biomechanical model constrains these calculations to angles that are anatomically possible. The output is continuous joint angle data for every joint in all three movement planes throughout the recording.

The relevant question for this study is whether Xsens data is accurate enough to detect kinematic differences between running conditions. Nijmeijer et al. [16] compared Xsens joint angles directly to optical motion capture in sport-specific tasks including jumping and landing and changes of direction. The two systems agreed closely for sagittal-plane angles at the hip and knee, with differences below 5° on average. A study at the University of Innsbruck tested Xsens specifically during running in 17 recreational runners on two different surfaces [17]. Within the same session, the system could detect kinematic differences between surfaces reliably, with intraclass correlation coefficients (ICC) above 0.80 for sagittal-plane angles. Reliability was lower for frontal-plane angles and when comparing across different sessions on different days.

These findings directly shape the analysis choices in this study. Sagittal-plane ROM at the lower-limb joints is the primary kinematic outcome, because that is where the evidence for Xsens accuracy is strongest.

On the scientific side, IMU-based running studies have confirmed the biomechanical patterns described in Section 2.1. Lin et al. [18] used IMU data to drive a musculoskeletal model, estimating not just joint angles but joint moments and forces on individual muscle-tendon units during treadmill running at different speeds. These joint moment estimates were very similar to lab-based inverse dynamics across most of the gait cycle. However, this study does not use musculoskeletal modeling: the outputs here are joint angles and temporal metrics, where the accuracy of IMU-derived data is more directly established.

Two sources of error are particularly relevant for treadmill IMU studies. The sensors are mounted in straps or a wearable suit placed over the body segments. Even with secure fixation, the sensor assembly can shift relative to the underlying bone during running, and that movement introduces error that the model cannot distinguish from actual limb motion. Magnetic interference from the treadmill motor and surrounding lab equipment can also disturb the sensor and cause slow drift in the estimated orientation. Calibration sensitivity is a separate consideration: the calculated joint angles depend on the posture the participant holds during the calibration procedure at the start of the session, and any deviation from the standard protocol carries through to all subsequent angle estimates. A 2025 study showed that using a dynamic calibration movement rather than a static pose reduces these errors, particularly in participants whose movement is restricted [19]. For healthy recreational runners following a standardized protocol, static calibration is adequate for within-session condition comparisons.

## 2.4 Wearable Physiological Monitoring

Modern running watches combine GPS tracking with optical heart rate sensing and built-in accelerometers that record running dynamics with every stride. Garmin was selected for this study because it is the most widely used brand among recreational runners and its devices output the biomechanically relevant stride metrics this study requires: cadence, ground contact time (GCT), vertical oscillation (VO), stride length, vertical ratio, and GCT balance. These metrics give a picture of how a runner is moving from one stride to the next, without any lab equipment.

Heart rate reflects cardiovascular demand. It increases with both speed and incline, and is the most direct measure of physiological load available from a consumer device. At a given pace, a higher heart rate on an incline compared to flat ground reflects the greater total mechanical work per unit time.

Cadence is the number of steps per minute. It increases with speed, partly because contact time decreases and partly because stride length cannot keep increasing indefinitely. At the same speed, a higher cadence means shorter strides, which reduces how far the foot lands in front of the center of mass. Overstriding in this sense has been associated with higher impact loading rates and greater injury risk.

GCT (Ground Contact Time) is the duration of the stance phase in milliseconds. It decreases as speed increases. GCT is closely linked to leg stiffness: a stiffer leg applies force more quickly and leaves the ground sooner. Loading rate is the speed at which ground reaction force builds up at the foot during impact. It depends on how hard the foot strikes and how fast. Because GCT reflects how long the foot is in contact with the ground, it is a practical proxy for the mechanical stress imposed on bones and soft tissues per stride. Shorter GCT is generally associated with better running economy, but also with higher peak loading rates, which have been linked to bone stress injury risk [20].

Vertical oscillation is the vertical displacement of the center of mass per stride, in centimeters. A high VO means the runner is travelling more vertically than horizontally. The vertical ratio normalizes VO by stride length, giving a percentage that reflects how much of the runner's energy goes into vertical rather than forward movement. Both metrics change with speed and tend to be lower in more economical runners.

These metrics are not just consumer features. One study validated cadence, GCT, and VO from a commercial fitness watch against simultaneous optical motion capture in 20 runners [20], finding good to excellent agreement for cadence and VO (ICC 0.93 and 0.96 respectively) and acceptable agreement for GCT (ICC 0.75). The metrics are accurate enough to detect condition-level differences in running form, which is exactly what this study uses them for.

GCT balance is the left-right percentage split in contact time, and it is the only asymmetry metric the watch provides directly. Garmin's own development data found correlations between GCT imbalance and injury in some runner cohorts, and the documentation notes that imbalances tend to increase on hills and with fatigue [21]. No peer-reviewed study has directly validated Garmin GCT balance against force-plate-derived contact time asymmetry. In this study, GCT is treated as a continuous monitoring variable rather than a validated asymmetry index.

At the population level, the Garmin-RUNSAFE Running Health Study [22] enrolled at least 20,000 runners, collecting running dynamics data via Garmin Connect alongside quarterly injury questionnaires over 18 months. This confirms that wearable running metrics have the resolution to detect differences relevant to injury epidemiology at scale. What this design cannot provide is the joint-level and muscle-level detail needed to explain any associations found. That requires concurrent EMG and kinematic recording in the same session, which is what this study provides.

## 2.5 Summary and Research Gap

Speed is the dominant driver of neuromuscular and mechanical demand in running. It increases EMG amplitudes, shortens GCT, raises cadence, and increases sagittal-plane joint ROM. This holds consistently across all the literature reviewed above. Incline redistributes work across joints: uphill running increases positive work at the hip and ankle, while downhill running increases eccentric knee loading. But the effect of incline on EMG amplitude is secondary to speed. The only published factorial speed × incline EMG study [3] confirmed this hierarchy, showing that incline effects at up to ±15% grade were smaller and less consistent than speed effects across the same muscles.

Joint moments respond to grade more strongly than joint angles do. Similar joint angles at two different inclines can coincide with very different muscle activation levels. This means kinematics alone are not sufficient to characterize the neuromuscular demands of graded running. Combined EMG and kinematic measurement is necessary to see the full picture.

IMU-based sagittal-plane kinematics are reliable within a session [16], [17], which fits the design of this study. Garmin running metrics are valid at the condition level for cadence and VO [20], with acceptable agreement for GCT.

Bilateral asymmetry adds a layer of complexity. Moderate asymmetries are common in healthy runners [9], [10] and their relationship with injury is not straightforward [11]. Monitoring asymmetry across both EMG and kinematic modalities could help clarify which aspects of asymmetry track with mechanical load and which do not.

The gap this pilot study fills is specific. No published study has combined multi-channel bilateral EMG with both full-body IMU kinematics and consumer wearable running metrics in the same participants. None has done so across a factorial speed × incline design at normal bodyweight on a standard treadmill. The closest prior EMG work [3] used an Alter-G with partial bodyweight support, which changes the mechanical environment. How EMG activation and IMU-derived kinematics relate to the running dynamics a consumer watch records, across systematically varied speed and incline conditions, has not been quantified.

This study provides that pilot dataset. The results describe how muscle activation and lower-limb kinematics respond to speed and incline in a setting representative of recreational training, and how those changes map onto the wearable metrics that injury prediction pipelines have access to in the field.

# 3. Market Analysis

Running is one of the most practiced sports in Spain. In 2023, 10.9% of the Spanish population reported running regularly [23]. Participation in organised road races continues to grow, and so does interest in technology that supports performance and health management. The global sports technology market was valued at USD 14.7 billion in 2023 and is projected to reach USD 55.1 billion by 2030, with a compound annual growth rate of 20.8% [24]. Wearables and data analytics platforms represent a central part of this growth.

The current market offers several platforms for training management and performance monitoring. The most established is TrainingPeaks, a US-based platform used by coaches and competitive athletes [25]. It provides training load metrics, periodisation tools, and integration with Garmin and other devices. TrainerPlan is a Spanish platform targeting coaches focused on training plan creation and athlete communication [26]. Train2Go is a Spanish triathlon coaching platform that offers training management and perceived exertion tracking via the Borg scale [27]. None of these platforms predict injury. They manage training volume and communication between coach and athlete.

***Table 1.*** *Comparison of running performance and coaching platforms.*

| Feature | TrainingPeaks | TrainerPlan | Train2Go | Myalbatross |
|---|---|---|---|---|
| Training plan management | Yes | Yes | Yes | **Yes** |
| Wearable integration | Yes | Yes | Yes | **Yes** |
| Injury risk indicator | No | No | No | **Yes (IEG)** |
| AI assistant | No | No | No | **Yes (Albi)** |
| Coach-to-athlete monitoring | Yes | Yes | Yes | **Yes** |
| Custom Hardware required | No | No | No | **No** |

Myalbatross is a Catalan platform for training planning, performance analysis, and injury prevention [1]. The platform is designed for coaches managing a portfolio of athletes. Its core metric is the IEG (Global Stress Index), a proprietary value that combines physiological load, structural load, and subjective wellness into a single number. This allows coaches to see injury risk at a glance across all their athletes and to prioritise attention before a problem becomes an injury. The platform monitors more than 50 variables per athlete continuously, including acute-to-chronic workload ratio, physiological balance, and self-reported sensations. Athletes report sensations and discomfort through their own app, and the platform crosses that input with load history and the IEG to surface early warning signals. An AI assistant called Albi can generate training blocks, analyse sessions, and produce performance reports on request. By quantifying how muscle activation changes with speed and incline, the data from this study can inform what loading thresholds are meaningful and which variables are worth tracking at the muscular level. This is a first step, not a finished model, but it is the type of ground-truth data that injury prediction tools require to move beyond generic training load metrics.

# 4. Concept Engineering

## 4.1 Study Concept

Running injury rates in recreational runners are high [2], and most injuries are overuse in nature. They result from repeated biomechanical loading that accumulates over time rather than from a single traumatic event. Understanding how that loading changes with speed and incline is a necessary step toward predicting and preventing it. What is missing from the literature is a study that maps muscle activation, joint kinematics, and running dynamics simultaneously across a systematic grid of speed and incline conditions in the same participants.

This study is a pilot that tests whether that combination is feasible and what the preliminary patterns look like. A group of recreational runners each completed a fixed walking baseline followed by a set of running conditions spanning a systematic speed and incline grid. We recorded surface EMG, full-body IMU kinematics, and Garmin running metrics simultaneously in each session. Recording all modalities in the same session means that for each condition, activation patterns can be interpreted alongside the joint movement they produce and the physiological load they correspond to. The technical implementation is in Section 5.

## 4.2 Alternative Approaches Considered

Before securing access to the CREB laboratory, I conducted research into alternative methods for collecting the data this study required. The main candidate was OpenCap, a markerless motion capture system that estimates lower-limb kinematics from smartphone video without requiring IMU sensors or specialised lab infrastructure. It uses computer vision to extract joint angles from multiple camera angles, making it usable in any space with sufficient lighting and a consumer camera. I also reviewed OpenSim as a simulation framework that could estimate muscle forces and joint moments from kinematic input, which would have allowed modelling of loading patterns even without direct EMG measurement.

This research showed that a fully instrumented approach was preferable if lab access could be secured. The Xsens IMU suit provides higher accuracy for joint angle estimation in a treadmill setting than video-based methods, and the Delsys EMG system adds direct muscle activity recording that neither OpenCap nor OpenSim can replace. Once access to the CREB lab was confirmed, the instrumented approach was adopted.

The OpenCap and OpenSim frameworks remain relevant for future work. If the protocol were extended to outdoor running, OpenCap could provide kinematic estimates without lab equipment. OpenSim could be applied to the IMU data already collected in this study to estimate joint moments and muscle forces, which is listed as a future line in Section 10.2.

## 4.3 System Block Diagram

The study pipeline runs in five sequential stages, from participant recruitment to final results. **Figure 1** shows the full architecture.


***Figure 1.*** *Study pipeline overview.*

Data collection used two wearable biomechanics systems (the Trigno EMG system from Delsys and the Xsens MVN Awinda suit) alongside a Garmin Forerunner 255 for running dynamics and cardiovascular load. Each participant completed 10 treadmill conditions: one fixed walking baseline and 9 running conditions in a randomised order. Data processing ran three independent Python pipelines, one per recording system, each producing a set of condition-level metrics. Analysis combined those metrics to describe speed effects, incline effects, bilateral asymmetry, and cross-modal relationships. The outputs are the activation profiles, joint kinematics, and running dynamics reported in Section 5.3.

## 4.4 Concept-Level Design Decisions

**Why multi-modal recording**

Surface EMG and IMU-based kinematics address different aspects of the same movement. EMG records which muscles are active and by how much, but it says nothing about the joint movement that results. IMU-based motion capture records joint angles and range of motion, but it cannot identify which muscles are generating the movement. Adding Garmin metrics connects the biomechanical picture to the physiological load and stride mechanics that a consumer device can measure. Recording all three in the same session produces a linked dataset where activation, kinematics, and load correspond to identical conditions in the same participants. No single modality could provide that.

**Why a treadmill rather than outdoor running**

The treadmill allows exact control of speed and incline. When a participant runs at 10 km/h and 5% incline, those values are fixed for the entire condition. This means differences in muscle activation and kinematics between conditions can be attributed to speed and incline rather than to anything else. Outdoor running does not allow this: a runner self-selects and fluctuates their pace, terrain changes continuously, and the incline is never constant. Isolating the effect of two specific variables requires a controlled environment. The acknowledged trade-off is that treadmill mechanics differ from outdoor running in documented ways, which is discussed in Section 5.4.7.[28]

**Why walking baseline normalization rather than MVC**

MVC normalization requires a dynamometer to apply controlled resistance to each muscle individually during a maximal voluntary contraction. The CREB lab did not have this equipment. The chosen alternative was to normalize each EMG channel to the mean RMS amplitude from the fixed walking baseline (5 km/h, 0% incline), always recorded first in each session before any running trials. The normalization divides each condition's RMS by that baseline value and produces a dimensionless percentage of walking-speed activation. This preserves between-condition comparability within this dataset. What it does not allow is direct comparison against MVC-normalized studies, because the reference contraction is different. The specific formula and parameters are in Section 5.2.2.

**Why Python**

All data processing and analysis was done in Python. The same pipeline could have been implemented in MATLAB or R, both of which have established signal processing and statistics libraries. We chose Python for convenience: we were already familiar with it, which reduced implementation time and the risk of coding errors. NumPy and SciPy handle signal processing, Pandas handles data organisation, and Matplotlib generates the figures.

**Why Delsys EMG and Xsens IMU**

The EMG and IMU systems were not selected by comparison against alternatives. The CREB lab had a Trigno wireless EMG system (Delsys Inc., Natick, MA, USA) and an Xsens MVN Awinda suit (Xsens Technologies B.V., Enschede, The Netherlands), and these were used because they were available. Both are validated research-grade systems used in peer-reviewed biomechanics studies [29], so the constraint of lab availability did not compromise data quality. Full technical specifications are in Section 5.1.4.

# 5. Detail Engineering

## 5.1 Study Design

### *5.1.1 Preliminary Study (INEFC Dataset)*

Before the main data collection at CREB, I visited Prof. Michel Marina Evrard at INEFC (Institut Nacional d'Educació Física de Catalunya). He had supervised a TFM on treadmill running EMG and had practical experience with the kind of protocol I was designing. The visit was an opportunity to ask about electrode placement decisions, signal quality issues, and how to structure the conditions before committing to a final protocol. As part of that conversation, Prof. Marina Evrard shared the raw EMG data from his student's TFM so I could examine what the data would look like before my own collection began.

The dataset came from one participant recorded on two separate days under identical conditions: treadmill running at 8, 10, and 12 km/h at 0% and 10% incline, giving a 3×2 design with no walking baseline. The data was normalized with MVC. The EMG system was a Biometrics Systems wireless device sampled at 2000 Hz, with 5 mm electrode diameter and 2 cm inter-electrode distance. Both sessions used the same protocol.

Working through this dataset before the main study was useful in two ways. It showed me what raw surface EMG from a running protocol actually looks like: the amplitude ranges, the artifact patterns, and the differences between conditions. It also informed several design decisions for the main study, including the choice to add a 5% incline condition to create a more evenly spaced grid and the decision to use a walking baseline for normalization rather than MVC, given the equipment constraints at CREB. The results from this preliminary dataset are in Section 5.3.1.

### *5.1.2 Experimental Design*

4 participants, aged 21 to 54, all of whom signed an informed consent form, each completed 10 treadmill conditions. The first was always a fixed walking baseline at 5 km/h and 0% incline. The remaining 9 were running conditions arranged in a 3×3 grid: speeds of 8, 10, and 12 km/h crossed with inclines of 0%, 5%, and 10%, randomised in order across participants.

***Table 2.*** *Running conditions. Each cell represents one condition.*

| CONDITIONS | 0% | 5% | 10% |
|---|---|---|---|
| 8 km/h | ✓ | ✓ | ✓ |
| 10 km/h | ✓ | ✓ | ✓ |
| 12 km/h | ✓ | ✓ | ✓ |

The speed range of 8 to 12 km/h corresponds to the typical training range of recreational runners [30]. The incline range of 0% to 10% covers the full range available on the treadmill used, spaced in equal 5% steps. Negative inclines were not possible with this treadmill, which is acknowledged as a limitation in Section 5.4.7. The baseline condition was always the first trial in every session to ensure a consistent, unfatigued normalization reference. The 9 running conditions were randomised independently for each participant. Randomisation tables are in Annex C.

#### *5.1.3 Participants*

4 participants were recruited as a convenience sample, which is appropriate for a pilot study of this type. The inclusion criteria were: being a recreational runner, being 18 years or older, and being able to sustain running at 12 km/h on a treadmill. Participants were excluded if they had a musculoskeletal injury in the 6 months prior to the session or any condition affecting normal gait.

***Table 3.*** *Table of participants.*

| Participant | Sex | Age | Height | Body mass |
|---|---|---|---|---|
| **P1** | F | 21 y | 1.68 m | 58 kg |
| **P2** | M | 21 y | 1.86 m | 72 kg |
| **P3** | F | 52 y | 1.62 m | 52 kg |
| **P4** | M | 54 y | 1.81 m | 70 kg |

The sample includes 2 men and 2 women, and 2 younger participants (21 years) and 2 older participants (52 and 54 years), which adds descriptive variety to a pilot dataset. All participants signed an informed consent form before the session and completed a health questionnaire on the same day. Both documents are in Annex A and Annex B respectively. One of the four participants is me, the researcher conducting the study. This data was collected and processed identically to all others.

Training backgrounds vary across the group. P3 runs 4 days per week on road and is the highest-volume runner in the sample. P4 runs 3 days per week at approximately 30 km per week. P2 and P1 train 3 to 4 times per week through team sport, P2 in football and P1 in basketball, and both maintain a high weekly training load despite low running mileage.

#### *5.1.4 Instrumentation*

Data were collected using three systems simultaneously: surface EMG, full-body IMU, and a wrist-worn running watch.

**Surface EMG**

Muscle activity was recorded using the Trigno wireless EMG system (Delsys Inc., Natick, MA, USA). 16 sensors were placed bilaterally across 8 muscles per leg. The system samples at 2000 Hz and uses parallel-bar dry electrodes with a fixed inter-electrode distance of 10 mm. Electrode placement followed SENIAM guidelines for each muscle [12].

**Inertial Measurement Unit system**

Full-body kinematics were recorded using the Xsens MVN Awinda suit (Xsens Technologies B.V., Enschede, The Netherlands). The system consists of 17 IMU sensors distributed across the body segments and uses sensor fusion to estimate joint angles in real time. Validity against optical motion capture for lower-limb joint angles during running has been established in the literature [17].

**Garmin Forerunner 255**

Running dynamics and cardiovascular load were recorded using a Garmin Forerunner 255 worn on the wrist throughout each session. The device records heart rate, cadence, ground contact time, vertical oscillation, and stride length at 1 Hz.

**Treadmill**

All conditions were performed on a NordicTrack T11.5 treadmill (Model No. NETL10713.0). The treadmill allows incline settings from 0% to 10% in 1% steps and speed settings up to 20 km/h.

### *5.1.5 Experimental Protocol*

Each session followed the same sequence across all participants.

Participants arrived in appropriate running clothing and were required to wear their own running shoes. The first step was skin preparation: the areas over each of the 8 target muscles per leg were shaved and cleaned with alcohol to reduce electrode impedance. 16 Trigno EMG sensors were then placed bilaterally following SENIAM guidelines. Placement locations and palpation landmarks for each muscle are described in Annex D. After electrode placement, the Xsens MVN Awinda suit was fitted and calibrated according to the manufacturer's protocol. The Garmin Forerunner 255 was worn on the wrist throughout the session, with manual lap markers used to synchronise condition boundaries in post-processing.

***Figure 2.*** *Experimental setup. Left: participant fitted with the Xsens MVN Awinda suit and Delsys Trigno EMG sensors. Centre: IMU calibration procedure before the start of the protocol. Right: participant running on the NordicTrack T11.5 treadmill during data collection.*

Before the main protocol, participants completed a 5-minute treadmill familiarisation in which speed and incline were progressively varied. This allowed participants to adapt to the treadmill and gave the researcher time to verify signal quality across all channels before the main recording began. The main protocol consisted of 10 conditions. The first was always the baseline: walking at 5 km/h and 0% incline for 1 minute. The remaining 9 running conditions (**Table 2**) followed in randomised order, each lasting 1 minute. Between conditions, participants rested with 2 minutes of walking at 4 km/h. Total session duration was 60 - 100 minutes depending on preparation and calibration time.

The analysis window for EMG and IMU data was seconds 20 to 50 of each condition, corresponding to steady-state activity after stabilisation. For Garmin data, the analysis window was seconds 10 to 60 of each condition. The first 10 seconds were excluded to allow adaptation to each new condition, and the window extends to second 60 to capture the peak cardiac frequency response, which typically occurs towards the end of the condition.

## 5.2 Data Processing Pipeline

### *5.2.1 Pipeline Overview*

All data processing was done in Python. All processing scripts are publicly available at https://github.com/maxvdaa6/tfg-running-emg-pipeline. The pipeline runs as three independent tracks, one per recording system. **Figure 3** shows the full architecture.

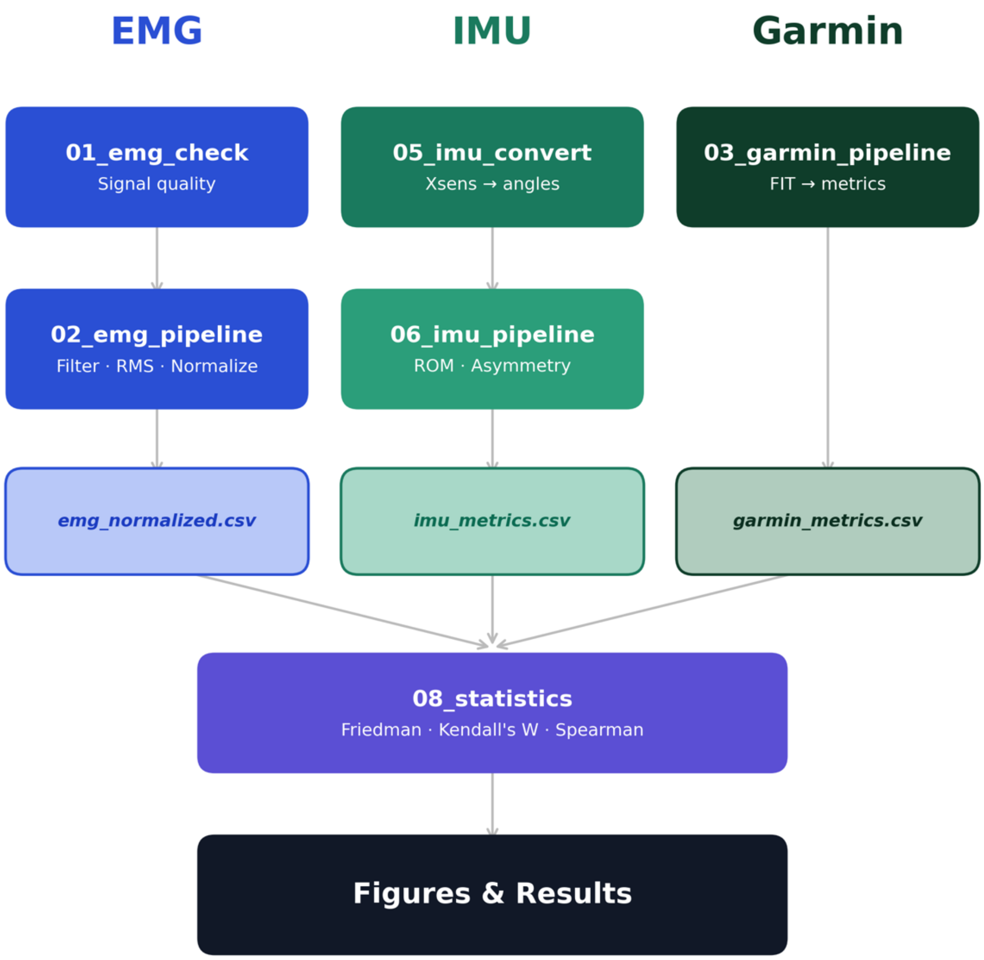


***Figure 3.*** *Data processing pipeline overview.*

The EMG track runs through signal quality checking, filtering, normalization, and channel exclusion before producing per-condition activation metrics. The IMU track converts raw Xsens output to joint angle metrics per condition. The Garmin track extracts running dynamics from FIT files using lap markers for condition synchronisation. The three tracks run independently and produce separate CSV files. These are combined in a final statistics and figures stage. The scripts are named sequentially: *"01_emg_pipeline"*, *"02_figures" "03_garmin_pipeline"*, *"04_garmin_figures"*, *"05_imu_convert"*, *"06_imu_pipeline"*, *"07_imu_figures"*, and *"08_statistics*". The full pipeline is reproducible from raw data files with no manual steps other than the channel exclusions described in Section 5.2.3.

#### *5.2.2 EMG Processing Pipeline*

Raw EMG signals were processed using the script "*01_emg_pipeline.py*" following five sequential steps. **Figure 4** illustrates steps 1 through 4 applied to one representative channel (Tibialis Anterior, right leg, P2, condition 10 km/h at 0% incline).

**Step 1: Spike removal.** Samples exceeding 10 × MAD (median absolute deviation) of the raw signal were flagged as spikes. A 10 ms buffer was applied around each flagged sample, and the affected region was replaced by linear interpolation between the nearest clean samples. This step removes electrical transients without distorting the surrounding signal.

**Step 2: Bandpass filtering.** The cleaned signal was filtered with a 4th-order Butterworth bandpass filter between 20 and 500 Hz, applied zero-phase using forward-backward filtering [31]. The 20 Hz lower cutoff removes movement artefacts and slow baseline drift. The 500 Hz upper cutoff is consistent with the Nyquist limit of the 2000 Hz sampling rate.

**Step 3: Post-filter clipping.** Residual high-amplitude samples in the filtered signal were clipped to ±4 × MAD of the filtered signal. This step handles artefacts that survive the bandpass filter without introducing ringing.

**Step 4: Rectification and RMS envelope.** The filtered signal was full-wave rectified and smoothed using a 100 ms sliding RMS window (200 samples at 2000 Hz). The resulting envelope represents local muscle activation amplitude over time.

**Step 5: Normalization to baseline.** For each muscle and each participant, the mean RMS during the baseline condition (walking at 5 km/h, 0% incline) served as the reference value. All running conditions were then expressed as a percentage of that reference. This approach avoids the need for maximum voluntary contractions, which are difficult to standardize in a running context. Some locomotion-based reference tasks like this one have been shown to provide reliable normalization for gait EMG analysis [32].

The analysis window was seconds 20 to 50 of each condition, giving 30 seconds of steady-state signal per muscle and per condition. The first 20 seconds were excluded to allow the participant to reach a stable running pattern at each new speed and incline. The output of the script was "*emg_normalized.csv*", containing the mean RMS and 95th percentile RMS normalized to baseline, per muscle, per condition, and per participant.[1]

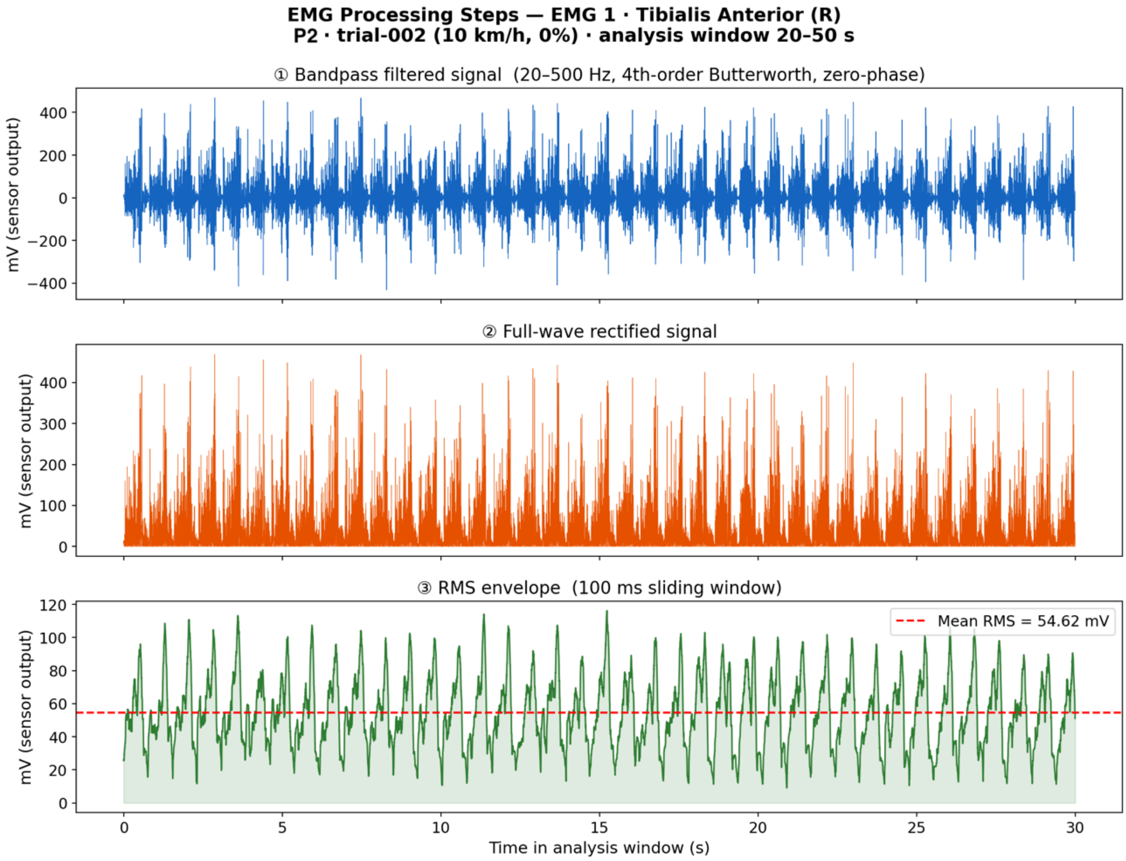


***Figure 4****. Visualization of rectification and RMS envelope.*

### *5.2.3 EMG Data Quality Control and Channel Exclusions*

All EMG channels were reviewed before analysis using the diagnostic script "*00b_diagnostic_plots.py*", which generated visual plots of the raw signal and the preprocessed RMS envelope for each participant, muscle, and trial. Channels were excluded when the signal showed clear signs of electrode failure or motion artefact.

Two types of exclusions were applied. Full-channel exclusions removed a muscle from all trials of a given participant. Trial-specific exclusions removed a single trial from one channel while keeping the remaining trials.

EMG 3 (Rectus Femoris, right leg) produced a flat signal in all 4 participants across all trials. This indicates the electrode was not functioning from the start of the session, likely due to poor initial contact. It is the most consequential exclusion, as it removes the right Rectus Femoris from all group-level analyses.

[1] Note on units: the Delsys Trigno system applies a hardware gain of approximately 909 to the raw EMG signal. The CSV values therefore represent amplified sensor output in volts, not true biological EMG amplitude in mV. Since all results are expressed as percentages of baseline, absolute amplitude values are not reported.

Several other channels were excluded across all trials due to sustained signal problems. Sweat accumulation during exercise can degrade electrode contact over time, leading to extremely high or unstable values that do not reflect true muscle activity. This was the most likely cause for the high-amplitude channels in P2 (Soleus left), P1 (Rectus Femoris left, Semitendinosus left), and P4 (Vastus Lateralis right). In P4, the Semitendinosus left showed values consistently below the baseline during running, which suggests the electrode shifted position during the session.

Trial-specific artefacts were identified in 9 additional channel-trial combinations across P1, P2, and P4. These were excluded individually and the remaining trials for those channels were retained.

**Table 4** summarises all exclusions by participant, channel, and trial.

***Table 4.*** *Table of exclusions*

| Participant | Channel | Muscle | Trial(s) excluded |
|---|---|---|---|
| **P1** | EMG 3 | RF_r | All |
| **P1** | EMG 9 | RF_l | All |
| **P1** | EMG 10 | ST_l | All |
| **P1** | EMG 4 bis | GM_r | 2 and 4 |
| **P1** | EMG 7 | SO_l | 3 |
| **P1** | EMG 11 | BF_l | 8 and 9 |
| **P1** | EMG 12 | GM_l | 6 |
| **P2** | EMG 3 | RF_r | All |
| **P2** | EMG 7 | SO_l | All |
| **P2** | EMG 9 | RF_l | 3 and 6 |
| **P2** | EMG 6 | MG_l | 9 |
| **P3** | EMG 3 | RF_r | All |
| **P4** | EMG 3 | RF_r | All |
| **P4** | EMG 2 bis | VL_r | All |
| **P4** | EMG 10 | ST_l | All |
| **P4** | EMG 8 | VL_l | 6 and 7 |
| **P4** | EMG 9 | RF_l | 3, 5 and 6 |

#### *5.2.4 IMU Processing Pipeline*

The Xsens MVN Awinda system exports joint angles directly from its onboard fusion algorithm, computed from the inertial sensor data. The script "*05_imu_convert.py*" extracted the "Joint Angles ZXY" sheet from each trial Excel file and saved it as a CSV. No additional filtering was applied to the joint angles, as the Xsens firmware already applies sensor fusion and smoothing internally.

The script "*06_imu_pipeline.py*" then computed biomechanical metrics from the extracted angles. The analysis window was frames 1200 to 3000, corresponding to seconds 20 to 50 at 60 Hz, matching the EMG analysis window exactly.

4 joints were analysed in the sagittal plane, plus hip abduction: hip flexion/extension, hip abduction/adduction, knee flexion/extension, and ankle dorsiflexion/plantarflexion, for both the right and left leg (8 signals total).

For each signal, 5 metrics were computed: mean angle, standard deviation, maximum peak, minimum peak, and range of motion (ROM). ROM was computed as the difference between the 5th and 95th percentiles (p95 - p5) rather than the absolute peak-to-peak range, to reduce the influence of transient artefacts in the IMU signal.

A symmetry index (SI) was also computed [33] for each joint and metric, comparing right and left sides:

$$SI = \frac{R - L}{0.5 \cdot (|R| + |L|)} \cdot 100$$

A positive SI indicates right-side dominance, and a negative SI indicates left-side dominance. SI = 0 means perfect symmetry.

The baseline trial (walking at 5 km/h, 0% incline) was excluded from the IMU analysis. Walking is biomechanically distinct from running and would introduce systematic differences that are not comparable to the running conditions. The output of the pipeline was "*imu_metrics.csv*", containing all metrics and symmetry indices per condition and per participant.

### *5.2.5 Garmin Processing Pipeline*

The Garmin Forerunner 255 records running metrics at 1 Hz as a single continuous file throughout the entire session. To mark the start of each condition during data collection, the lap function of the watch was used, creating a lap marker at the beginning of each trial. These lap timestamps were then stored in "*garmin_annotations.csv*", which contains one row per participant and trial with the corresponding start time in seconds within the continuous recording. The script "*03_garmin_pipeline.py*" used these timestamps to extract the relevant window for each condition.

The analysis window was seconds 10 to 60 relative to the start of each condition, giving 50 seconds of data per trial. The first 10 seconds were excluded to allow adaptation to the new speed and incline. This window is wider than the EMG and IMU windows in both directions: it starts 10 seconds earlier and extends 10 seconds further. Starting earlier gives a longer window for computing the mean heart rate, which makes the average more representative of the sustained cardiovascular effort during the condition. Extending to second 60 ensures the heart rate peak is captured, since heart rate rises progressively and often reaches its maximum toward the end of the condition.

5 metrics were extracted per condition: mean heart rate (bpm), maximum heart rate (bpm), cadence (steps/min), mean ground contact time (ms), and mean vertical oscillation (mm). Cadence was computed by doubling the raw Garmin value, which reports steps per minute for one foot only.

One trial was excluded from the Garmin analysis: P4, trial-003 (12 km/h, 10% incline), where heart rate showed abnormally low values inconsistent with the exercise intensity, indicating a likely sensor contact error during that trial.

The output of the script was "*garmin_metrics.csv*", containing all 5 metrics per condition and per participant.

### *5.2.6 Statistical Analysis*

A sample of four participants rules out parametric testing. Normality cannot be verified at this scale, and standard parametric tests such as ANOVA would be unreliable. All analyses therefore use non-parametric methods.

To test whether running condition had a consistent effect on each outcome variable, we applied the Friedman non-parametric test. The test treats the nine running conditions as the repeated factor and the four participants as blocks. It ranks the values within each participant across conditions and checks whether those rankings are consistent across the group. A significant result indicates that at least one condition consistently differs from the others. We quantified effect size as Kendall's W, which ranges from 0 (no rank agreement across participants) to 1 (perfect agreement). We set the significance threshold at $p < 0.05$.

With $n = 4$ participants, we applied no pairwise follow-up tests. The minimum achievable p-value in any pairwise non-parametric test at this sample size is 0.125, which means no comparison can reach significance at $p < 0.05$ regardless of the observed difference. We describe condition differences directly from group means and medians in sections 5.3.2 to 5.3.4.

For cross-modal correlations, we computed Spearman rank correlation separately for each participant across the nine running conditions and then averaged ρ across the four participants. The Spearman correlation measures the strength and direction of a monotonic relationship without assuming linearity. We selected three associations for analysis based on two criteria: a direct biomechanical or physiological rationale linking the two variables, and a consistent correlation direction across all four participants in exploratory screening. The selected associations are reported in Section 5.3.5.

## 5.3 Results

### *5.3.1 Preliminary Study Results (INEFC)*

The preliminary study recorded one participant across 6 conditions. Three speeds (8, 10, and 12 km/h) were combined with two inclines (0% and 10%), giving a 3×2 design. Eight muscles were recorded: Tibialis Anterior, Medial Gastrocnemius, Biceps Femoris, Semitendinosus, Vastus Lateralis, Vastus Medialis, Gluteus Maximus, and Rectus Femoris. The muscle set partially overlaps with the main study and includes Vastus Medialis and Gluteus Maximus instead of Soleus and Gluteus Medius.

Activation was normalized per muscle to the peak value recorded during a squat MVC. The squat was used as a practical reference but does not represent a true MVC for all muscles. Posterior chain muscles such as BF and ST are not primary movers in a squat, so their reference values were low (72 μV and 87 μV respectively), which inflates their normalized values relative to what a muscle-specific MVC would produce. For the figures in this section, activation values were additionally normalized within each muscle to the 8 km/h 0% condition, setting it to 100% and expressing all others relative to it. This approach removes the squat MVC limitation for visualization and focuses the comparison on relative changes across conditions.

ST and Gluteus Maximus showed the largest relative increases. ST reached 210% of the reference at 12 km/h 10% incline, and Gluteus Maximus reached 211% at the same condition. BF also showed a large incline-driven increase, reaching 192% at 12 km/h 10%. MG rose consistently with both speed and incline, reaching 142% at 10 km/h 10%; the cell at 12 km/h 10% was masked due to an artifact consistent with electrode displacement. VL and Vastus Medialis showed moderate increases at higher speeds and incline, reaching 173% and 159% respectively at 12 km/h 10%. TA showed a non-monotonic pattern, dropping to 86% at 10 km/h 0% before returning to 101% at 12 km/h 0%, and remained close to the reference across all incline conditions (91% to 99%). RF showed minimal variation across conditions (99% to 136%).

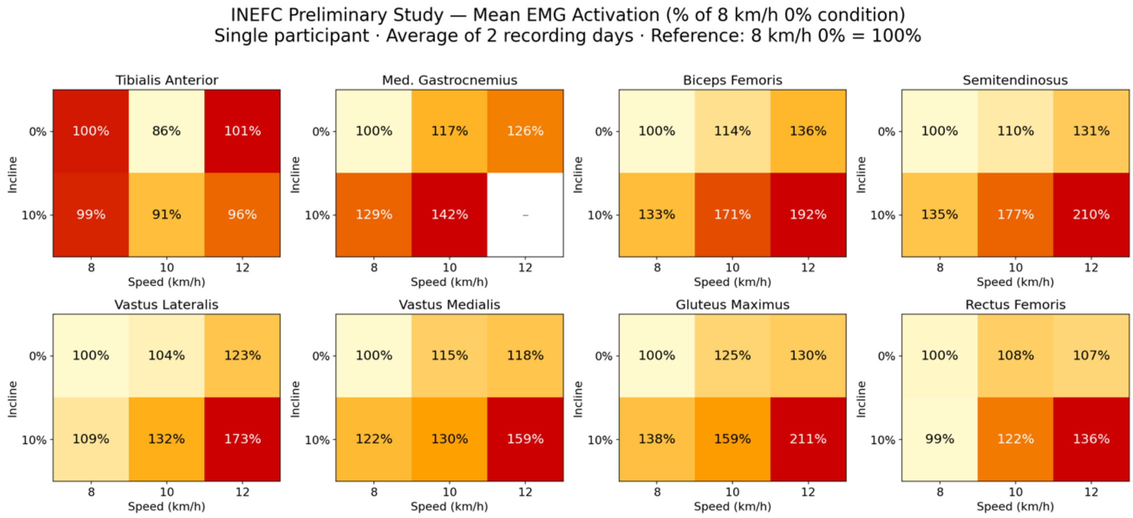


***Figure 5****. Mean EMG activation across the 6 conditions and 8 muscles, normalized to the 8 km/h 0% condition (100%). Average of 2 recording days.*

**Figure 6** shows the same data as line plots, separated by incline level. The divergence between the 0% and 10% incline lines increases with speed for the posterior chain muscles, particularly ST, BF, and Gluteus Maximus. This indicates that the combined effect of high speed and high incline is larger than either factor alone. For TA, the two lines overlap closely across all speeds, confirming that incline had little effect on anterior compartment activation. But we still see a clear increase in EMG activity when either speed or incline increases.

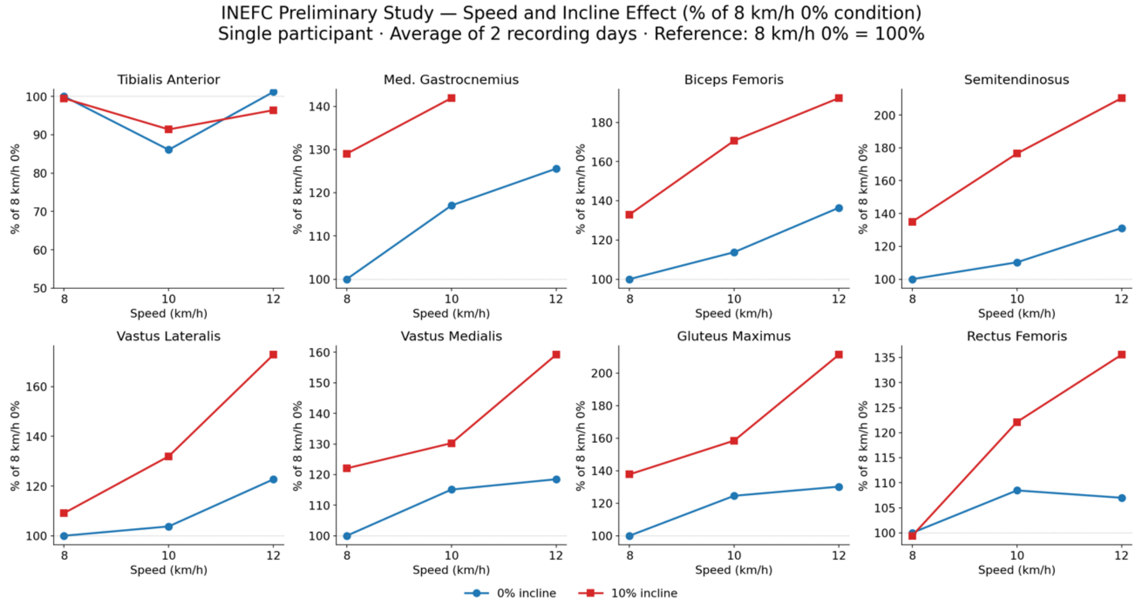


***Figure 6.*** *Speed and incline effects on EMG activation per muscle, normalized to 8km/h 0% = 100%. Lines represent 0% (blue) and 10% (red) incline. Average of 2 recording days.*

Day-to-day reproducibility was high. Corrected p-values for mean activation were 1.00 across all conditions and muscles, indicating no significant difference between the two recording sessions. This confirmed that the pipeline produced stable outputs under repeated identical conditions.

Two additional analyses were performed: peak activation (p95 of the RMS envelope) and time above a 20 µV recruitment threshold. Both confirmed the same directional trends as the mean activation. This confirmed that mean RMS is a sufficient summary metric for condition-level comparisons. The main study therefore reports mean RMS only. BF and ST showed the highest relative increases in peak bursts, and recruitment duration increased consistently with both speed and incline for the posterior chain muscles. Full results are reported in Annex E.

The preliminary study confirmed that the pipeline produced valid and reproducible outputs. The posterior chain muscles, particularly BF and ST, were the most responsive to both speed and incline, which informed the analysis priorities for the main study.

### *5.3.2 EMG Results*

All values are normalised to the walking baseline condition (5 km/h, 0%), so a value of 300% means the muscle produced three times the RMS amplitude recorded during the reference walk. Each participant's activation map is presented as a series of 3×3 grids, one per muscle and side. Within each grid, columns represent speed (8, 10, 12 km/h from left to right) and rows represent incline (0%, 5%, 10% from bottom to top). The top-right cell therefore corresponds to the highest speed and the steepest incline. The colour scale within each 3×3 grid is set independently relative to that muscle's own value range for that participant, so darkness can only be compared across conditions within the same muscle and participant, not across muscles or across participants.

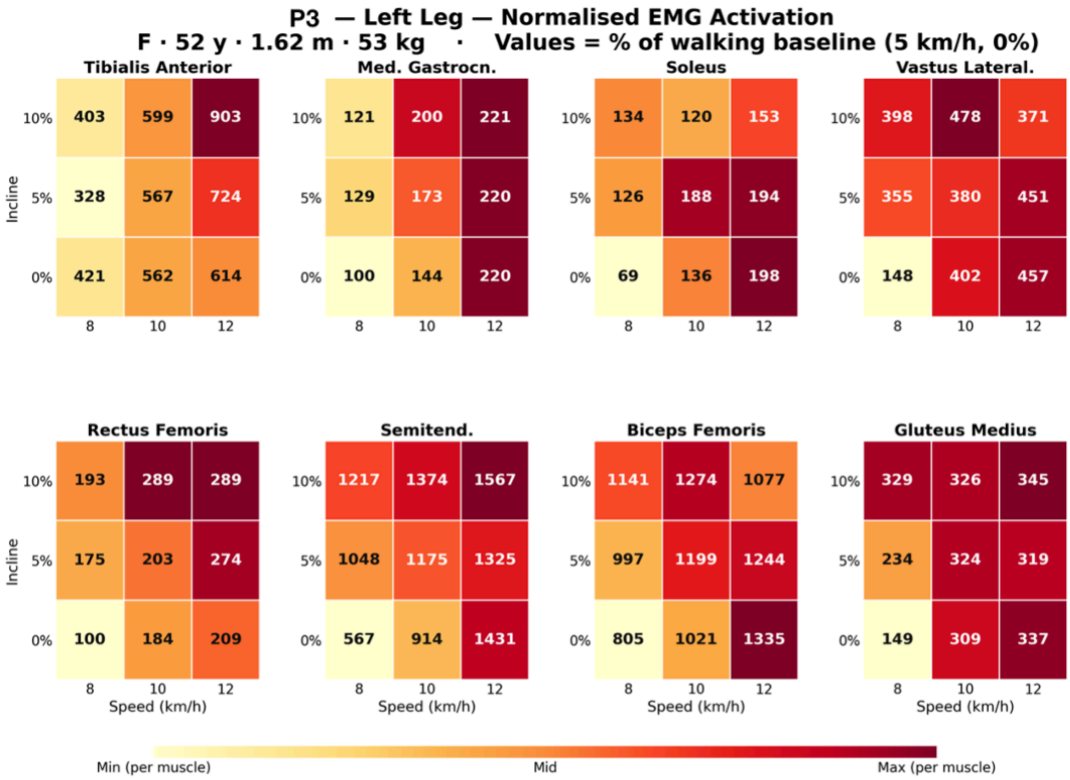


*Figure 7.* *Normalised EMG activation map for P3, Left Leg. Each cell shows mean RMS amplitude as a percentage of the walking baseline (5 km/h, 0%). Columns: speed (8, 10, 12 km/h). Rows: incline (0%, 5%, 10%, bottom to top). Colour scale is independent per muscle. Grey cells: excluded channels*

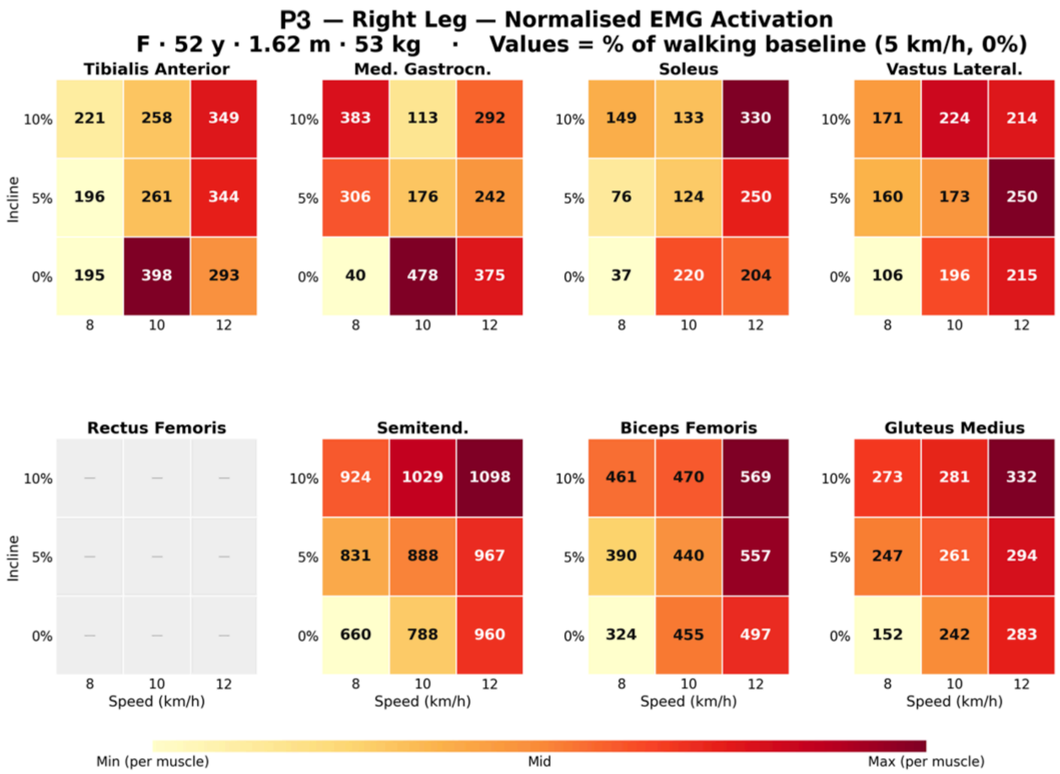


*Figure 8.* *Normalised EMG activation map for P3, Right Leg*

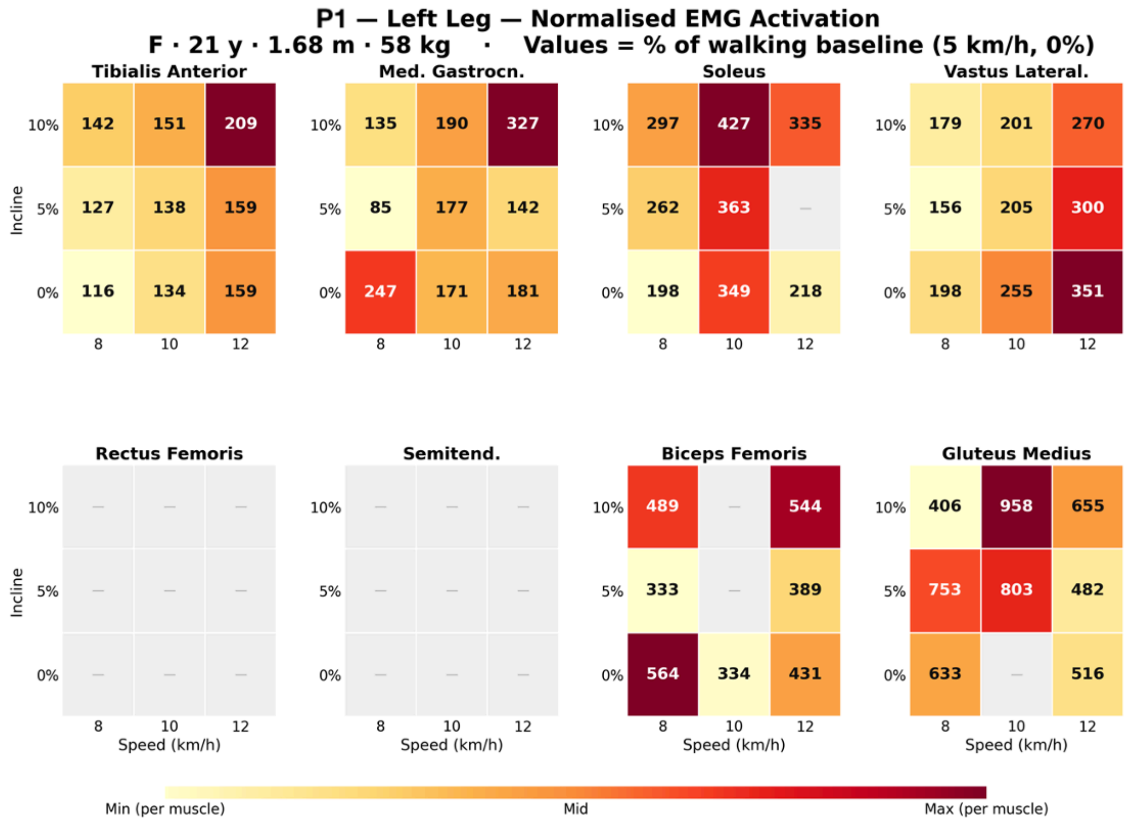


*__Figure 9.__ Normalised EMG activation map for P1, Left Leg*

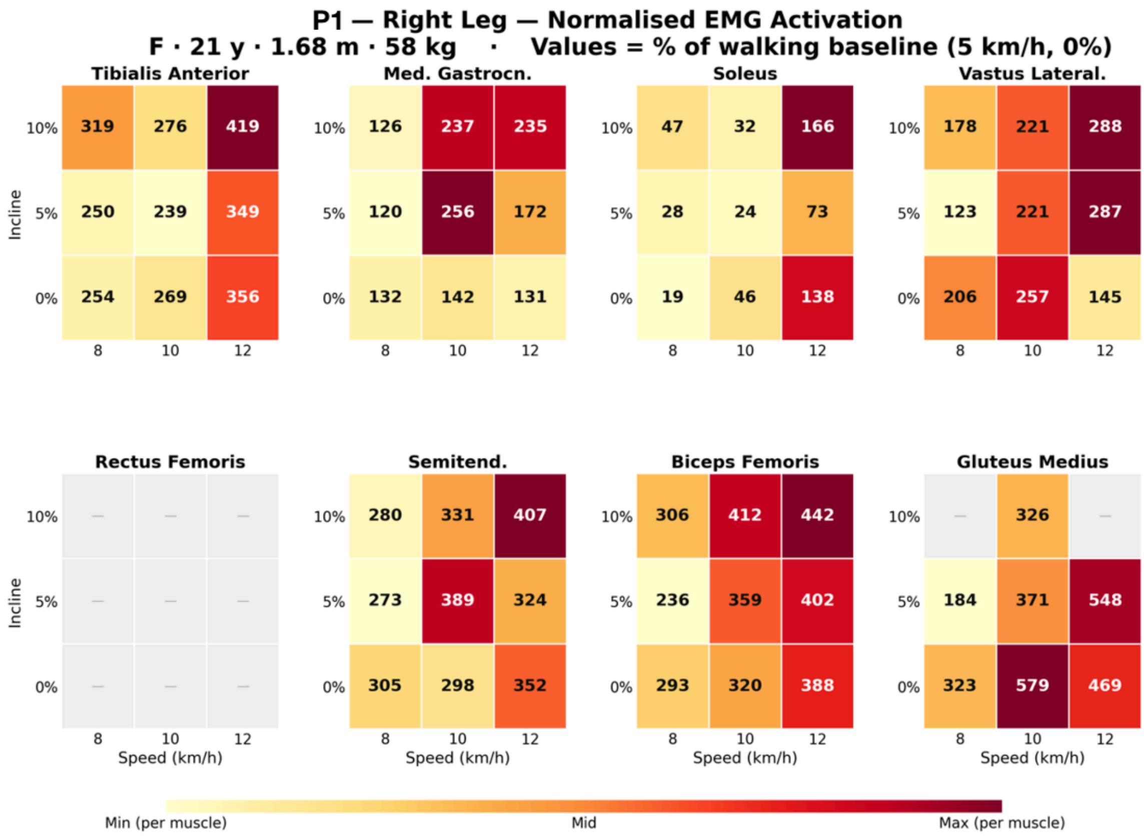


*__Figure 10.__ Normalised EMG activation map for P1, Right Leg*

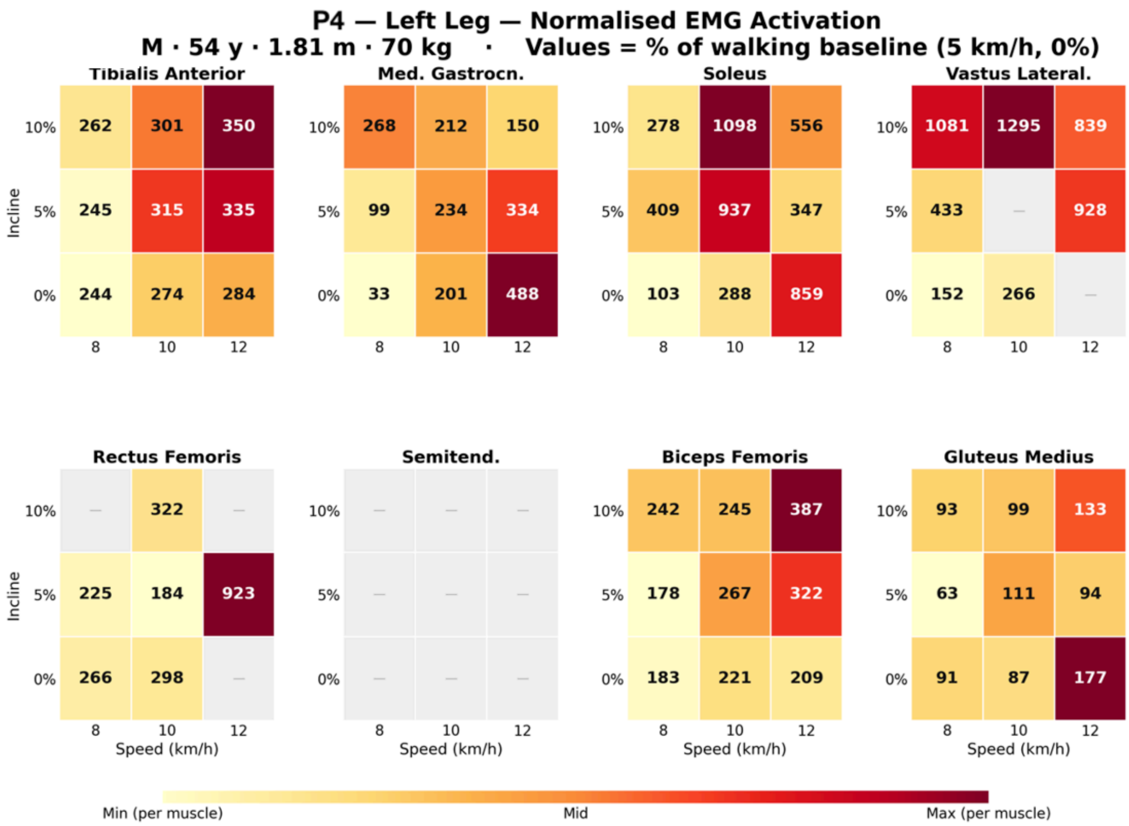


***Figure 11.*** *Normalised EMG activation map for P4, Left Leg*

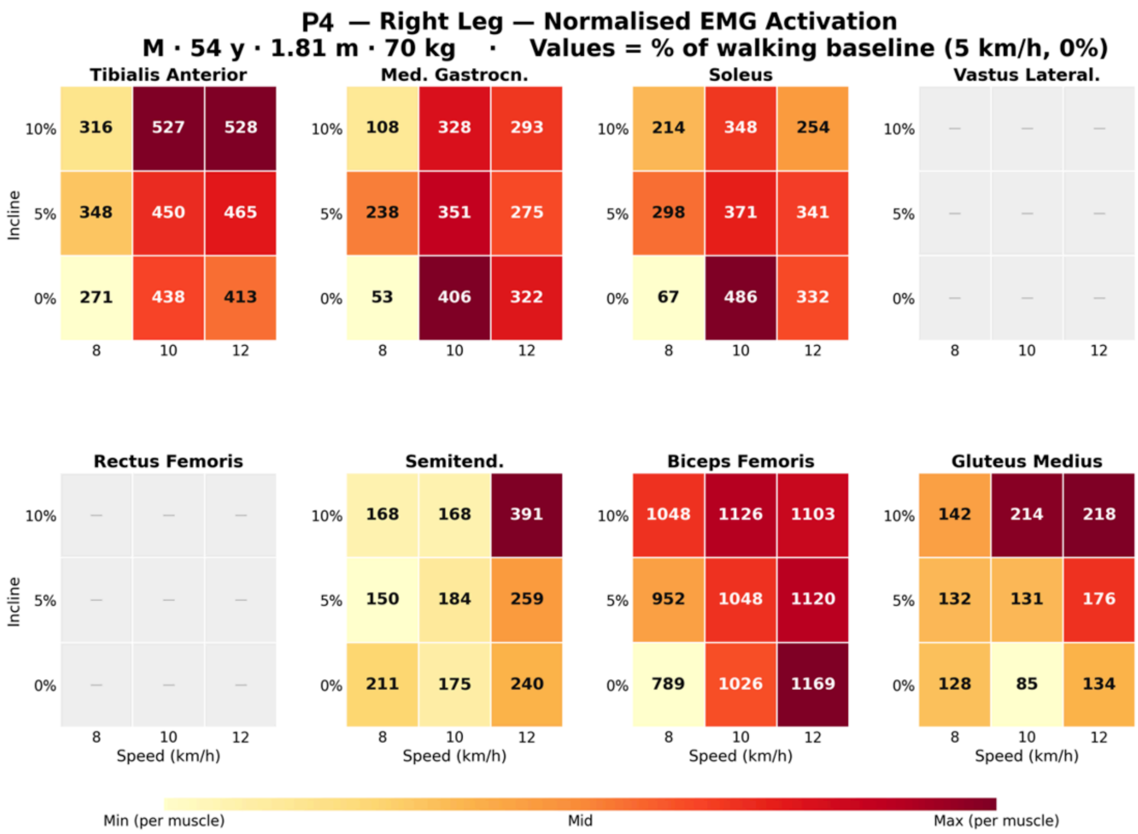


***Figure 12.*** *Normalised EMG activation map for P4, Right Leg*

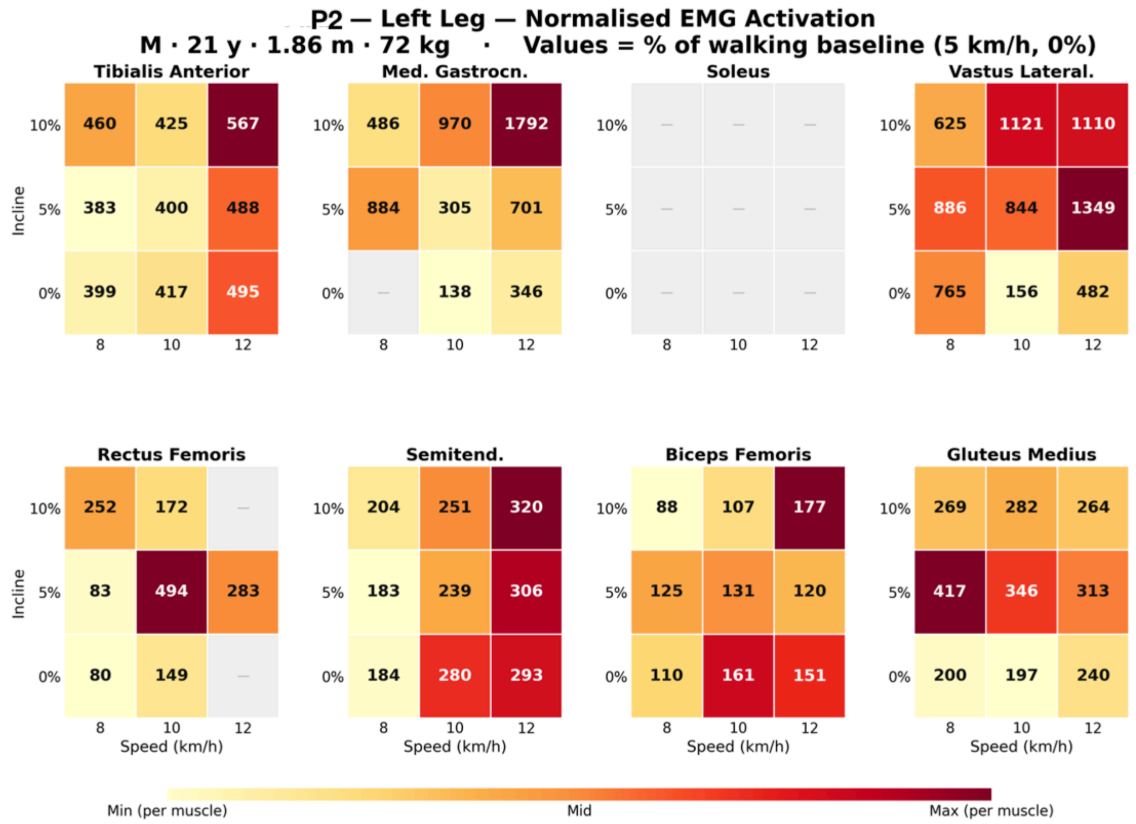


***Figure 13.*** *Normalised EMG activation map for P2, Left Leg*

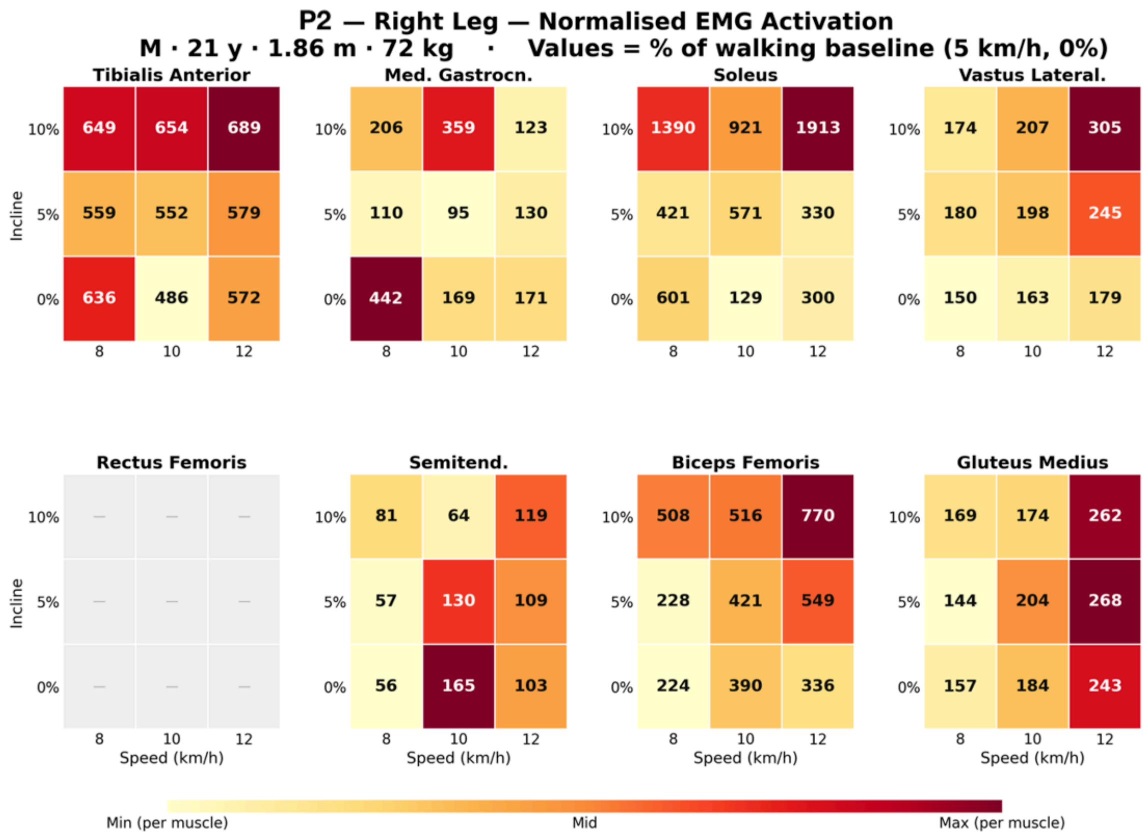


***Figure 14.*** *Normalised EMG activation map for P2, Right Leg*

For most muscles and participants, activation increases with both speed and incline, producing progressively darker cells toward the top-right of each subplot. However, not all muscles and not all participants follow this pattern consistently. Some muscles show no clear directional response, some show a response to speed but not to incline, and in a few cases activation decreases or stays flat across conditions. This is expected in a pilot study of this size. With 4 participants, a convenience sample, and electrode placements that were not optimal for every muscle site, some channels capture the physiological signal reliably and others do not. The maps should be read as descriptive summaries of what was recorded, not as definitive characterisations of each muscle's behaviour. Inter-participant variability is large: values for the same condition and muscle can differ by a factor of two or more between individuals, which is expected in a pilot sample spanning a wide age range and different training backgrounds.

Excluded channels appear as grey cells with a dash. P1 has the most excluded channels, with 7 muscles showing at least one excluded condition. The Rectus Femoris right is the only channel excluded in all four participants and has no valid data at group level. Detailed exclusion decisions are reported in Section 5.2.3. All group-level analyses in the following subsections use only non-excluded observations.

**Figure 15** shows the group-level effect of speed and incline on normalised EMG activation. Each panel corresponds to one muscle, and each of the three lines represents one incline level: 0% in blue, 5% in orange, and 10% in red.

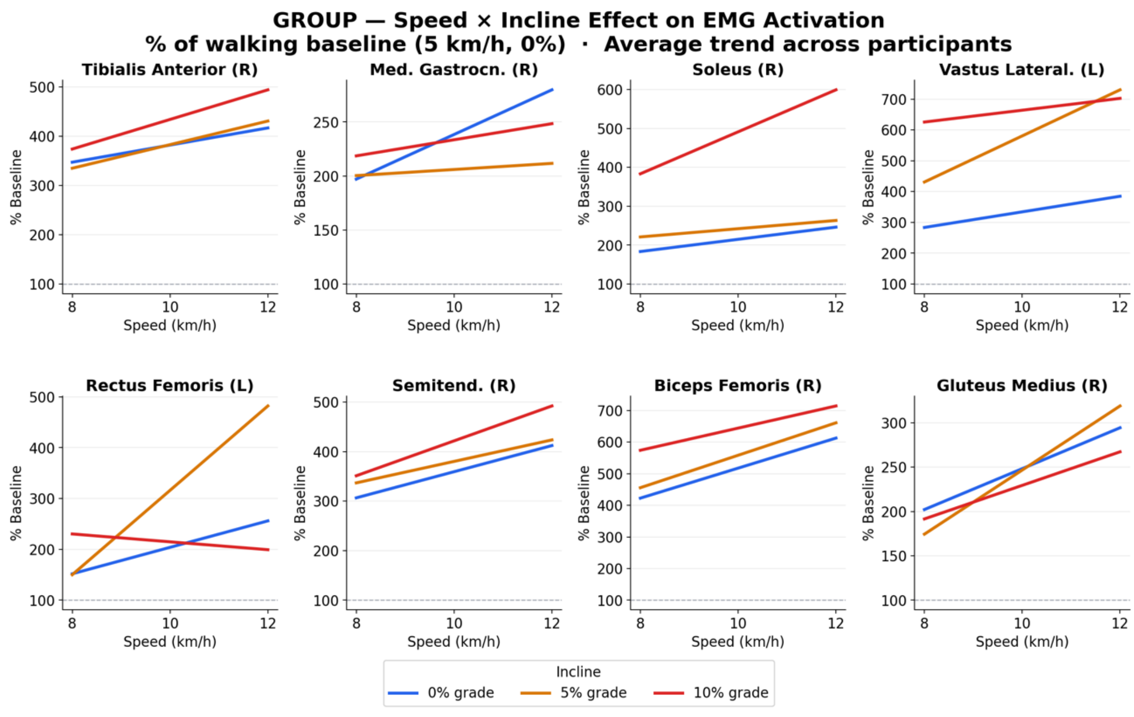


*__Figure 15.__ Group average EMG activation trend versus speed, by incline level. Lines represent the mean of individual linear regressions per participant. Values as percentage of walking baseline (5 km/h, 0%).*

The figure displays 8 muscles instead of the full 16 channels. For each muscle, one side was selected based on data completeness: the side with fewer exclusions across all participants and conditions.

The group trend for each muscle and incline was computed as follows. For each participant, a linear regression was fitted between speed (8, 10, 12 km/h) and mean normalised activation. This gives one slope and one intercept per participant per incline level. The group line shown in the figure is the average of those individual slopes and intercepts.

The clearest patterns appear in SO, ST, and BF, where all three incline lines trend upward with speed and maintain the expected order throughout the speed range. Higher incline produces higher activation at both the lower and upper ends of the speed range. Other muscles show more variability. RF shows a negative average slope at 10% incline, which reflects the high number of exclusions for that channel and the limited data available for the group regression. GM shows lines that are not consistently ordered across the speed range, indicating high inter-individual variability in gluteus medius recruitment strategy.

### *5.3.3 IMU Results*

The XSENS inertial measurement system recorded joint angles continuously throughout each trial. From these signals, we extracted the range of motion (ROM) for four joints: hip flexion/extension, knee flexion/extension, ankle dorsiflexion/plantarflexion, and hip abduction/adduction. ROM is reported in degrees. Individual heatmaps show right and left limbs separately. Group figures show the mean of both limbs across all four participants.

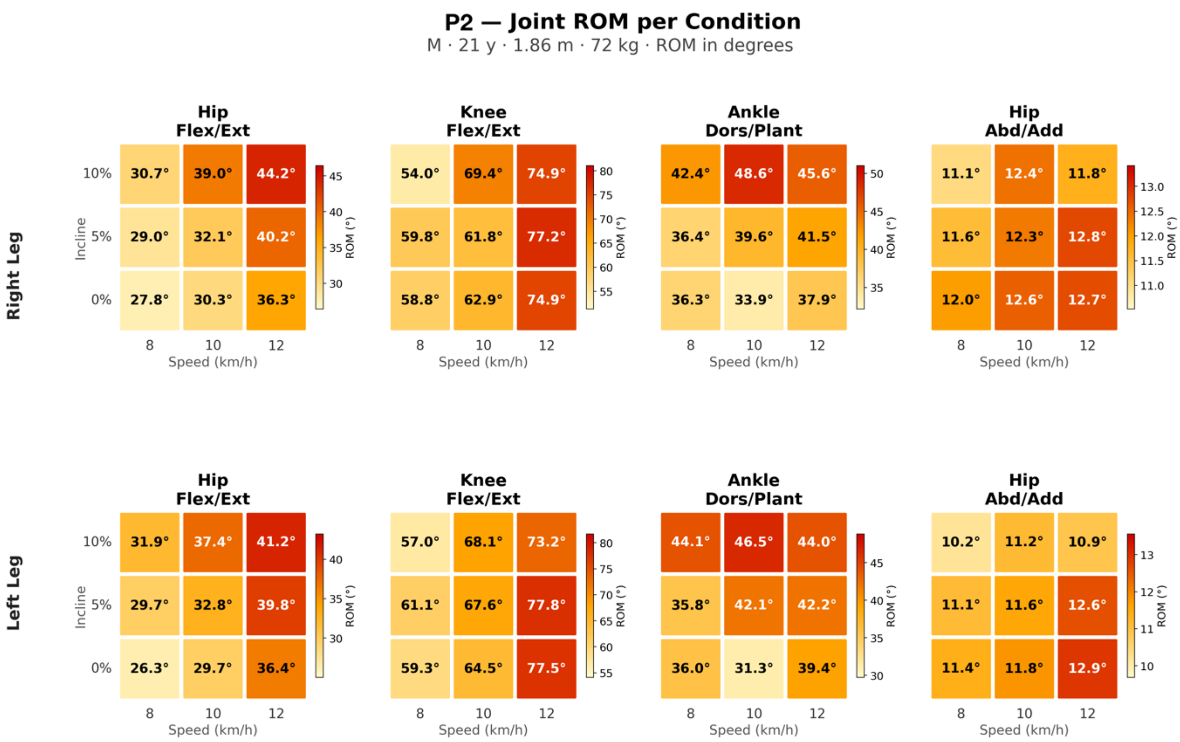


***Figure 16.*** *Joint ROM per condition for P2. Each cell shows mean ROM in degrees. Columns: speed (8, 10, 12 km/h). Rows: incline (0%, 5%, 10%, bottom to top). Top row: right leg. Bottom row: left leg. Colour scale is independent per joint.*

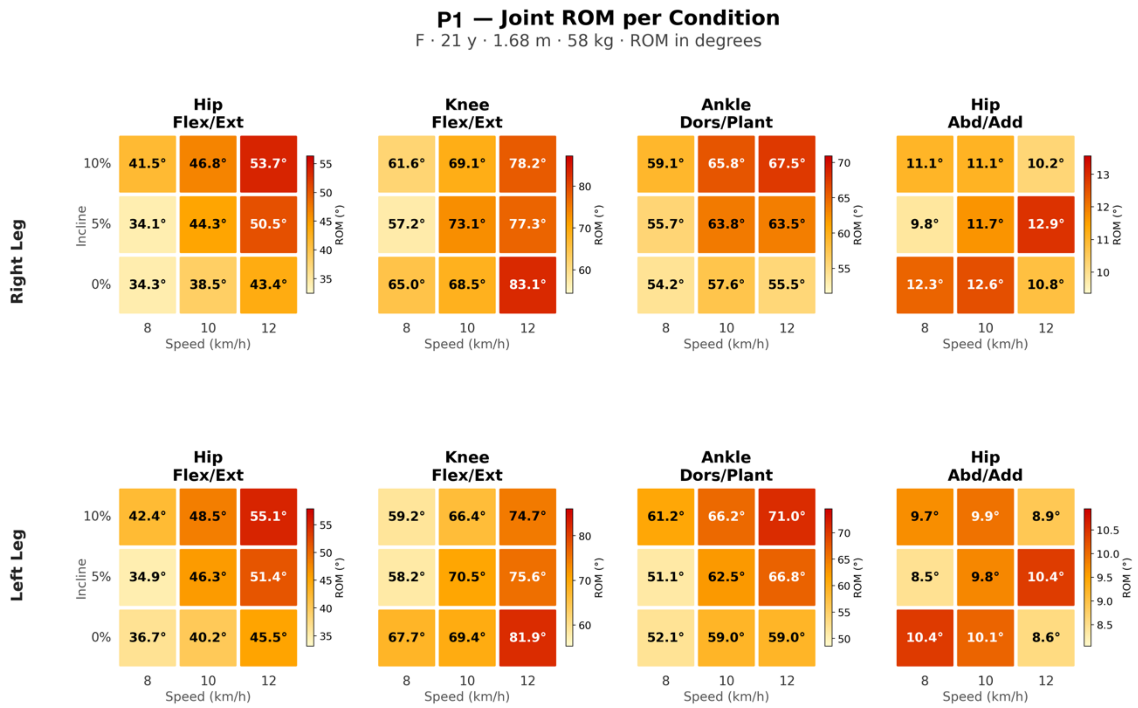


*Figure 17. Joint ROM per condition for P1.*

Individual ROM heatmaps for P3 and P4 are provided in Annex F. P1 and P2 were selected for the main text because they show the clearest speed effect across all four joints.

ROM increases with speed at the hip, knee, and ankle in both participants. Averaged across incline levels, hip flexion ROM increases by 36% from 8 to 12 km/h in P2 (29.2° to 39.7°) and by 34% in P1 (37.3° to 49.9°). Knee flexion ROM follows the same pattern, rising by 30% in P2 (58.3° to 75.9°) and by 28% in P1 (61.5° to 78.5°). P1 shows higher ankle dorsiflexion ROM than P2 across all conditions, with a mean difference of approximately 20° across equivalent speeds and inclines. This difference is addressed in Section 5.4.

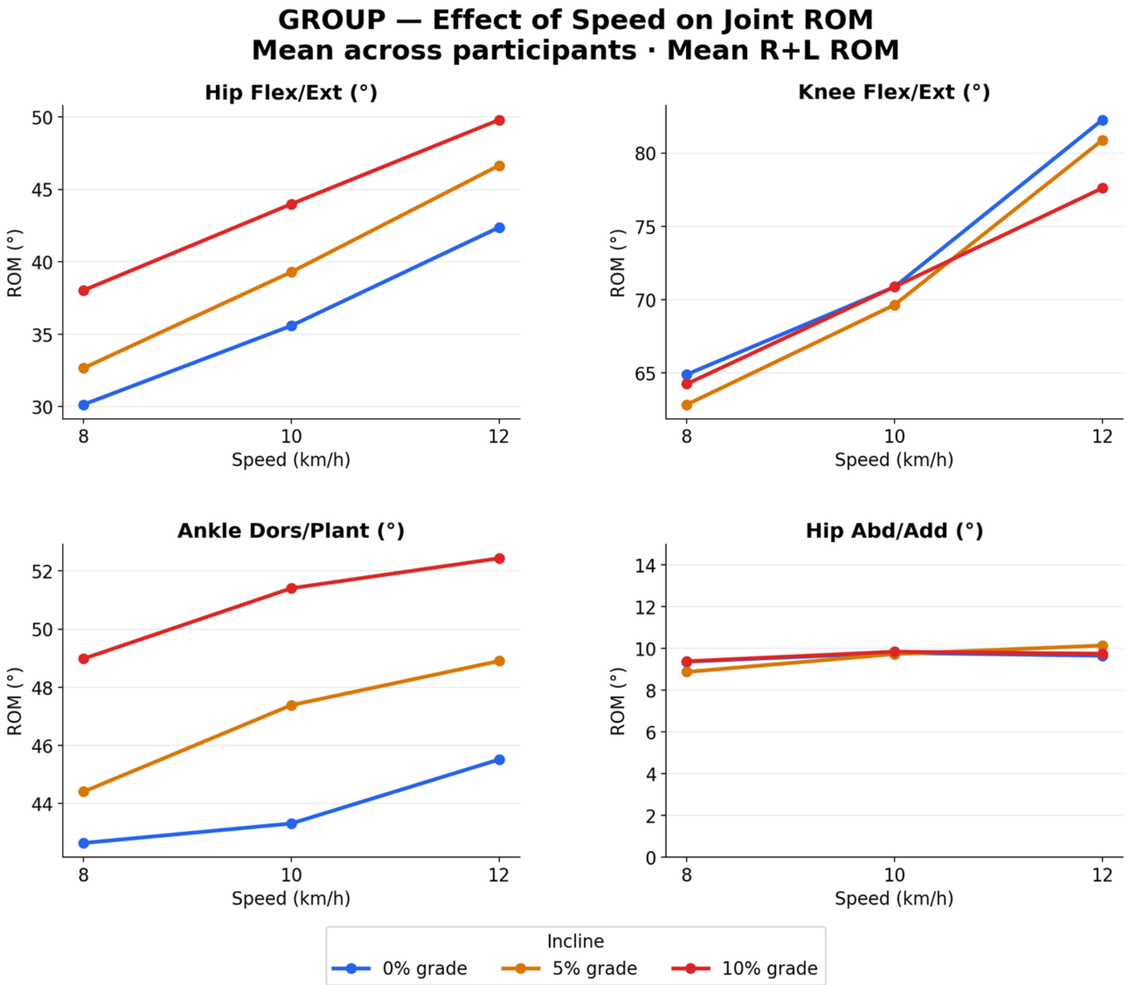


*Figure 18. Group mean ROM versus speed, by incline level. Each panel shows one joint. Lines represent the mean across all four participants. Blue: 0% grade; orange: 5% grade; red: 10% grade.*

The speed effect is consistent: higher speed increases ROM at the hip, knee, and ankle, but not at the hip abductor. The incline effect is more selective: only hip flexion and ankle dorsiflexion increase with incline; knee flexion and hip abduction do not.

This pattern is visible in **Figure 18**. In the hip flexion and ankle panels, the three incline lines are ordered with blue (0%) at the bottom and red (10%) at the top across all speeds, confirming that higher incline produces higher ROM at these joints. In the knee flexion and hip abduction panels, the three lines overlap throughout the speed range, confirming that incline has no effect on these joints.

Averaged across incline levels, group mean hip flexion ROM increases from 33.6° at 8 km/h to 46.3° at 12 km/h (+38%), knee flexion ROM from 64.0° to 80.3° (+25%), and ankle dorsiflexion ROM from 45.3° to 48.9° (+8%). Hip abduction ROM stays flat across all speeds, with group mean values around 9.6° regardless of condition. Averaged across speed levels, hip flexion ROM increases from 36.0° at 0% grade to 43.9° at 10% grade, and ankle dorsiflexion ROM from 43.8° to 50.9°. Knee flexion group mean values are 72.7°, 71.1°, and 70.9° at 0%, 5%, and 10% grade respectively.

Hip abduction ROM shows high inter-individual variability (CV 19.6% across conditions), which is consistent with this joint being more dependent on individual running technique than on the external demands of speed or incline.

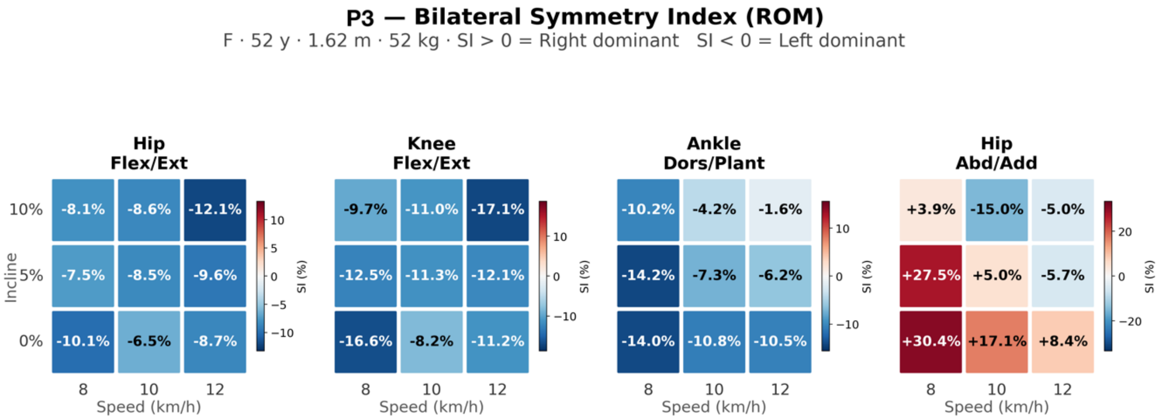


*__Figure 19.__ Bilateral symmetry index (SI) per condition for P3. SI > 0 indicates right-side dominance; SI < 0 indicates left-side dominance. Columns: speed (8, 10, 12 km/h). Rows: incline (0%, 5%, 10%, bottom to top).*

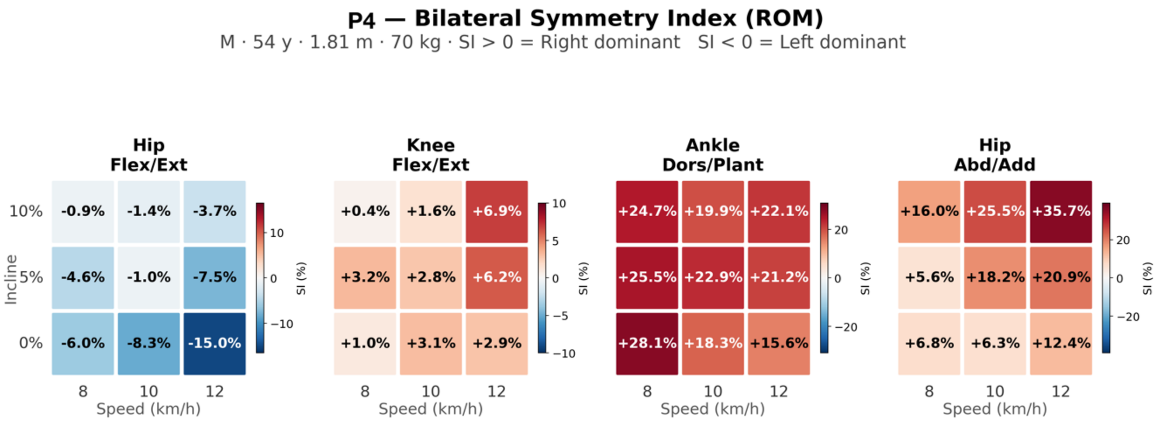


*__Figure 20.__ Bilateral symmetry index (SI) per condition for P4.*

SI heatmaps for P1 and P2 are provided in Annex F. P3 and P4 were selected for the main text because they show the most consistent and interpretable asymmetry patterns across conditions.

P3 shows a persistent left-side dominance in hip flexion and knee flexion ROM across all conditions. Hip flexion SI values range from −6% to −12% and knee flexion SI values from −8% to −17%, with no systematic change across speeds or inclines. P4 shows a persistent right-side dominance in ankle dorsiflexion, with SI values between +15% and +28% that remain stable across all conditions.

Hip abduction SI shows a different pattern in both participants, and the two tendencies are opposite. In P3, hip abduction SI decreases from strongly right dominant at low speed and low incline (+30% at 8 km/h, 0%) to left dominant at high speed and high incline (−15% at 10 km/h, 10%). In P4, hip abduction SI increases from moderate right dominance at low speed and low incline (+7% at 8 km/h, 0%) to strong right dominance at high speed and high incline (+36% at 12 km/h, 10%). Unlike the asymmetries in hip flexion, knee flexion, and ankle dorsiflexion, hip abduction asymmetry in these two participants does change systematically with the demands of the task.

### *5.3.4 Garmin Results*

The Garmin running watch recorded heart rate, cadence, ground contact time (GCT), and vertical oscillation continuously throughout each trial. Mean values were extracted per condition for each participant.

P1 and P2 were selected for the main text because both have complete datasets across all nine running conditions (P3 is missing one condition: 12 km/h, 10%), and because their figures illustrate the widest contrast in heart rate response, which is one of the key patterns described in this section. Individual Garmin heatmaps for P3 and P4 are provided in Annex F.

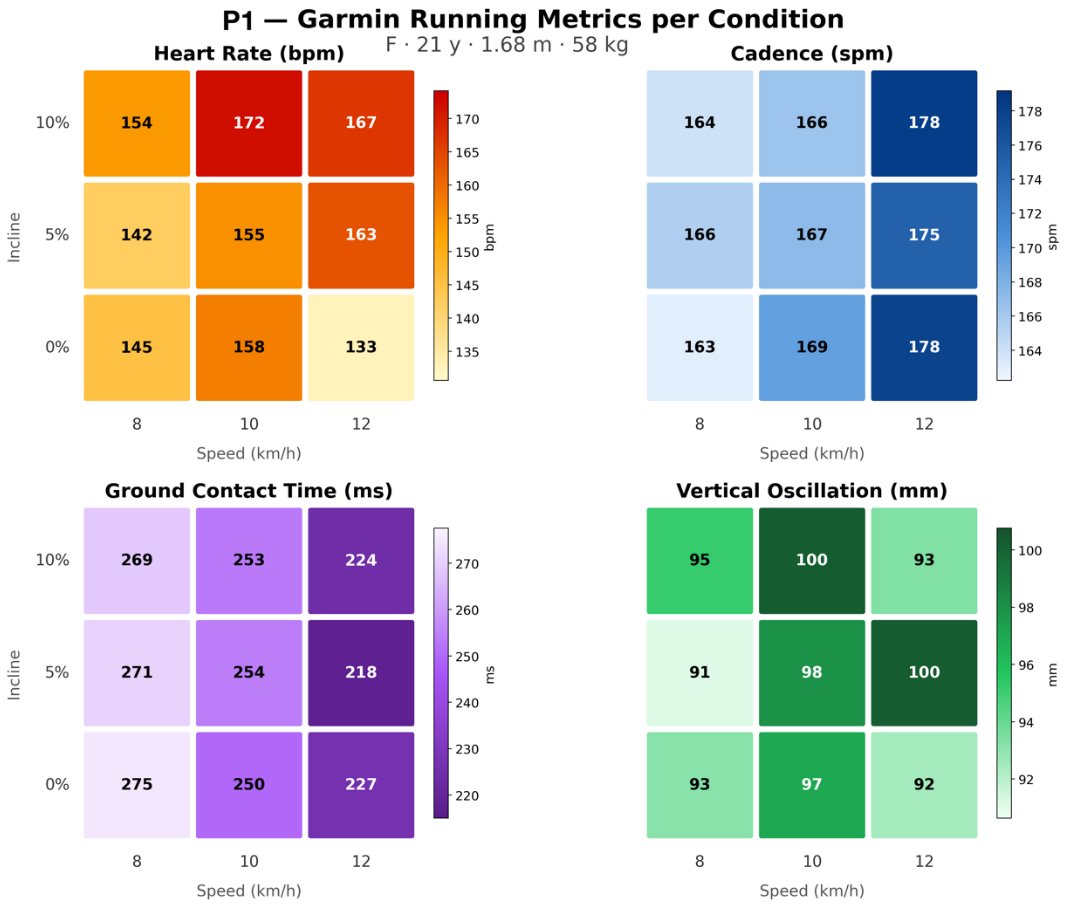


***Figure 21.*** *Garmin running metrics per condition for P1. Each cell shows the mean value across the condition window. Columns: speed (8, 10, 12 km/h). Rows: incline (0%, 5%, 10%, bottom to top). Colour scale is independent per metric.*

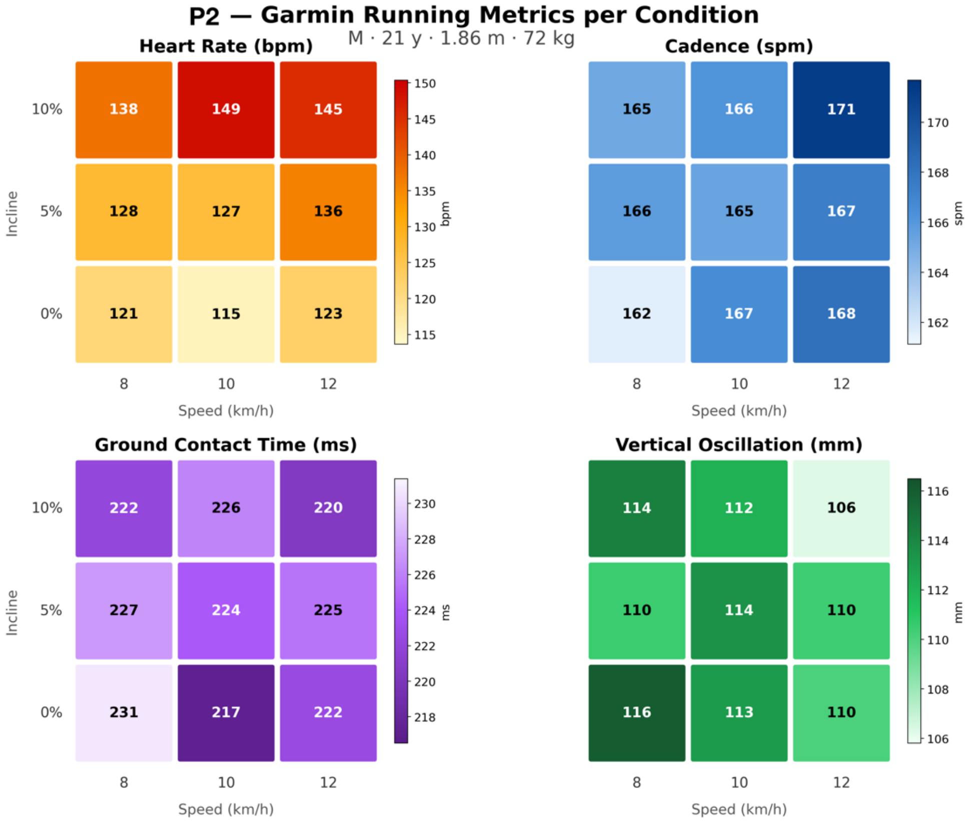


*Figure 22. Garmin running metrics per condition for P2.*

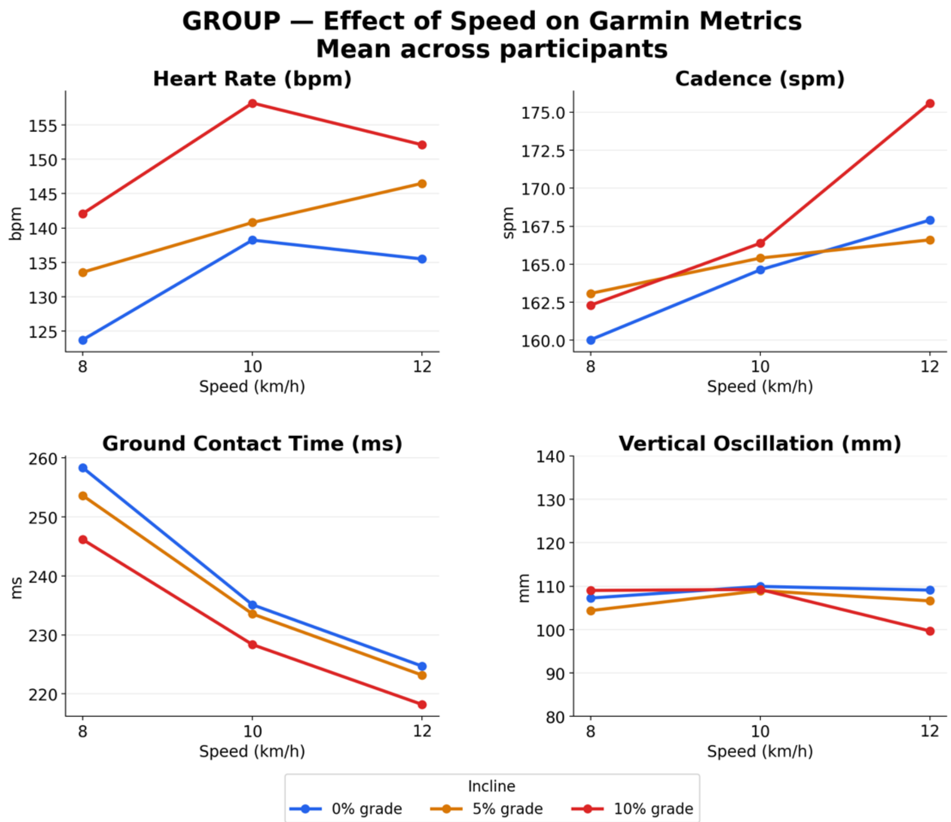


*Figure 23. Group mean Garmin metrics versus speed, by incline level. Lines represent the mean across all four participants. Blue: 0% grade; orange: 5% grade; red: 10% grade*

Speed increases cadence and decreases GCT. Group mean cadence increases from 161.8 spm at 8 km/h to 169.5 spm at 12 km/h. Group mean GCT decreases from 252.7 ms at 8 km/h to 222.4 ms at 12 km/h. The incline effect on these two metrics is small: cadence changes from 164.2 spm at 0% grade to 167.4 spm at 10% grade, and GCT from 239.4 ms to 232.1 ms.

Heart rate shows a different pattern. The incline effect is larger than the speed effect: group mean HR increases from 132.5 bpm at 0% grade to 150.7 bpm at 10% grade (+14%), while the speed effect is smaller and less consistent across the 8–12 km/h range. Vertical oscillation is flat across all conditions, with group mean values between 105.6 and 109.4 mm regardless of speed or incline.

This contrast is consistent with the physiological cost of running uphill: incline increases metabolic demand without substantially changing the temporal structure of the stride.

Inter-individual differences are present in GCT and cadence. P2 and P4 show lower mean GCT than P1 and P3 across all conditions (224 ms and 222 ms vs 249 ms and 251 ms respectively). P3 shows lower mean cadence than the other three participants (155.8 spm vs 166–170 spm).

### *5.3.5 Statistical Analysis*

We applied the Friedman non-parametric test to assess whether running condition produced a consistent within-participant effect on each outcome variable. Condition is treated as the repeated factor (nine running conditions) and participant as the block. Kendall's W quantifies the effect size, where W = 1 indicates perfect rank agreement across participants and W = 0 indicates no agreement. Results for all variables are shown in **Figure 24**. Given the sample size of four participants, non-significant results should be interpreted alongside W rather than as an absence of effect. We are looking for variables where both p is significant and W is high, meaning the condition effect is not only statistically detectable but consistent in direction across all four participants.

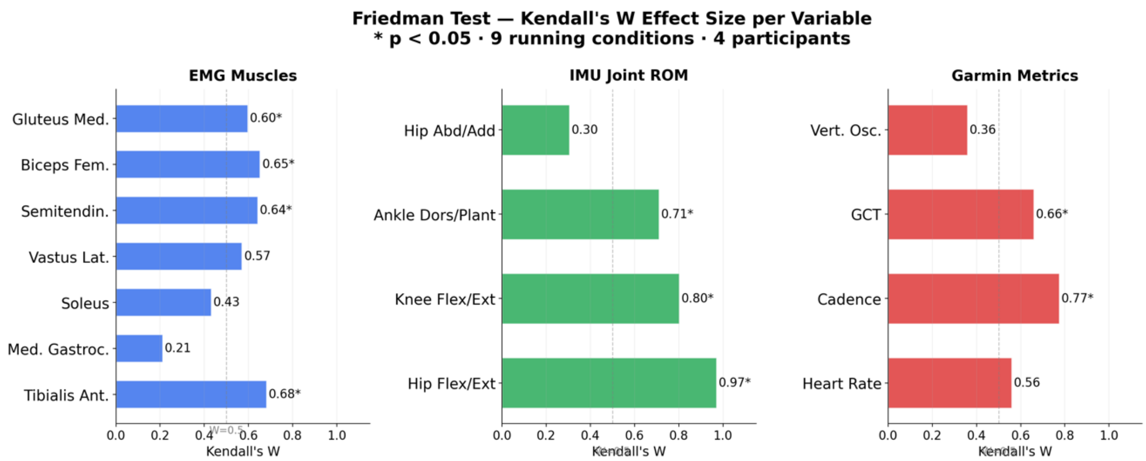


***Figure 24.** Kendall's W effect size from the Friedman test for all measured variables, grouped by modality. Asterisks indicate p < 0.05. Nine running conditions, four participants.*

Joint ROM showed the strongest condition effects of the three modalities. Hip flexion ROM reached W = 0.971 ($p < 0.001$), knee flexion W = 0.802 ( $p = 0.001$), and ankle dorsiflexion W = 0.710 (p =

0.004). Hip abduction was not significant ($p = 0.284$, $W = 0.304$), consistent with the flat response to condition described in Section 5.3.3.

Within the EMG data, four muscles reached significance: tibialis anterior ($W = 0.681$, $p = 0.005$), semitendinosus ($W = 0.642$, $p = 0.009$), biceps femoris ($W = 0.652$, $p = 0.008$), and gluteus medius ($W = 0.596$, $p = 0.015$). Medial gastrocnemius did not reach significance ($p = 0.566$, $W = 0.210$). Soleus and vastus lateralis were borderline ($p = 0.087$ and $p = 0.090$), with vastus lateralis showing a moderate effect size ($W = 0.570$) despite not crossing the 0.05 threshold. Rectus femoris had insufficient valid measurements across conditions and was excluded from this analysis.

For the Garmin metrics, cadence showed the largest condition effect ($W = 0.774$, $p = 0.017$) and ground contact time was also significant ($W = 0.659$, $p = 0.045$). Heart rate did not reach significance ($p = 0.098$, $W = 0.559$). Vertical oscillation showed no condition effect ($p = 0.375$, $W = 0.359$).

Three cross-modal associations were selected for analysis: heart rate versus muscle activation, tibialis anterior activation versus ground contact time, and hamstring activation versus knee flexion ROM. These were chosen based on two criteria: a direct biomechanical or physiological rationale linking the two variables, and a consistent correlation direction across all four participants in exploratory analysis.

**Heart rate and muscle activation.**

**Figure *25*** shows the association between relative heart rate (%HRmax, estimated as 220 − age)[2] and muscle activation for four representative muscles. One muscle was selected per functional group: tibialis anterior (left) for dorsiflexion, medial gastrocnemius (right) for plantarflexion, vastus lateralis (left) for knee extension, and biceps femoris (right) for knee flexion and hip extension. Within each group, the side with fewer excluded conditions was used, giving two left and two right muscles. All four muscles show a positive overall trend between %HRmax and activation across participants. Vastus lateralis shows the most consistent individual slopes (P1: $\rho = +0.500$, P2: $\rho = +0.700$, P3: $\rho = +0.738$, P4: $\rho = +0.679$; mean $\rho = +0.654$). Tibialis anterior shows the most inter-individual variability in slope, while medial gastrocnemius and biceps femoris are intermediate.

The figure also shows that participants worked at different ranges of %HRmax across the nine conditions. P2 worked at the lowest relative intensities, from 58% to 75% HRmax. P1 and P3 were intermediate, ranging from 67% to 87% and from 57% to 88% respectively, with P3 showing the widest span of any participant. P4 worked at the highest relative intensities throughout, reaching up to 99% of his estimated HRmax. This inter-individual variation at equivalent absolute loads may reflect differences in fitness level and training experience, and is discussed further in Section 5.4.

[2] Estimated HRmax (220 − age) carries a standard error of roughly ±10 bpm at the individual level [34], so these relative intensities are approximate. P4's near-maximal values in particular should be read as indicating high relative effort rather than a precise percentage of true maximum

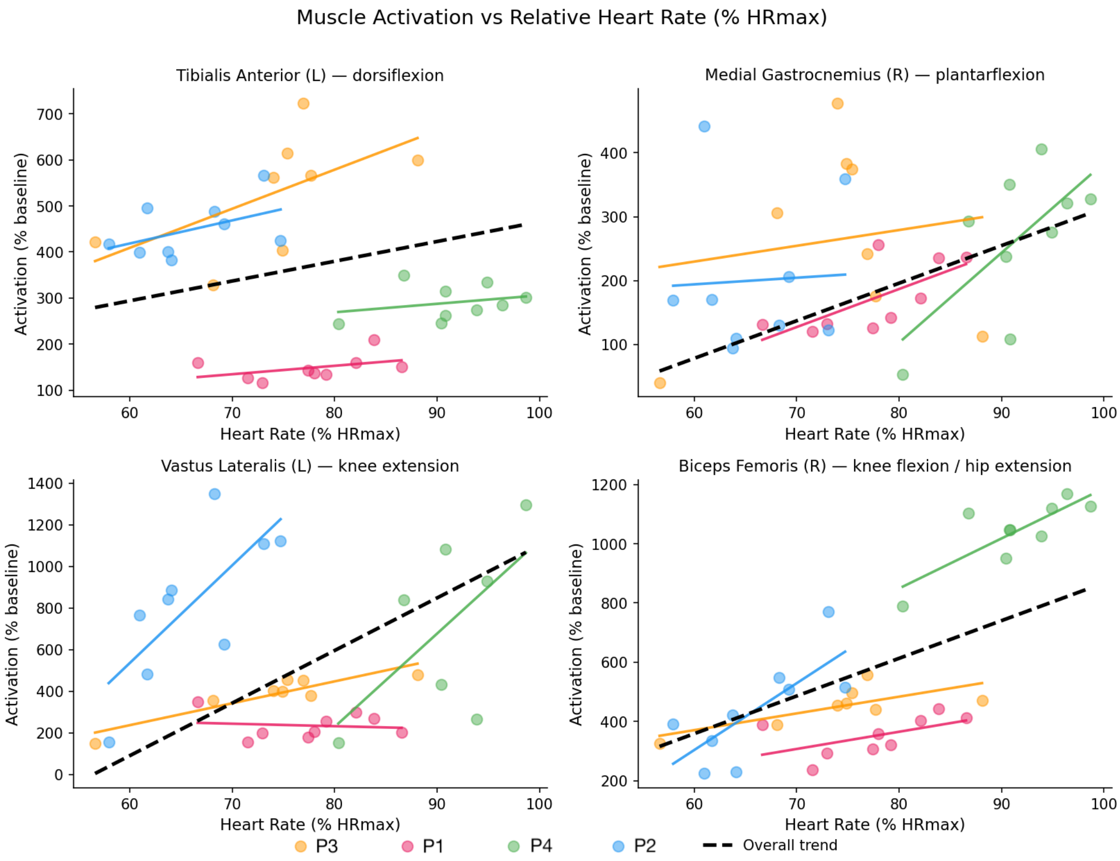


**Figure 25.** Muscle activation (% walking baseline) versus relative heart rate (%HRmax, estimated as 220 − age) for four representative muscles, one per functional group. Each dot represents one running condition. Lines show individual participant trends. The dashed line shows the overall trend across all participants.

### Tibialis anterior activation and ground contact time

**Figure 26** shows the association between tibialis anterior activation and ground contact time across the nine running conditions. All four participants show a negative correlation (P1: $\rho = -0.800$, P2: $\rho = -0.167$, P3: $\rho = -0.619$, P4: $\rho = -0.867$; mean $\rho = -0.613$). The correlation was significant for P1 ($p = 0.010$) and P4 ($p = 0.003$). P3 was borderline ($p = 0.102$, $n = 8$ valid conditions). P2 showed a weak association that did not reach significance ($p = 0.668$). Excluding P2, the mean across the other three participants is $\rho = -0.762$. Despite the variability in strength, the direction is negative for all four participants. Shorter ground contact time leaves less time for swing-phase dorsiflexion. The tibialis anterior must contract faster to achieve foot clearance and prepare for the next heel strike.

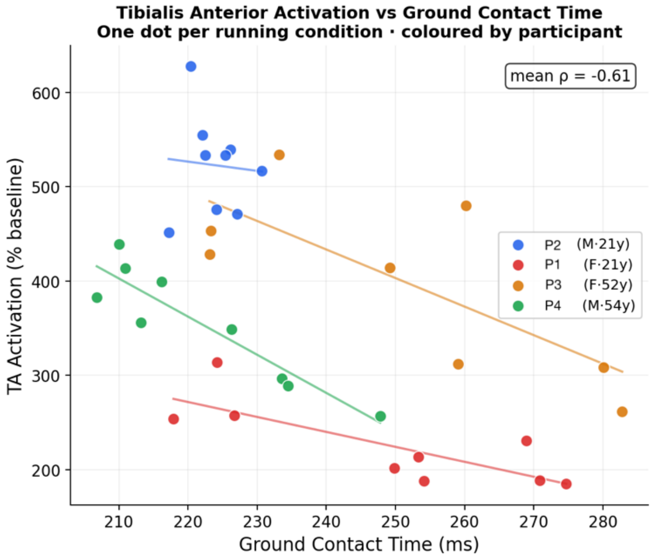


*__Figure 26.__ Tibialis anterior activation (% walking baseline) versus ground contact time (ms) across the nine running conditions. Lines show individual participant trends. Mean Spearman $\rho = -0.613$.*

**Hamstring activation and knee flexion ROM**

**Figure 27** shows the association between mean hamstring activation (mean of semitendinosus and biceps femoris) and knee flexion ROM across the nine running conditions. All four participants show a positive correlation (P1: $\rho = +0.750$, P2: $\rho = +0.700$, P3: $\rho = +0.433$, P4: $\rho = +0.850$; mean $\rho = +0.683$). The correlation reached significance for P1 ($p = 0.020$), P2 ($p = 0.036$), and P4 ($p = 0.004$). P3 showed the weakest association ($p = 0.244$). Conditions with greater knee flexion ROM require greater hamstring output to drive knee flexion in swing phase and to decelerate the lower leg before foot contact.

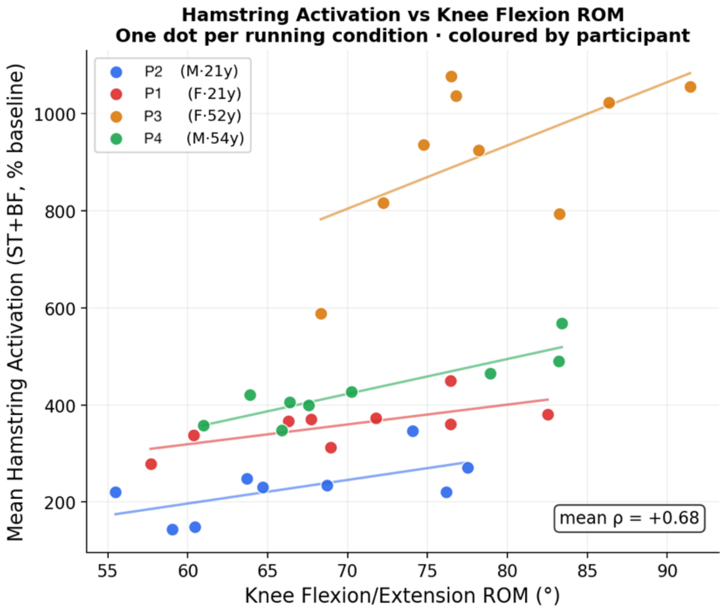


*__Figure 27.__ Mean hamstring activation (semitendinosus + biceps femoris, % walking baseline) versus knee flexion ROM (°) across the nine running conditions. Each dot represents one condition. Lines show individual participant trends. Mean Spearman $\rho = +0.683$.*

## 5.4 Discussion

### *5.4.1 Speed and incline effects on neuromuscular and biomechanical load*

Unless otherwise stated, all values in this section are group means across the four participants.

Speed increased load consistently across all three measurement systems and across all four participants. Plantarflexor activation increased 1.53× and knee extensor activation 1.39× from 8 to 12 km/h. Hip flexion ROM increased 12.7° and knee flexion ROM 16.3°. Ground contact time dropped 30 ms and heart rate rose 11 bpm. The reason is straightforward: faster running requires more power output per stride. To maintain a higher speed, the neuromuscular system recruits more motor units across all muscle groups [35], and the hip and knee must move through more range to produce a longer stride. These are not independent adaptations. The kinematic demand drives the muscular demand. A larger ROM requires greater force from the muscles that produce and control that range, which is why the EMG, IMU, and Garmin responses all scale together with speed.

Incline increased cardiovascular and kinematic load consistently across all four participants, but the EMG response was not consistent. Heart rate rose 18.2 bpm from flat to 10% incline, hip flexion ROM increased 7.9°, and ankle dorsiflexion increased 7.1°. Only two muscles showed consistent activation increases across all four participants: BF_r (1.24×) and TA_l (1.16×). The cardiovascular and kinematic adaptations make sense as shared constraints: running uphill requires more total mechanical work per step, which drives heart rate up, and the forward lean and longer push-off phase require more hip flexion and ankle dorsiflexion from every runner regardless of individual strategy [6], [7]. The EMG response is different because muscle recruitment is not a fixed constraint. The body can distribute the additional load across different muscles in different ways, and two participants can produce the same kinematics through different combinations of activation. This redundancy explains why the incline EMG response varies across participants while the joint and cardiovascular responses do not. [14]

Knee flexion ROM showed a different incline response from the other joints. Bilateral knee flexion ROM decreased 1.8° from flat to 10% incline (72.7° to 70.9°), showing a clear flat response. This contrasts with the speed response, where knee flexion ROM increased 16.3°. On incline, knee flexion ROM does not increase. At the same time, quadriceps activation increases. The knee is working harder but moving less. On flat ground, the knee bends and extends with each step to absorb impact and return energy, like a spring. On incline, it stays more rigid. The quadriceps contract to hold the knee at a fixed angle, not to drive it through a range of motion. The leg acts as a firm column, and the hip and ankle take on the propulsive work. Roberts and Belliveau [36] described this shift in knee strategy during incline running, showing that the knee contributes less mechanical work on slope while the hip takes on a larger share of propulsion.

### *5.4.2. Statistical consistency across conditions*

Kendall's W measures rank agreement across participants, not absolute values. A high W means all four participants ordered the conditions from least to most in the same way, even if their individual magnitudes differed. The pattern of W values across variables reflects why some outcomes are more tightly coupled to running condition than others.

Joint ROM showed the highest W values of all measured variables. Hip flexion reached W = 0.971 and knee flexion W = 0.802. The reason is biomechanical. To run faster, the hip and knee must move through more range to produce a longer stride. This is a mechanical requirement, not a choice. Every participant faces the same constraint regardless of fitness or technique, which is why the rank ordering across conditions is near-identical across participants.

EMG showed lower W values, and several muscles did not reach significance. The musculoskeletal system is redundant: multiple muscles can contribute to the same joint moment, and participants can distribute load differently across them while producing the same kinematics [37]. One participant may rely more on biceps femoris for knee flexion; another may distribute more load to semitendinosus. Both are valid strategies. The condition effect on EMG still exists. Most muscles increase activation with speed and incline. But the specific distribution of load across muscles varies between participants, and this lowers rank agreement. The kinematics constrain the mechanical output; they do not constrain how the neuromuscular system gets there.

The variables that did not reach significance, hip abduction ROM, medial gastrocnemius, and vertical oscillation, fit the same logic. None of them are mechanically required to change in a consistent direction with speed or incline. Their flat response is not noise: it reflects that running condition does not impose a directional constraint on these variables.

### *5.4.3 Cross-modal associations*

Tibialis anterior activation and ground contact time were inversely correlated across conditions (mean $\rho = -0.613$). The reason is a time constraint. Faster or steeper conditions shorten GCT, and a shorter contact time means a shorter swing phase. The angular displacement TA needs to achieve for foot clearance does not change with speed: the foot must still reach the same position before ground contact. The same movement must happen in less time, which requires higher angular velocity and therefore higher muscle activation [38]. This explains why the correlation is stronger than for most other muscle-metric pairs in this study.

Hamstring activation and knee flexion ROM were positively correlated across conditions (per-participant mean $\rho = +0.683$). Conditions with greater knee flexion ROM require the hamstrings to do more work in both directions. During swing they drive the knee into flexion, and before foot contact, they decelerate the lower leg eccentrically. Eccentric contractions under greater stretch generate higher forces [14], [18]. Conditions that demand a larger ROM therefore place a higher eccentric load on the hamstrings, which is reflected in the higher activation levels.

All four representative muscles showed a positive association between activation and relative heart rate across conditions (**Figure *25***). Vastus lateralis showed the most consistent relationship across participants (mean $\rho = +0.654$), while tibialis anterior showed the most inter-individual variability in slope. Medial gastrocnemius and biceps femoris were intermediate. The pattern is consistent with the interpretation that as running conditions become more demanding, cardiovascular and neuromuscular load rise together. Heart rate is available from any consumer wearable without additional sensors, and its association with muscle activation across conditions suggests it carries information about neuromuscular load that goes beyond cardiovascular effort alone. The implications for load monitoring are discussed in Section 5.4.6.

#### *5.4.4 Asymmetry patterns*

P3 shows persistent left-side dominance in hip flexion and knee flexion ROM across all nine conditions. Hip flexion SI ranged from −6% to −12% and knee flexion SI from −8% to −17%, with no systematic change with speed or incline. P4 shows persistent right-side dominance in ankle dorsiflexion, with SI values between +15% and +28% that remain stable across all conditions. These asymmetries are condition-independent. They do not respond to changes in external load, which suggests they reflect structural or habitual characteristics of each individual rather than a task-driven adaptation. Persistent bilateral asymmetries of this kind are consistent with what has been reported in recreational runners across a range of speeds and conditions [9], [10], [11]. P4's knee flexion SI values of −8% to −17% fall within the range considered clinically relevant in the asymmetry monitoring literature [11].

Hip abduction asymmetry behaves differently from the other joints. In P3, hip abduction SI shifts from strong right dominance at low demand (+30% at 8 km/h, 0%) to left dominance at high demand (−15% at 10 km/h, 10%). In P4, it moves in the opposite direction, increasing from moderate right dominance (+7%) to strong right dominance (+36%) as speed and incline increase. This pattern is condition-dependent and individual in direction. Hip abduction contributes to lateral stability rather than propulsion. As running demands increase, participants appear to adapt their lateral stabilisation strategy, and they do so differently. This also explains the non-significant Friedman result for hip abduction ROM reported in Section 5.3.5: the changes exist, but they go in opposite directions between participants and cancel out at group level.

Persistent asymmetries are stable enough to track longitudinally from IMU data without requiring knowledge of the specific running condition. Condition-dependent asymmetries, like those seen in hip abduction, only emerge under higher demands and would be missed if monitoring were limited to easy running. Both types carry potential relevance for injury risk assessment, as discussed in Section 5.4.6.

#### *5.4.5 Inter-individual variability*

Absolute EMG activation levels varied between participants across all conditions. These differences are expected. Individual factors including age, sex, body composition, and neuromuscular strategy all contribute to differences in absolute EMG amplitude between individuals [13]. Normalisation to each participant's own walking baseline removes the contribution of electrode placement and hardware gain, but genuine inter-individual differences in neuromuscular activation remain. The relevant question for this study is not whether participants activate the same absolute amount, but whether they respond to changes in speed and incline in the same direction. That trend is what the condition-level analysis captures, and it is more consistent across participants than the absolute values.

Cardiovascular load at the same absolute condition differed between participants. Across the nine running conditions, P2 worked between 58% and 75% HRmax, P1 between 67% and 87%, P3 between 57% and 88%, and P4 between 80% and 99%. These differences reflect individual cardiovascular fitness and running-specific adaptation. Participants with a longer history of regular aerobic training develop a higher cardiovascular capacity, which means the same absolute running speed places a smaller relative demand on their system. P2, with the longest athletic background, showed the lowest relative cardiovascular load across all conditions. P4, as the least runningadapted participant, reached near-maximal heart rates at conditions that were moderate for the others. A participant operating close to their aerobic ceiling faces a fundamentally different physiological situation than one with substantial reserve, and this contributes to the variability in neuromuscular responses across participants at identical conditions.

Biomechanical characteristics also differed between participants. **Figure 28** shows foot strike patterns for P1 and P2 during treadmill running.


***Figure 28.*** *Foot strike pattern during treadmill running. Left: P1 (midfoot strike). Right: P2 (heel strike). Images captured during data collection at CREB.*

P1 lands closer to the midfoot, while P2 uses a heel strike. This difference is visible in the ankle dorsiflexion ROM data: P1 showed approximately 20° higher ankle dorsiflexion ROM than P2 across equivalent conditions (**Figure 16** and **Figure 17**). A midfoot strike places the ankle in a more dorsiflexed position at contact and requires a different range of motion through the gait cycle. The same running condition therefore produces different joint kinematics depending on the individual's habitual movement pattern, which contributes to inter-individual variability in both IMU and EMG data.

### *5.4.6 Implications for Myalbatross*

The long-term goal of Myalbatross is to predict injury risk using only consumer wearable data: speed, incline, heart rate, ground contact time, and cadence. No EMG sensors, no inertial measurement suits. The runner carries only a watch. Reaching that goal requires two steps. The first is establishing what watch metrics reflect in terms of muscle activation and joint load. The second is translating that load information into injury risk predictions. This study contributes to the first step. To build the mapping between watch data and neuromuscular state, it is necessary to record both simultaneously across a range of conditions. That is what this pilot provides.

By recording EMG, IMU, and Garmin data in parallel across nine running conditions, this pilot maps what the watch measures to what muscles and joints do. The cross-modal relationships identified in Section 5.4.3 are the direct output of this mapping. Ground contact time correlates with tibialis anterior activation (mean $\rho = -0.613$). Heart rate correlates with vastus lateralis activation (mean $\rho = +0.654$). These relationships suggest that Garmin metrics carry information about neuromuscular state beyond their conventional interpretation as cardiovascular or timing variables. If these relationships hold in a larger population, watch data could be used to estimate muscle load without requiring EMG equipment.

The asymmetry indices derived from IMU data add a further layer. Persistent bilateral asymmetries, like those observed in P3 and P4, are detectable from joint angle data and stable across conditions. Asymmetry is associated with injury risk in the running literature [9], [10], [11]. If IMU-derived SI values can be estimated from running kinematics captured by a multi-axis watch or a single sacral IMU, they become a practical monitoring metric.

This pilot is not sufficient to build or validate a prediction model. Four participants across nine conditions cannot establish the population-level relationships needed for reliable injury risk estimation. What it does establish is the methodology and the first evidence that the relevant relationships exist. The next step is replication in a larger and more diverse cohort, with the same multi-modal recording protocol, to determine which Garmin metrics are the most robust proxies for neuromuscular load across different runner profiles.

As a practical output of this collaboration, interactive data visualisation dashboards were developed to allow coaches and trainers to explore the condition-mapped dataset. Each dashboard summarises the full results for one participant across all nine conditions, combining EMG activation, joint kinematics, and Garmin running metrics in a single interactive interface. These tools provide a first bridge between the raw dataset and the end users Myalbatross aims to serve. Screenshots of the dashboards are included in Annex G. The full interactive versions are available as supplementary digital material.

#### *5.4.7 Limitations*

Four participants is a small sample to draw conclusions about recreational runners in general. Individual responses vary for many reasons, and what holds for four people may not hold for a broader population. This is why the study is framed as a pilot. The goal was not to produce definitive findings but to test the methodology, identify the relevant variables, and document the range of responses. The trends observed are consistent enough to justify a larger follow-up study, but they should not be interpreted as population-level conclusions.

A second limitation is that each participant completed the protocol once. There is no test-retest data, and we cannot assess whether the EMG, IMU, or Garmin values would replicate on a different day, under different levels of prior fatigue, or at a different point in the training season. Single-session designs are standard in pilot work but limit the reliability interpretation of any individual measurement.

Another limitation concerns the condition space. Only positive inclines from 0% to 10% were tested. Downhill running was not possible with the available treadmill. Negative inclines produce a fundamentally different loading pattern, with greater eccentric demand on the quadriceps and a different ground contact time and foot strike profile. The absence of downhill conditions is a gap in the dataset that limits its applicability to trail or road running scenarios where descent is common.

Each condition lasted one minute, with two minutes of active recovery between conditions. This duration is sufficient to reach steady-state for most variables, but it does not capture the effect of sustained fatigue. Muscle activation patterns change with fatigue, particularly in the later stages of longer runs. Whether the relationships observed here hold over a 30-minute or 60-minute run is unknown. Fatigue was neither controlled nor measured in this study.

EMG data quality was also limited by electrode failures and signal artefacts. The right rectus femoris channel was non-functional across all participants due to a dead electrode, removing this muscle from all analyses. Additional trials were excluded in multiple channels due to sweat artefacts and contact failures, reducing the completeness of the bilateral EMG dataset.

All data were collected on a motorised treadmill. Treadmill and outdoor running are broadly comparable in terms of lower limb kinematics and muscle activation [28], and the controlled setting was a deliberate choice to isolate the effects of speed and incline. That said, outdoor running introduces variability that a treadmill cannot replicate: uneven terrain and natural pacing adjustments both modulate neuromuscular demand in ways not captured here. How the findings extend to more variable real-world environments is a question for future work.

A final limitation is the absence of ground reaction force data. Force measurements would allow direct quantification of joint loading and would strengthen the interpretation of the EMG findings in terms of mechanical stress on tissues. Without GRF, the link between muscle activation and actual loading remains indirect, which limits the immediate applicability of the dataset to injury risk modelling.

# 6. Execution Schedule

## 6.1 Work Breakdown Structure

A Work Breakdown Structure (WBS) decomposes the project into a hierarchy of tasks grouped by phase. The project is structured into five phases: Project Initiation and Planning, Preliminary Study at INEFC, Main Study Data Collection, Data Processing and Analysis, and Written Memory and Presentation. **Figure 29** shows the full decomposition.

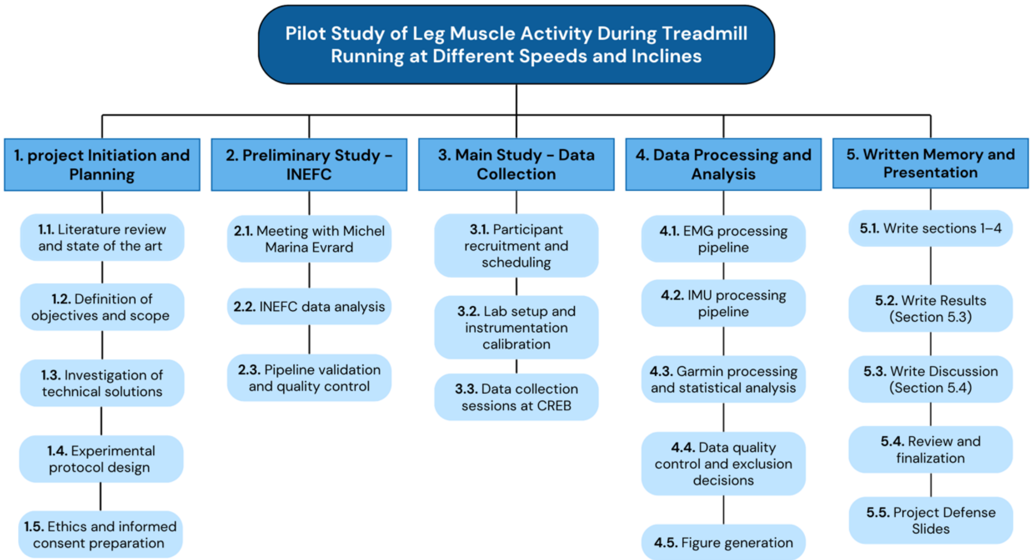


***Figure 29.*** *WBS Diagram.*

## 6.2. Precedence Analysis

The precedence analysis defines the logical dependencies between tasks and estimates their duration. **Table 5** lists the 21 tasks with their estimated durations and predecessors.

***Table 5.*** *Precedence analysis of the project tasks, including estimated duration.*

| ID | Task | Duration (Days) | Predecessors |
|---|---|---|---|
| 1.1 | Literature review and state of the art | 15 | - |
| 1.2 | Definition of objectives and scope | 10 | 1.1 |
| 1.3 | Investigation of technical solutions | 10 | 1.2 |
| 1.4 | Experimental protocol design | 12 | 1.3 |
| 1.5 | Ethics and informed consent preparation | 5 | 1.4 |
| 2.1 | Meeting with Michel Marina Evrard | 1 | 1.1 |
| 2.2 | INEFC data analysis | 7 | 2.1 |
| 2.3 | Pipeline validation and quality control | 5 | 2.2 |
| 3.1 | Participant recruitment and scheduling | 5 | 1.5 |
| 3.2 | Lab setup and instrumentation calibration | 6 | 3.1 |
| 3.3 | Data collection sessions at CREB | 3 | 3.2 |
| 4.1 | EMG processing pipeline | 7 | 3.3, 2.3 |
| 4.2 | IMU processing pipeline | 7 | 3.3 |
| 4.3 | Garmin processing and statistical analysis | 4 | 4.1, 4.2 |
| 4.4 | Data quality control and exclusion decisions | 2 | 4.1, 4.2, 4.3 |

| | | | |
|---|---|---|---|
| 4.5 | Figure generation | 2 | 4.4 |
| 5.1 | Write sections 1–4 | 10 | 1.2 |
| 5.2 | Write Results (Section 5.3) | 5 | 4.5 |
| 5.3 | Write Discussion (Section 5.4) | 8 | 5.2 |
| 5.4 | Review and finalization | 3 | 5.1, 5.2, 5.3 |
| 5.5 | Project Defense Slides | 4 | 5.4 |

## 6.3 PERT Diagram

**Figure 30** shows the project network in activity-on-arrow format. Each node displays the early start (green) and late start (red) in days from project start. The critical path is shown in red and spans 101 days, from March 1 to June 10, 2026.

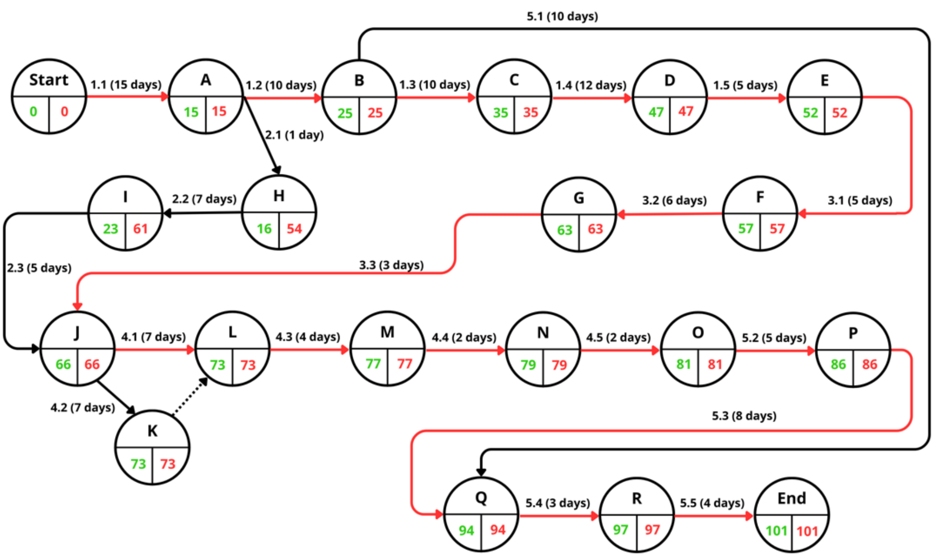


*__Figure 30.__ PERT diagram of the project.*

## 6.4 Gantt Chart

**Figure 31** shows the project schedule as a Gantt chart, with critical tasks, flexible tasks, and available float shown for each activity.

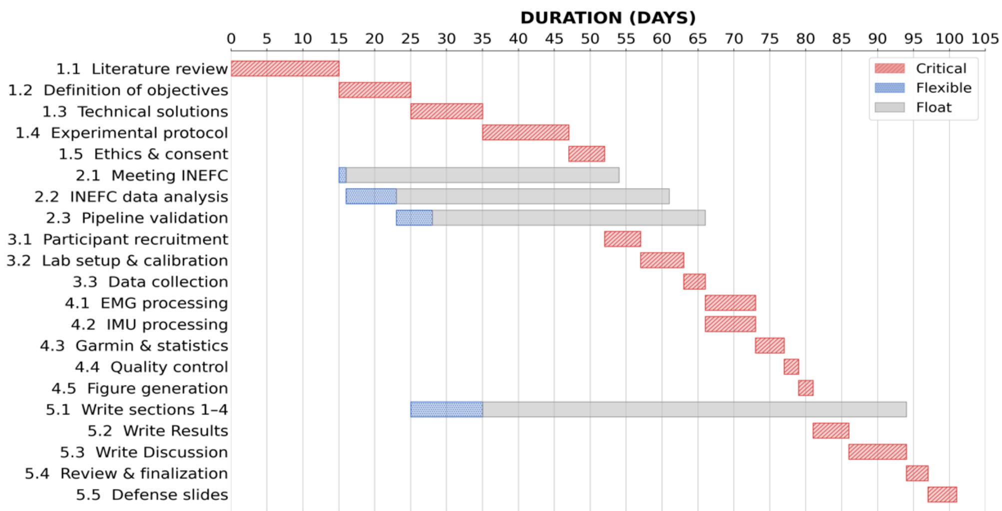


*__Figure 31.__ Gantt chart of the project.*

# 7. Technical Feasibility and SWOT Analysis

## 7.1 SWOT Analysis

**Table 6** presents the SWOT analysis of the project, summarising the internal strengths and weaknesses of the study design and the external opportunities and threats relevant to its continuation and application.

***Table 6.*** *SWOT analysis of the study.*

| Strengths | Weaknesses |
|---|---|
| • Multi-modal pipeline (EMG + IMU + Garmin) recorded in a single session | • Small sample (n=4): trends visible but not generalizable |
| • Prior experience with Python and validated pipeline from INEFC preliminary study | • Right Rectus Femoris absent for all participants (dead electrode, channel 3) |
| • Realistic treadmill conditions covering the recreational running range | • No MVC normalisation: absolute values not comparable across MVC-normalised studies |
| • Myalbatross collaboration: direct applied context for the results | • No downhill running: treadmill limited to 0–10% incline |
| **Opportunities** | **Threats** |
| • Scalable to larger cohorts using the same hardware and Python scripts | • Electrode placement requires a trained operator, limiting reproducibility |
| • OpenSim extension to estimate joint moments and muscle forces | • Treadmill-to-outdoor generalisation not validated |
| • Cross-modal associations as candidate inputs for the Myalbatross injury prediction model | • EMG hardware cost limits replication in low-resource settings |
| • Extension to clinical populations: apply the pipeline to runners with injury history | • Session duration of 60–120 min per participant may limit scalability to larger cohorts |

## 7.2 Technical Feasibility Assessment

The pipeline ran end-to-end for all 4 participants. All processing steps are scripted in Python and produce reproducible outputs from raw files. No manual intervention is required between raw data and final figures, except for quality control of channel exclusions, which requires visual inspection of the raw EMG signal.

Two aspects of the protocol limit how quickly the study can be scaled up. First, electrode placement across 16 channels takes approximately 45 to 60 minutes per participant and requires trained personnel familiar with SENIAM guidelines. Second, session duration of 60 to 120 minutes constrains the number of participants that can be recorded in a single working day. Both are manageable in a larger study, but they should be accounted for in planning.

The study is technically feasible within the existing CREB infrastructure. All hardware is available in the lab and all software is open-source. A follow-up study with 15 to 20 participants could use the same pipeline and the same equipment, with additional operator time budgeted for electrode placement and session management.

# 8. Economic Feasibility

Equipment costs are estimated using straight-line amortisation. The cost attributed to this project corresponds to the fraction of each asset's useful life consumed during the 101-day project duration. All hardware was provided by the CREB laboratory at ETSEIB (UPC) and no equipment was purchased for this study. All data processing software is open-source and carries no licensing cost, except for the Xsens MVN Animate license required for motion capture data export.

***Table 7.*** *Full project budget, including amortised equipment costs and personnel.*

| Item | Market Price | Useful Life | Cost attributed to project |
|---|---|---|---|
| **Equipment** | | | |
| Xsens MVN Awinda (17-sensor full system) | 18,000 € | 10 years | 498 € |
| Delsys Trigno Research+ (16-channel EMG) | 20,000 € | 10 years | 554 € |
| Garmin Forerunner 255 | 300 € | 5 years | 17 € |
| NordicTrack T11.5 treadmill | 1,500 € | 10 years | 42 € |
| Laptop | 1,200 € | 5 years | 66 € |
| **Software** | | | |
| Xsens MVN Animate license | 2,500 € | 1 year | 691 € |
| Open-source (Python, OpenSim) | 0 € | | 0 € |
| **Personnel** | | | |
| Researcher (Biomedical Student) | 15 €/h x 300 h | | 4,500 € |
| CREB technical support | 20 €/h x 10 h x 2 researchers | | 400 € |
| **TOTAL** | | | **6,768 €** |

The total estimated cost of the project is €6,768. This reflects the real economic cost of conducting the study. No external funding was required.

# 9. Regulations and Ethical Aspects

This study involved 4 healthy adult volunteers performing treadmill running under controlled conditions. All measurements were non-invasive: surface EMG electrodes, an IMU suit, and a wrist-worn Garmin device. No drugs, biological samples, or clinical interventions were used.

All participants signed an informed consent form before data collection began. The form described the study purpose, the procedures involved, the possible discomforts, the right to withdraw at any time without consequence, and the conditions under which participant names may appear in the thesis. The consent form is available in Catalan and English in Annex A. Each participant also completed a health questionnaire to screen for exclusion criteria before the session (Annex B).

Participant data is stored securely, used exclusively for academic purposes, and handled in compliance with EU Regulation 2016/679 (GDPR) [39]. Participants are identified in all outputs by anonymous codes (P1 to P4). All devices used in the study (the Xsens MVN Awinda, the Delsys Trigno Research+, and the Garmin Forerunner 255) are CE-marked commercial products. All sessions were conducted under CREB laboratory safety protocols at ETSEIB (UPC). The treadmill was supervised by the researcher at all times throughout each trial.

# 10. Conclusions and Future Lines

## 10.1 Conclusions

This project successfully built and validated a multi-modal pipeline for simultaneous recording and analysis of EMG, full-body kinematics, and Garmin running metrics during treadmill running. The pipeline ran end-to-end for all four participants and produced reproducible outputs from raw files.

Speed increased neuromuscular and biomechanical load consistently across all four participants. Muscle activation rose across most channels, joint range of motion increased at the hip, knee, and ankle, and ground contact time shortened. The response to incline was more selective. Heart rate and hip flexion and ankle dorsiflexion ROM increased consistently with grade, but the EMG response varied between participants. Only the hamstrings and tibialis anterior showed consistent activation increases across all four participants at higher inclines. The difference between the speed and incline EMG responses reflects neuromuscular redundancy: the body can distribute load across different muscles while producing the same kinematics, and participants do not all do it the same way.

Joint kinematics were more consistent across participants than EMG. Speed increased hip flexion and knee flexion ROM in the same direction and by similar magnitudes in all four participants. Incline increased hip flexion and ankle dorsiflexion ROM but had no effect on knee flexion ROM. Kinematics are mechanically constrained by the task in a way that muscle activation is not, which explains the higher statistical consistency in the IMU data.

Bilateral asymmetries were present and stable in two of the four participants. P3 showed persistent left-side dominance in hip flexion and knee flexion ROM across all nine conditions. P4 showed persistent right-side dominance in ankle dorsiflexion. Hip abduction asymmetry was condition-dependent and went in opposite directions between participants. These asymmetries are detectable from IMU data and do not require EMG to identify.

Cross-modal associations between Garmin metrics and muscle activation and joint kinematics were identified across all nine conditions. Consumer watch data carries information about neuromuscular state that goes beyond its conventional interpretation as a cardiovascular or timing variable. The pilot dataset produced by this study is a first step toward building a structured evidence base for injury prediction: a condition-mapped record of what muscles and joints do at each combination of speed and incline, paired with the watch metrics already available in any recreational runner's training data.

## 10.2 Future Lines

The most immediate next step is to increase the sample size. Four participants are sufficient to identify trends and test the pipeline, but not to draw population-level conclusions or build predictive models. A follow-up study with 15 to 20 participants, using the same protocol and the same pipeline, would allow proper statistical inference and would establish whether the cross-modal relationships observed here hold across a broader range of runner profiles.

A longitudinal design would add a dimension that a single-session study cannot provide. Recording the same participants across a full training season would allow tracking of how muscle activation patterns and bilateral asymmetries change with training load, fatigue accumulation, and fitness progression. This would bring the dataset much closer to what is needed for injury risk modelling, where the relevant signal is cumulative load over time rather than a snapshot of one session.

Outdoor validation is a natural extension of the treadmill protocol. The controlled setting was the right choice for this pilot, but real-world running involves terrain variability and natural pacing adjustments that a treadmill cannot replicate. Applying the same pipeline to outdoor running would test how well the treadmill findings generalise and would extend the dataset to the conditions that most recreational runners actually train in.

The protocol should also be extended to negative inclines. Downhill running was not possible with the treadmill used at CREB, and it is a meaningful gap. Downhill running places a higher eccentric demand on the quadriceps and produces a different foot strike and ground contact profile. Including downhill conditions would complete the incline range and add data that is relevant for trail runners and road runners who train on hilly routes.

On the analysis side, integrating OpenSim would allow estimation of joint moments and muscle forces from the IMU kinematics already collected. This would move the dataset from describing what joints do to quantifying the mechanical load they carry, which is the variable most directly linked to overuse injury risk.

The Myalbatross injury prediction model is the long-term applied goal of this line of work. The cross-modal relationships identified in this study show that consumer watch data carries information about neuromuscular state. The next step for Myalbatross is to replicate those relationships in a larger dataset and use them to train a model that estimates muscle load from watch metrics alone. Once that mapping is established, the model can be extended to link estimated load with injury outcomes, drawing on longitudinal data from runners who sustain injuries during a monitored training period.

A final and more ambitious direction is the extension of this pipeline beyond running and into clinical populations. The same hardware and the same processing approach used here can be applied to patients with neurological conditions that affect gait, such as Parkinson's disease. Parkinson's produces measurable changes in stride length, cadence, muscle activation timing, and bilateral symmetry, all of which this pipeline can detect. Applying the methodology to a clinical setting would allow characterisation of pathological gait patterns and, over time, monitoring of disease progression or response to treatment. As a biomedical engineering project developed in collaboration with a research lab, this is a natural bridge between the sports science context of this study and the clinical applications that motivate the field.

# Bibliography

[1] "myalbatross - Tool para gestionar la salud de tus atletas." Accessed: Jun. 03, 2026. [Online]. Available: https://www.myalbatross.ai/es/

[2] R. N. van Gent, D. Siem, M. van Middelkoop, A. G. van Os, S. M. A. Bierma-Zeinstra, and B. W. Koes, "Incidence and determinants of lower extremity running injuries in long distance runners: a systematic review," *Br. J. Sports Med.*, vol. 41, no. 8, pp. 469–480; discussion 480, Aug. 2007, doi: 10.1136/bjsm.2006.033548.

[3] R. Whiteley, C. Hansen, A. Thomson, V. Sideris, and M. G. Wilson, "Lower limb EMG activation during reduced gravity running on an incline. Speed matters more than hills irrespective of indicated bodyweight," *Gait Posture*, vol. 83, pp. 52–59, Jan. 2021, doi: 10.1016/j.gaitpost.2020.09.029.

[4] A. Saito, A. Tomita, R. Ando, K. Watanabe, and H. Akima, "Muscle synergies are consistent across level and uphill treadmill running," *Sci. Rep.*, vol. 8, no. 1, p. 5979, Apr. 2018, doi: 10.1038/s41598-018-24332-z.

[5] S. C. Swanson and G. E. Caldwell, "An integrated biomechanical analysis of high speed incline and level treadmill running," *Med. Sci. Sports Exerc.*, vol. 32, no. 6, pp. 1146–1155, Jun. 2000, doi: 10.1097/00005768-200006000-00018.

[6] G. Vernillo *et al.*, "Biomechanics of graded running: Part I - Stride parameters, external forces, muscle activations," *Scand. J. Med. Sci. Sports*, vol. 30, no. 9, pp. 1632–1641, Sep. 2020, doi: 10.1111/sms.13708.

[7] A. Khassetarash *et al.*, "Biomechanics of graded running: Part II-Joint kinematics and kinetics," *Scand. J. Med. Sci. Sports*, vol. 30, no. 9, pp. 1642–1654, Sep. 2020, doi: 10.1111/sms.13735.

[8] J. Kovše, I. Papuga, M. Drobnič, A. Buyukaslan, V. Strojnik, and M. Supej, "Alterations in pelvic kinematics with speed, incline, and fatigue in female runners," *Front. Sports Act. Living*, vol. 7, p. 1721641, doi: 10.3389/fspor.2025.1721641.

[9] S. Mo *et al.*, "Bilateral asymmetry of running gait in competitive, recreational and novice runners at different speeds," *Hum. Mov. Sci.*, vol. 71, p. 102600, Jun. 2020, doi: 10.1016/j.humov.2020.102600.

[10] O. Girard, G. P. Millet, and J.-P. Micallef, "Constant low-to-moderate mechanical asymmetries during 800-m track running," *Front. Sports Act. Living*, vol. 6, p. 1278454, 2024, doi: 10.3389/fspor.2024.1278454.

[11] J. A. J. Keogh *et al.*, "Monitoring lower limb biomechanical asymmetry and psychological measures in athletic populations-A scoping review," *Scand. J. Med. Sci. Sports*, vol. 33, no. 11, pp. 2125–2148, Nov. 2023, doi: 10.1111/sms.14460.

[12] H. J. Hermens, B. Freriks, C. Disselhorst-Klug, and G. Rau, "Development of recommendations for SEMG sensors and sensor placement procedures," *J. Electromyogr. Kinesiol. Off. J. Int. Soc. Electrophysiol. Kinesiol.*, vol. 10, no. 5, pp. 361–374, Oct. 2000, doi: 10.1016/s1050-6411(00)00027-4.

[13] A. Burden, "How should we normalize electromyograms obtained from healthy participants? What we have learned from over 25 years of research," *J. Electromyogr. Kinesiol. Off. J. Int. Soc. Electrophysiol. Kinesiol.*, vol. 20, no. 6, pp. 1023–1035, Dec. 2010, doi: 10.1016/j.jelekin.2010.07.004.

[14] T. A. Akyürek, H. Ertan, and A. Darendeli, "Biceps Femoris EMG Activity During Incline Treadmill Running and Nordic Hamstring Task," *J. Strength Cond. Res.*, vol. 39, no. 5, pp. 540–546, May 2025, doi: 10.1519/JSC.0000000000005049.

[15] M. SATO, T. KRIEGER, A. D. GIDLEY, B. WEAVER, C. A. JOHNSON, and D. E. LANKFORD, "Physiological and Psychological Differences Between 20% Grade Incline Walking and Level-

Grade Jogging at Isocaloric Intensity," *Int. J. Exerc. Sci.*, vol. 17, no. 6, pp. 1318–1336, Dec. 2024, doi: 10.70252/CWWL1447.
[16] E. M. Nijmeijer, P. Heuvelmans, R. Bolt, A. Gokeler, E. Otten, and A. Benjaminse, "Concurrent validation of the Xsens IMU system of lower-body kinematics in jump-landing and change-of-direction tasks," *J. Biomech.*, vol. 154, p. 111637, Jun. 2023, doi: 10.1016/j.jbiomech.2023.111637.
[17] D. Debertin, A. Wargel, and M. Mohr, "Reliability of Xsens IMU-Based Lower Extremity Joint Angles during In-Field Running," *Sensors*, vol. 24, no. 3, p. 871, Jan. 2024, doi: 10.3390/s24030871.
[18] Y.-C. Lin *et al.*, "Assessing the Validity of Wearable Inertial Sensors in Evaluating Joint Kinetics and Hamstring Musculotendon Mechanics at Various Running Speeds," *Med. Sci. Sports Exerc.*, vol. 57, no. 11, pp. 2537–2549, Nov. 2025, doi: 10.1249/MSS.0000000000003786.
[19] C. Zuo *et al.*, "Transformer IMU Calibrator: Dynamic On-body IMU Calibration for Inertial Motion Capture," *ACM Trans Graph*, vol. 44, no. 4, p. 45:1-45:14, Jul. 2025, doi: 10.1145/3730937.
[20] D. Adams, F. Pozzi, A. Carroll, A. Rombach, and J. Zeni, "Validity and Reliability of a Commercial Fitness Watch for Measuring Running Dynamics," *J. Orthop. Sports Phys. Ther.*, vol. 46, no. 6, pp. 471–476, Jun. 2016, doi: 10.2519/jospt.2016.6391.
[21] "How Does the Ground Contact Time Balance Feature Work on Garmin Watches? | Garmin Customer Support," Garmin. Accessed: May 15, 2026. [Online]. Available: https://support.garmin.com/en-US/?faq=71FahMTBtT1J5bbu9YLcm9
[22] R. Ø. Nielsen *et al.*, "The Garmin-RUNSAFE Running Health Study on the aetiology of running-related injuries: rationale and design of an 18-month prospective cohort study including runners worldwide," *BMJ Open*, vol. 9, no. 9, p. e032627, Sep. 2019, doi: 10.1136/bmjopen-2019-032627.
[23] "Popularity of running in Spain 2023," Statista. Accessed: Jun. 03, 2026. [Online]. Available: https://www.statista.com/statistics/776948/annual-share-of-people-who-went-running-in-spain/
[24] "Sports Technology Market Size, Share | Industry Report, 2030." Accessed: Jun. 03, 2026. [Online]. Available: https://www.grandviewresearch.com/industry-analysis/sports-technology-market
[25] "Become a Coach," TrainingPeaks. Accessed: Jun. 03, 2026. [Online]. Available: https://www.trainingpeaks.com/become-a-coach/
[26] "Online Training Platform." Accessed: Jun. 03, 2026. [Online]. Available: https://trainerplan.co/en
[27] desafio, "Train2Go is born, a tool for coaches by Antón Ruanova," Triatlón Noticias. Accessed: Jun. 03, 2026. [Online]. Available: https://en.triatlonnoticias.com/material-2/nace-train2go-herramienta-para-entrenadores-de-la-mano-de-anton-ruanova/
[28] B. Van Hooren *et al.*, "Is Motorized Treadmill Running Biomechanically Comparable to Overground Running? A Systematic Review and Meta-Analysis of Cross-Over Studies," *Sports Med.*, vol. 50, no. 4, pp. 785–813, Apr. 2020, doi: 10.1007/s40279-019-01237-z.
[29] C. Jayaraman *et al.*, "Validity and reliability study of a novel surface electromyography sensor using a well-consolidated electromyography system in individuals with cervical spinal cord injury," *Spinal Cord*, vol. 62, no. 6, pp. 320–327, Jun. 2024, doi: 10.1038/s41393-024-00981-y.
[30] M. S. Orendurff *et al.*, "A little bit faster: Lower extremity joint kinematics and kinetics as recreational runners achieve faster speeds," *J. Biomech.*, vol. 71, pp. 167–175, Apr. 2018, doi: 10.1016/j.jbiomech.2018.02.010.
[31] C. J. D. Luca, "The Use of Surface Electromyography in Biomechanics," *J. Appl. Biomech.*, vol. 13, no. 2, pp. 135–163, May 1997, doi: 10.1123/jab.13.2.135.

[32] A. Ghazwan, S. M. Forrest, C. A. Holt, and G. M. Whatling, "Can activities of daily living contribute to EMG normalization for gait analysis?," *PloS One*, vol. 12, no. 4, p. e0174670, 2017, doi: 10.1371/journal.pone.0174670.
[33] R. O. Robinson, W. Herzog, and B. M. Nigg, "Use of force platform variables to quantify the effects of chiropractic manipulation on gait symmetry," *J. Manipulative Physiol. Ther.*, vol. 10, no. 4, pp. 172–176, Aug. 1987.
[34] H. Tanaka, K. D. Monahan, and D. R. Seals, "Age-predicted maximal heart rate revisited," *J. Am. Coll. Cardiol.*, vol. 37, no. 1, pp. 153–156, Jan. 2001, doi: 10.1016/s0735-1097(00)01054-8.
[35] S. S. M. Lee, M. de Boef Miara, A. S. Arnold, A. A. Biewener, and J. M. Wakeling, "Recruitment of faster motor units is associated with greater rates of fascicle strain and rapid changes in muscle force during locomotion," *J. Exp. Biol.*, vol. 216, no. 2, pp. 198–207, Jan. 2013, doi: 10.1242/jeb.072637.
[36] T. J. Roberts and R. A. Belliveau, "Sources of mechanical power for uphill running in humans," *J. Exp. Biol.*, vol. 208, no. Pt 10, pp. 1963–1970, May 2005, doi: 10.1242/jeb.01555.
[37] P. Morasso, "A Vexing Question in Motor Control: The Degrees of Freedom Problem," *Front. Bioeng. Biotechnol.*, vol. 9, p. 783501, Jan. 2022, doi: 10.3389/fbioe.2021.783501.
[38] S. Bajelan, W. A. T. Sparrow, and R. Begg, "The ankle dorsiflexion kinetics demand to increase swing phase foot-ground clearance: implications for assistive device design and energy demands," *J. Neuroengineering Rehabil.*, vol. 21, no. 1, p. 105, Jun. 2024, doi: 10.1186/s12984-024-01394-x.
[39] "General Data Protection Regulation (GDPR) – Legal Text," General Data Protection Regulation (GDPR). Accessed: May 01, 2026. [Online]. Available: https://gdpr-info.eu/

# Annexes

## Annex A: Informed Consent Form

### A1. English Informed Consent

# Informed Consent to Participate in a Pilot Biomechanics Study of Running

**Project title:** Pilot study of lower-limb muscle activity during treadmill running at different speeds and inclines.

**Responsible researcher:** Max van der Aa
**Centre:** Biomechanical Engineering Lab, CREB, ETSEIB
**Study type:** Pilot study

### Purpose of the study

You are being invited to participate in a pilot study aimed at analysing how lower-limb muscle activity changes during treadmill running when speed and incline are modified. The study will be conducted at the Biomechanical Engineering Lab of CREB and will include simultaneous recording of body movement using inertial sensors (IMUs) and muscle activity using surface electromyography (EMG).

### What participation involves

If you agree to participate, you will be asked to attend one data collection session at the laboratory. During the session, an XSENS suit will be used, some body measurements will be taken for calibration, IMU sensors will be placed on the body, and surface EMG electrodes will be placed on several muscles of both legs following an anatomical placement protocol.

Before placing the EMG electrodes, the skin may be cleaned with alcohol and, if necessary, small areas of the leg may be shaved with a disposable razor to improve signal quality. Afterwards, several treadmill running trials will be performed under different combinations of speed and incline.

### Estimated duration

The total duration of participation will be approximately 60 to 120 minutes, including preparation, sensor placement, calibration, rest periods between conditions, and removal of the equipment. The exact duration may vary depending on the time needed to prepare the skin, check the signals, and complete all planned conditions.

## Possible discomforts and risks

Participation in this study is considered low risk, but it may involve some minor discomforts. These may include discomfort from sensor placement, mild skin irritation caused by the adhesive or alcohol, physical fatigue from treadmill running, and temporary muscle fatigue after some conditions.

If at any point during the session pain, dizziness, excessive fatigue, or any other relevant discomfort occurs, the trial will be stopped immediately. Participation is completely voluntary and may be discontinued at any time without providing any explanation.

## Expected benefits

There may be no direct benefit to the participant. However, the data collected may contribute to the academic development of the project and to a better understanding of muscle activation patterns during locomotion under different conditions.

## Confidentiality and data handling

The data collected will be treated confidentially and used exclusively for academic and research purposes related to the TFG. Identifying personal data will be kept separate from experimental data where possible, and results will be presented in aggregated or coded form to avoid direct identification of participants.

## Voluntary participation

Participation is entirely voluntary. The decision not to participate, or to withdraw consent once the session has started, will not result in any penalty or negative consequence.

## Photo and video authorisation

Taking photographs or recording videos should not be considered automatically included in the general consent to participate; therefore, separate and specific authorisation is requested. This authorisation is optional and may be refused without affecting participation in the data collection. If authorised, the images and/or videos will be used exclusively for the final TFG presentation.

Please mark the appropriate option:

- [ ] I **authorise** the taking of photographs and/or videos during the session.
- [ ] I **do not authorise** the taking of photographs and/or videos during the session.

### Consent declaration

The participant has been informed about the nature of the study, the procedures to be carried out, the possible discomforts or foreseeable risks, and the voluntary nature of participation. By signing below, the participant declares that they have read this document, had the opportunity to ask questions, and freely agree to participate in the study.

**Participant's full name:** ________________________________

**Participant's signature:** ________________________________

**Date:** ____ / ____ / ______

**Name and signature of the researcher collecting the consent:**

________________________________

**Date:** ____ / ____ / ______

### Observations

Space for any relevant observations, limitations, incidents, or restrictions expressed by the participant:

*A2. Catalan Informed Consent*

# Consentiment informat per participar en un estudi pilot de biomecànica de la cursa

**Títol del projecte:** Estudi pilot de l'activitat muscular de la cama durant cursa en cinta amb diferents velocitats i desnivells.

**Investigador responsable:** Max van der Aa
**Centre:** *Biomechanical Engineering Lab* del CREB, ETSEIB
**Tipus d'estudi:** Estudi pilot

## Finalitat de l'estudi

Se li demana participar en un estudi pilot orientat a analitzar com canvia l'activitat muscular de les cames durant la cursa en cinta quan es modifiquen la velocitat i el desnivell. L'estudi es farà *Biomechanical Engineering Lab* del CREB amb registre simultani de moviment corporal mitjançant sensors inercials (IMUs) i activitat muscular mitjançant electromiografia de superfície (EMG).

## En què consisteix la participació

Si accepta participar, se li demanarà que assisteixi a una sessió de recollida de dades al laboratori. Durant la sessió s'utilitzarà una samarreta del sistema XSENS, es prendran algunes mesures corporals per a la calibració, es col·locaran sensors IMU al cos i elèctrodes EMG de superfície sobre diversos músculs de les dues cames, seguint un protocol de col·locació anatòmica.

Abans de col·locar els elèctrodes EMG, es podrà netejar la pell amb alcohol i, si és necessari, afaitar petites zones de la cama amb maquineta d'un sol ús per millorar la qualitat del senyal. Després es realitzaran diverses proves de cursa en cinta amb diferents combinacions de velocitat i desnivell.

## Durada prevista

La durada total aproximada de la participació serà d'entre 60 i 120 minuts, incloent preparació, col·locació de sensors, calibració, descansos entre condicions i retirada del material. La durada exacta pot variar segons el temps necessari per preparar la pell, verificar els senyals i completar totes les condicions previstes.

### Molèsties i riscos previsibles

La participació en aquest estudi es considera de risc baix, però pot comportar algunes molèsties lleus. Entre aquestes molèsties hi pot haver sensació d'incomoditat per la col·locació dels sensors, irritació cutània lleu per l'adhesiu o l'alcohol, cansament físic per córrer en cinta, i fatiga muscular temporal després d'algunes condicions.

Si durant la sessió apareix dolor, mareig, fatiga excessiva o qualsevol altra molèstia rellevant, la prova s'aturarà immediatament. La participació és totalment voluntària i es pot interrompre en qualsevol moment sense necessitat de donar explicacions.

### Beneficis esperats

És possible que la participació no comporti cap benefici directe per a la persona participant. Tanmateix, les dades obtingudes poden contribuir al desenvolupament acadèmic del projecte i a una millor comprensió dels patrons d'activació muscular durant la locomoció en diferents condicions.

### Confidencialitat i tractament de dades

Les dades recollides es tractaran de manera confidencial i s'utilitzaran exclusivament amb finalitats acadèmiques i de recerca associades al TFG. Les dades personals identificatives es mantindran separades de les dades experimentals sempre que sigui possible, i els resultats es presentaran de forma agregada o codificada per evitar la identificació directa de les persones participants.

### Caràcter voluntari de la participació

La participació és completament voluntària. La decisió de no participar, o de retirar el consentiment un cop iniciada la sessió, no comportarà cap perjudici ni cap conseqüència negativa.

### Autorització d'imatges i vídeos

La presa de fotografies o vídeos no s'ha de considerar inclosa automàticament en el consentiment general de participació, i per això es demana una autorització específica i separada. Aquesta autorització és opcional i es pot denegar sense afectar la participació en la recollida de dades. En cas d'autoritzar-la, les imatges i/o vídeos s'utilitzaran exclusivament per a la presentació final del TFG

Marqui l'opció corresponent:

- [ ] **Autoritzo** la realització de fotografies i/o vídeos durant la sessió.
- [ ] **No autoritzo** la realització de fotografies i/o vídeos durant la sessió.

### Declaració de consentiment

S'ha explicat en què consisteix aquest estudi, quins procediments es duran a terme, quines molèsties o riscos previsibles existeixen, i que la participació és voluntària. La persona signant declara que ha llegit aquest document, que ha pogut fer preguntes i que accepta participar lliurement en l'estudi.

**Nom i cognoms de la persona participant:** ________________________________

**Signatura de la persona participant:** ________________________________

**Data:** ____ / ____ / ______

**Nom i signatura de la persona investigadora que recull el consentiment:**
________________________________

**Data:** ____ / ____ / ______

### Observacions

Espai per indicar qualsevol observació rellevant, limitació, incidència o restricció expressada per la persona participant:

# Annex B: Health Questionnaire

## B1. English Health Questionnaire

# Initial Participant Questionnaire

**Projecte:** Pilot study of lower-limb muscle activity during treadmill running at different speeds and inclines
**Centre:** *Biomechanical Engineering Lab*, CREB, ETSEIB
**Purpose of the document:** Initial characterization of the sample and recording of factors that may influence the experimental session.

**Participant name:** ____________________
**Date:** ____ / ____ / ______

### 1. Basic information

- **Age:** __________ years
- **Sex:** __________________________________
- **Height:** __________ cm
- **Weight:** __________ kg
- **Dominant leg:** [ ]Right [ ] Left [ ] Both / do not know

### 2. Sports profile

- **Do you exercise regularly?** [ ]Yes [ ] No
- **How many days per week do you exercise?** __________ days/week
- **What type of sport do you mainly do?** __________________________________
- **How many days per week do you usually run?** __________ days/week

### 3. recent status before test

- **Have you trained in the last 24 hours?** [ ] Yes [ ] No
- **Have you done a high-intensity session in the last 48 hours?** [ ] Yes [ ] No
- **How would you rate your current fatigue?** [ ] 1 [ ] 2 [ ] 3 [ ] 4 [ ] 5

  *(1 = very rested, 5 = very fatigued)*
- **Did you sleep well last night?** [ ] Yes [ ] No
- **How many hours did you sleep approximately?** __________ hours
- **Have you eaten in the last 2–3 hours?** [ ] Yes [ ] No
- **Have you had caffeine today?** [ ] Yes [ ] No

### 4. Relevant experience

- **Do you have experience running on a treadmill** [ ] Yes [ ] No
- **Have you ever participated in a similar study or test involving sensors, EMG, IMUs, or treadmill running?** [ ] Yes [ ] No
- **If yes, briefly specify what kind of test it was:**

  ______________________________

### 5. Health and safety

- **Do you currently have any injury/pain in your legs?** [ ] Yes [ ] No
- **Have you had any recent leg injury in the last few months?** [ ] Yes [ ] No
- **Is there any condition that could affect today's test?** [ ] Yes [ ] No
- **Do you feel fit to run on the treadmill today?** [ ] Yes [ ] No

### 6. Observations

Space to add any information that may be relevant for interpreting the experimental session (unusual fatigue, discomfort, nerves, medication, etc.):

*B2. Catalan Health Questionnaire*

# Qüestionari inicial de participants

**Projecte:** Estudi pilot de l'activitat muscular de la cama durant cursa en cinta amb diferents velocitats i desnivells
**Centre:** *Biomechanical Engineering Lab* del CREB, ETSEIB
**Ús del document:** Caracterització inicial de la mostra i registre de factors que poden influir en la sessió experimental.

---

**Nom del participant:** ____________________
**Data:** ____ / ____ / _____

## 1. Dades bàsiques

- **Edat:** __________ anys
- **Sexe:** __________________________________
- **Alçada:** __________ cm
- **Pes:** __________ kg
- **Cama dominant:** [ ]Dreta     [ ] Esquerra     [ ] Ambdues / no ho sap

## 2. Perfil esportiu

- **Fas esport regularment?** [ ]Sí   [ ] No
- **Quants dies per setmana fas esport?** __________ dies/setmana
- **Quin tipus d'esport fas principalment?** __________________________________
- **Quants dies per setmana corres habitualment?** __________ dies/setmana

## 3. Estat recent abans de la prova

- **Has entrenat en les últimes 24 hores?** [ ] Sí   [ ] No
- **Has fet una sessió intensa en les últimes 48 hores?** [ ] Sí   [ ] No
- **Com valores la teva fatiga actual?** [ ] 1   [ ] 2   [ ] 3   [ ] 4   [ ] 5

  *(1 = molt descansat/da, 5 = molt fatigat/da)*
- **Has dormit bé aquesta nit?** [ ] Sí   [ ] No
- **Quantes hores has dormit aproximadament?** __________ hores
- **Has menjat en les últimes 2–3 hores?** [ ] Sí   [ ] No
- **Has pres cafeïna avui?** [ ] Sí   [ ] No

### 4. Experiència rellevant

- **Tens experiència corrent en cinta?** [ ] Sí [ ] No
- **Has participat alguna vegada en un estudi o prova semblant amb sensors, EMG, IMUs o cinta?** [ ] Sí [ ] No
- **En cas afirmatiu, indica breument quin tipus de prova era:**

  ______________________________

### 5. Salut i seguretat

- **Tens lesió/dolor actual a les cames?** [ ] Sí [ ] No
- **Has tingut alguna lesió recent a les cames en els últims mesos?** [ ] Sí [ ] No
- **Hi ha alguna condició que pugui afectar la prova d'avui?** [ ] Sí [ ] No
- **Et trobes apte per fer cursa en cinta avui?** [ ] Sí [ ] No

### 6. Observacions

Espai per afegir qualsevol informació que pugui ser rellevant per interpretar la sessió experimental (fatiga inusual, molèsties, nervis, medicació, etc.):

## Annex C: Randomisation Tables

The walking baseline (5 km/h, 0%) was always performed first and is not included in the randomisation. The nine running conditions were randomised independently for each participant. The table below show the order in which conditions were performed.

***Table C.1.*** *Randomised condition order for each participant. The walking baseline (5 km/h, 0%) was always performed first and is not included.*

| Order | P1 | P2 | P3 | P4 |
|---|---|---|---|---|
| 1 | 12 km/h, 0% | 10 km/h, 0% | 8 km/h, 0% | 8 km/h, 0% |
| 2 | 12 km/h, 10% | 12 km/h, 10% | 12 km/h, 10% | 12 km/h, 10% |
| 3 | 12 km/h, 5% | 12 km/h, 5% | 10 km/h, 10% | 12 km/h, 5% |
| 4 | 8 km/h, 10% | 10 km/h, 5% | 12 km/h, 5% | 8 km/h, 10% |
| 5 | 10 km/h, 0% | 12 km/h, 10% | 10 km/h, 5% | 12 km/h, 0% |
| 6 | 8 km/h, 5% | 8 km/h, 10% | 12 km/h, 0% | 10 km/h, 5% |
| 7 | 10 km/h, 10% | 10 km/h, 10% | 8 km/h, 5% | 10 km/h, 0% |
| 8 | 10 km/h, 5% | 8 km/h, 0% | 8 km/h, 10% | 8 km/h, 5% |
| 9 | 8 km/h, 0% | 8 km/h, 5% | 10 km/h, 0% | 10 km/h, 10% |

## Annex D: Electrode Placement Diagram and Photographs

The following pages show the electrode placement locations for each of the 8 muscles recorded per leg, following SENIAM guidelines. Orange crosses indicate electrode positions; blue dots indicate anatomical landmarks used for palpation. Electrodes were placed parallel to the muscle fibre direction, which follows the line from origin to insertion and is not always parallel to the underlying bone.

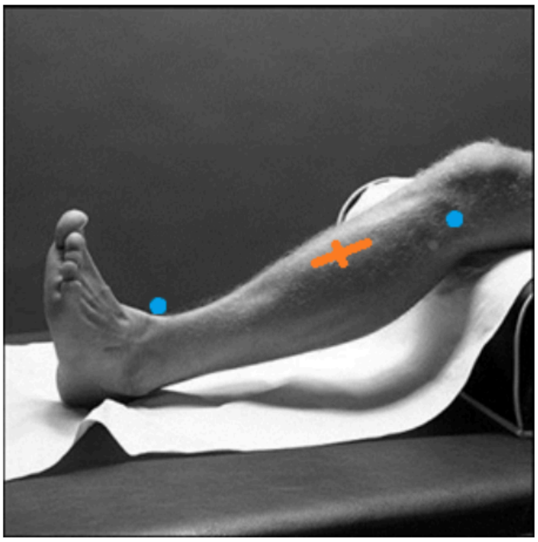

| **a. Tibialis anterior** | R sensor | L sensor |
|---|---|---|
| | | |

Position of the sensor:

- At ~ 1/3 of the line from tip of the fibula to tip of medial malleolus, as proximal as possible

Test contraction:

- Ask for dorsiflexion and inversion under resistance

| **b. Medial gastrocnemius** | R sensor | L sensor |
|---|---|---|
| | | |

Position of the sensor:

- At the most prominent bulge of the muscle

Test contraction:

- Ask plantar flexion of the foot under resistance while the knee is almost extended

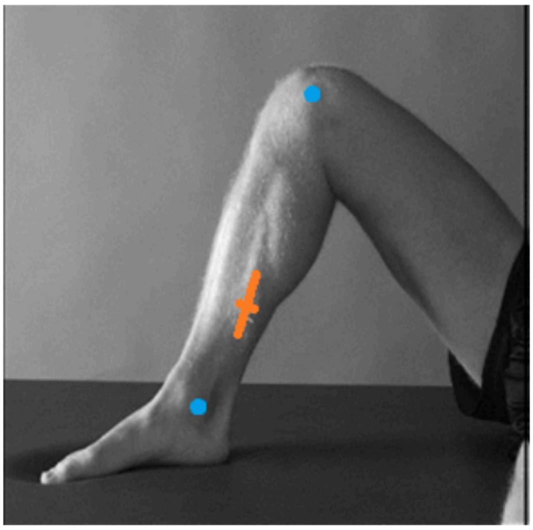

**c. Soleus**

| R sensor | L sensor |
|---|---|
| | |

Position of the sensor:

- At 2/3 of the line from the tip of the medial femur condyle and the tip of the medial malleolus

Test contraction:

- Move the foot passively in dorsiflexion and palpate the muscle
- In supine with flexed knee, ask for heel rise, pressing toes into the table, with resistance at the knee

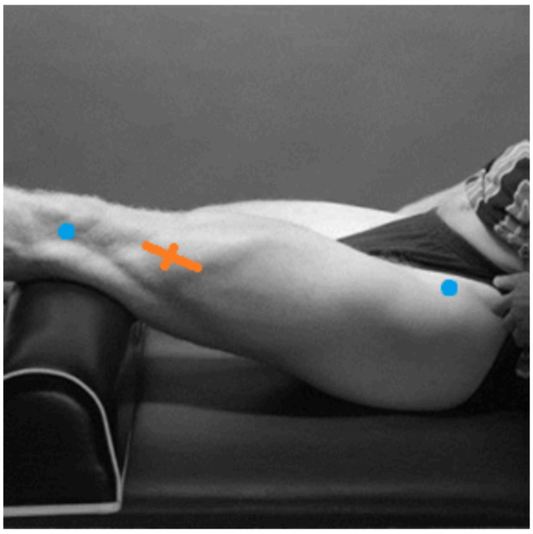

**d. Vastus lateralis**

| R sensor | L sensor |
|---|---|
| | |

Position of the sensor:

- At 2/3 of the line from the ASIS to the lateral side of the patella.

Test contraction:

- Ask to lift the extended leg or extend the knee without rotation in the hip

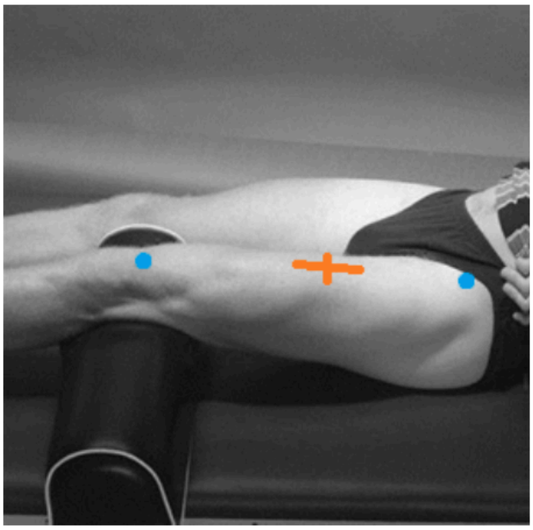

**e. Rectus femoris**

| R sensor | L sensor |
|---|---|
| | |

Position of the sensor:

- At ~1/2 of the line from the ASIS to the superior edge of the patella. Narrow muscle

Test contraction:

- Ask to lift the extended leg or extend the knee without rotation in the hip

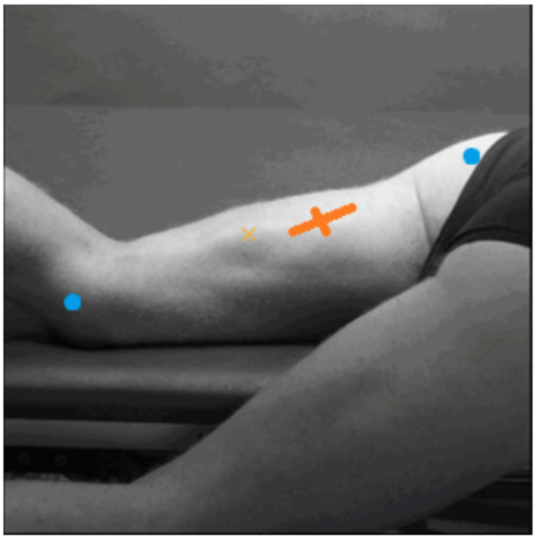

**f. Medial hamstrings / semitendinosus**

| R sensor | L sensor |
| --- | --- |
| | |

Position of the sensor:

- At 2/3 of the line between the ischial tuberosity and the medial epicondyle of the tibia
- ** according to SENIAM guidelines, should be at ~1/2, but we do 1/3 to avoid cross-talk with lateral ham.

Test contraction:

- Ask for knee flexion with resistance at the ankle

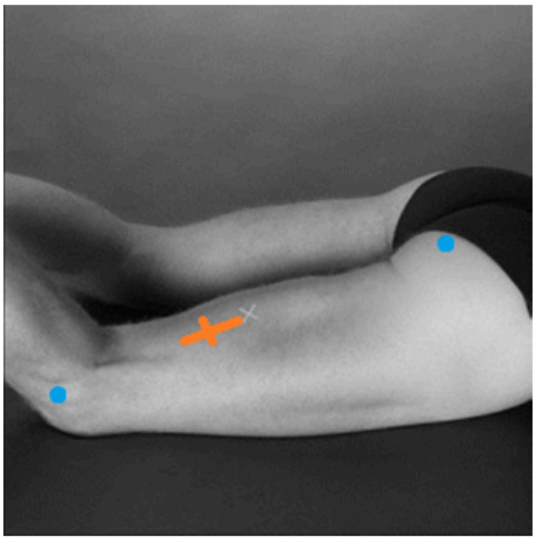

**g. Lateral hamstrings / Biceps femoris**

| R sensor | L sensor |
| --- | --- |
| | |

Position of the sensor:

- At 2/3 of the line between the ischial tuberosity and the lateral epicondyle of the tibia
- ** according to SENIAM guidelines, should be at ~1/2, but we do 2/3 to avoid cross-talk with medial ham.

Test contraction:

- Ask for knee flexion with resistance at the ankle

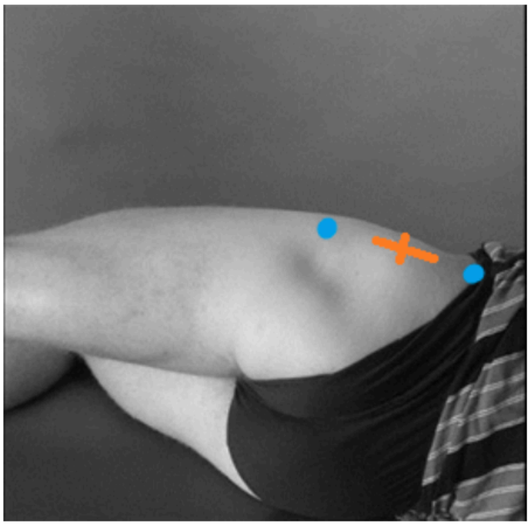

**h. Gluteus medius**

| R sensor | L sensor |
| --- | --- |
| | |

Position of the sensor:

- At ~1/2 of the line from the iliac crest to the greater trochanter
- Place electrode in stance

Test contraction:

- Palpate muscle when patient is standing on one leg
- Laying on one side, ask for abduction of the hip with extended knee with resistance at the ankle

Full-body kinematics were recorded using the Xsens MVN Awinda system. The system uses 17 IMU sensors distributed across the body segments. Placement followed the manufacturer's standard protocol.

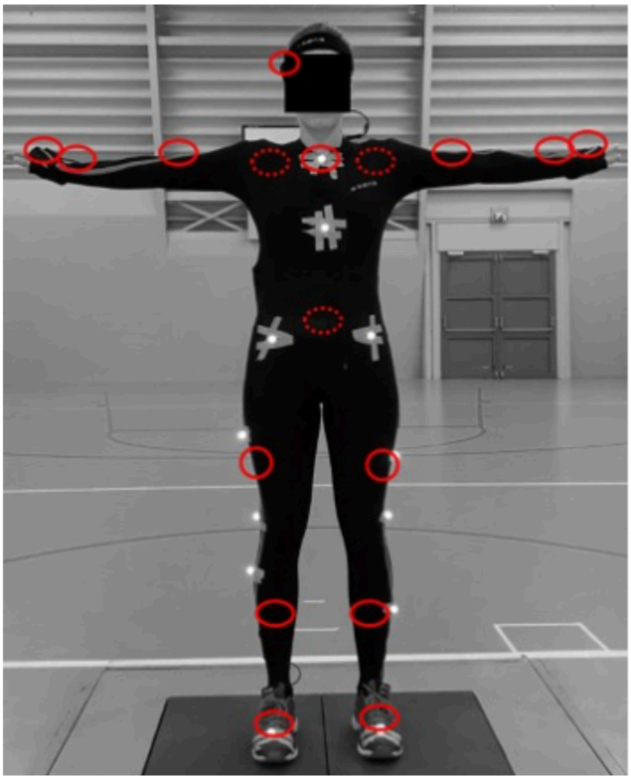

***Figure D.1.*** *IMU sensor placement for the Xsens MVN Awinda system. 17 sensors distributed across body segments following the manufacturer's standard protocol.*

## Annex E: INEFC Preliminary Study – Supplementary EMG Analyses

The main text reports mean RMS activation for the INEFC preliminary dataset (Section 5.3.1). Two additional analyses were performed on the same dataset to confirm that the directional trends were not specific to the mean activation metric. **Figure E.1** shows peak activation, computed as the 95th percentile of the RMS envelope per condition. This metric captures the highest burst amplitude within the analysis window, which is relevant for muscles that show phasic rather than tonic activation during running. **Figure E.2** shows recruitment duration, computed as the percentage of time within the analysis window where the RMS envelope exceeded a threshold of 20 µV. This metric reflects how consistently a muscle is recruited across the stride cycle, independent of the absolute amplitude of each contraction.

Both analyses confirmed the same directional trends as the mean activation. BF and ST showed the highest relative increases in peak bursts, and recruitment duration increased consistently with both speed and incline for the posterior chain muscles.

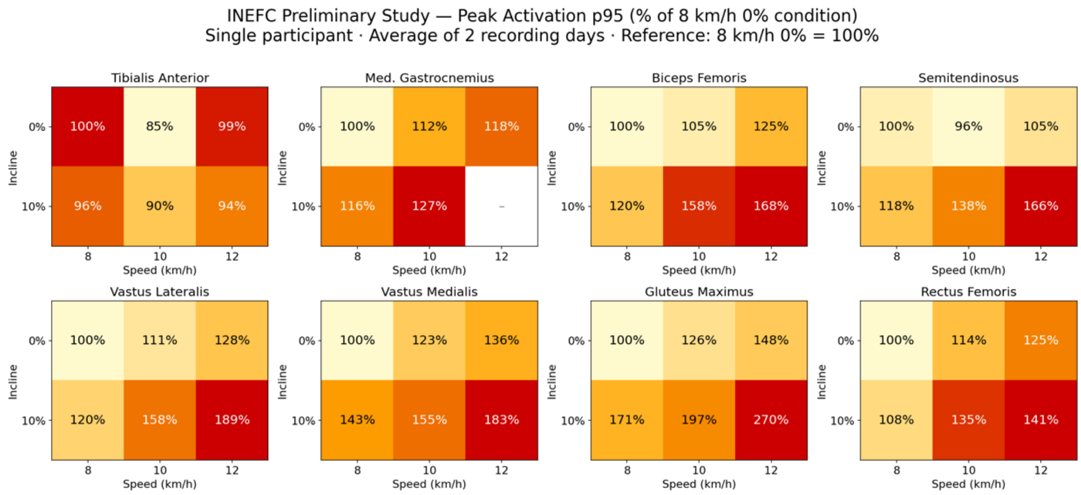


*__Figure E.1.__ Peak EMG activation (95th percentile of RMS envelope) for the INEFC dataset, normalised to the 8 km/h, 0% condition. Average of 2 recording days.*

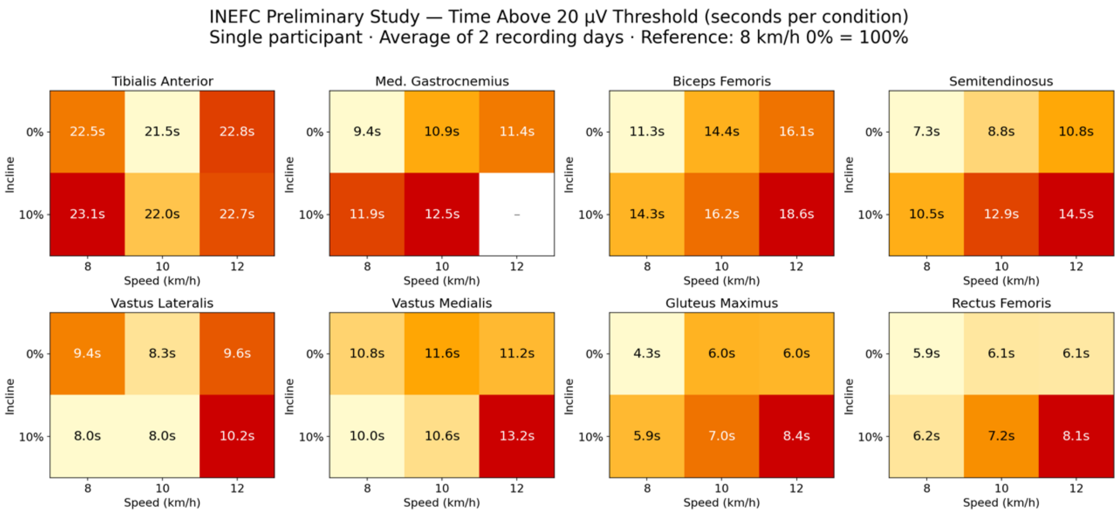


*__Figure E.2.__ Recruitment duration (percentage of time above 20 µV threshold) for the INEFC dataset. Average of 2 recording days.*

# Annex F: Supplementary Individual Figures

## *F.1 Joint ROM Heatmaps*

Individual ROM heatmaps for P1 and P2 are shown in the main text (**Figure 16** and **Figure 17**). The figures below show the same data for P3 and P4.

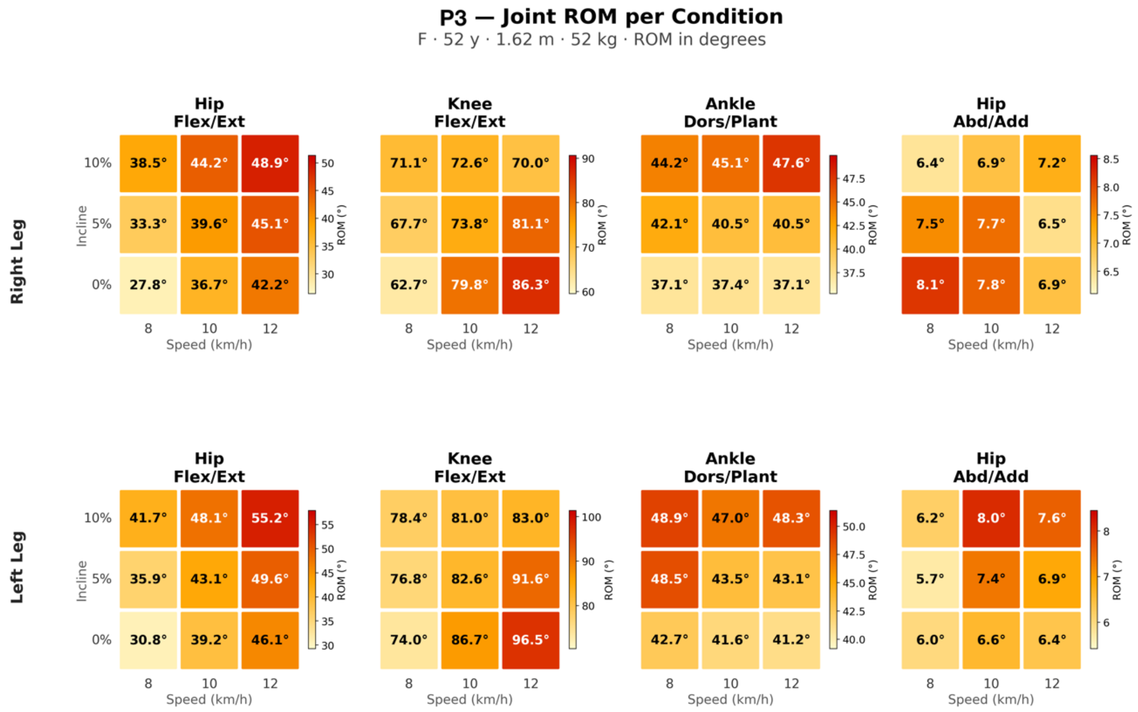


***Figure F.1****. Joint ROM per condition for P3.*

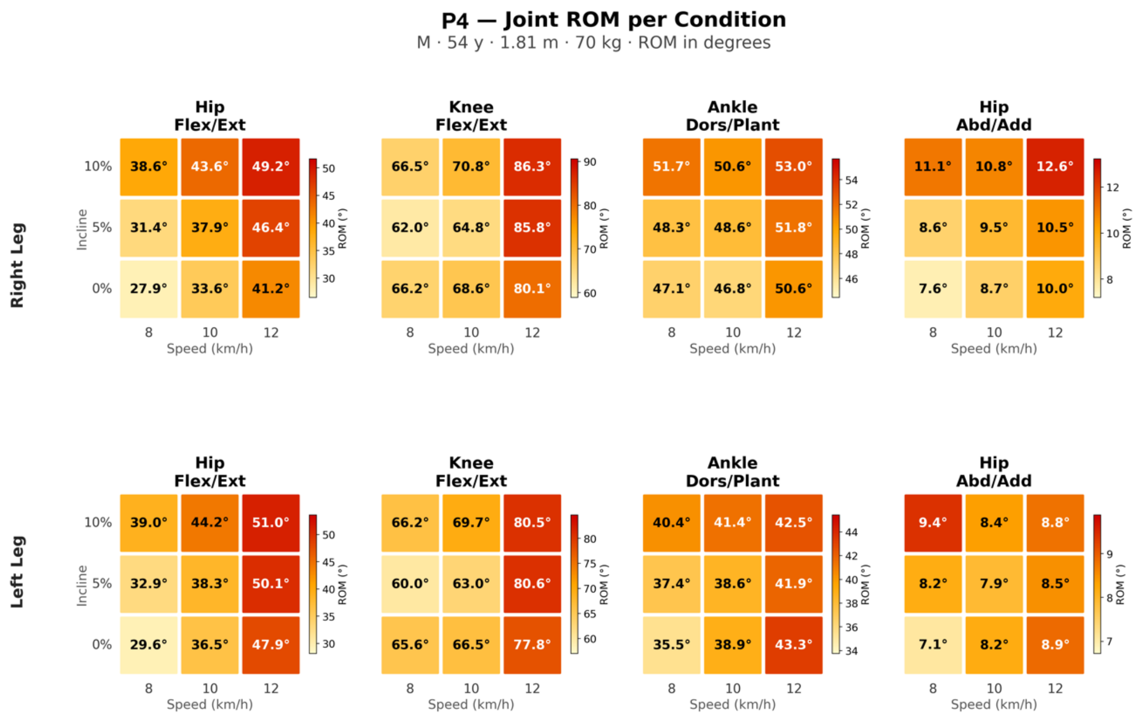


***Figure F.2****. Joint ROM per condition for P4.*

### F.2 Bilateral Symmetry Index Heatmaps

Individual SI heatmaps for P3 and P4 are shown in the main text (**Figure 19** and **Figure 20**). The figures below show the same data for P1 and P2.

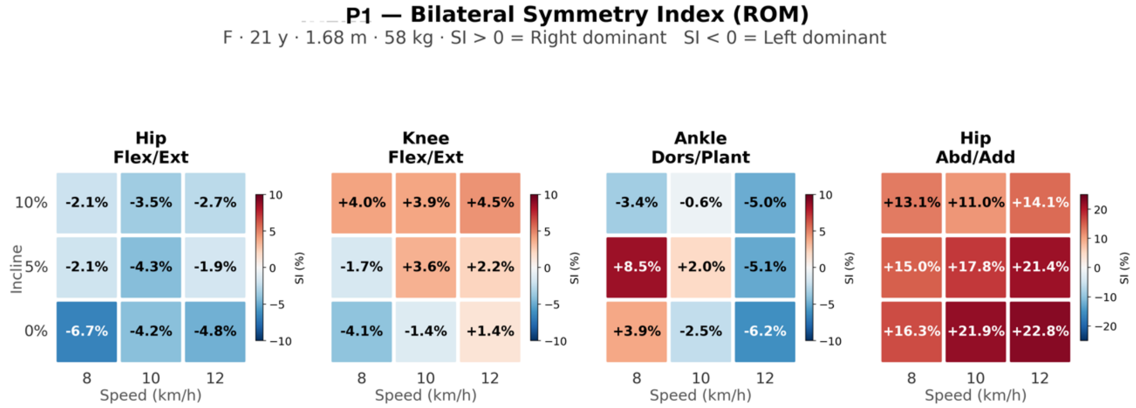


**Figure F.3.** *Bilateral symmetry index per condition for P1.*

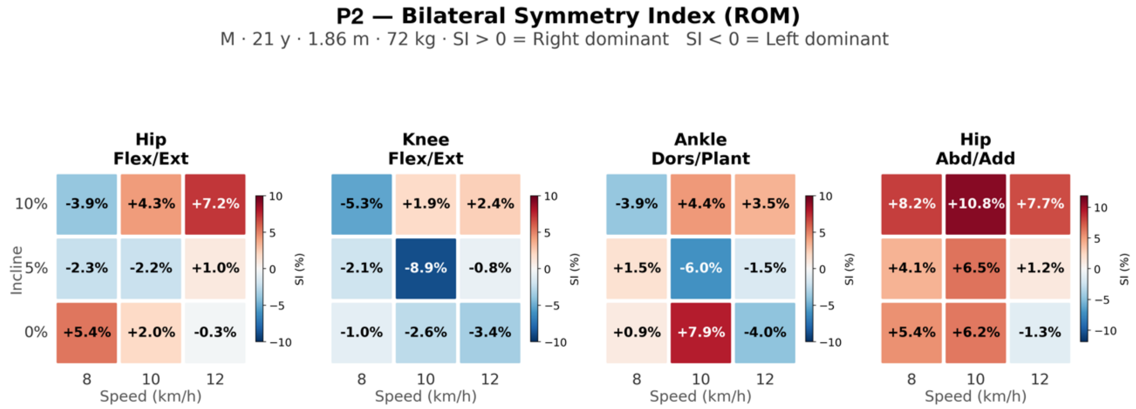


**Figure F.4.** *Bilateral symmetry index per condition for P2.*

### F.3 Garmin Heatmaps

Individual Garmin heatmaps for P1 and P2 are shown in the main text (**Figure 21** and **Figure 22**). The figures below show the same data for P3 and P4.

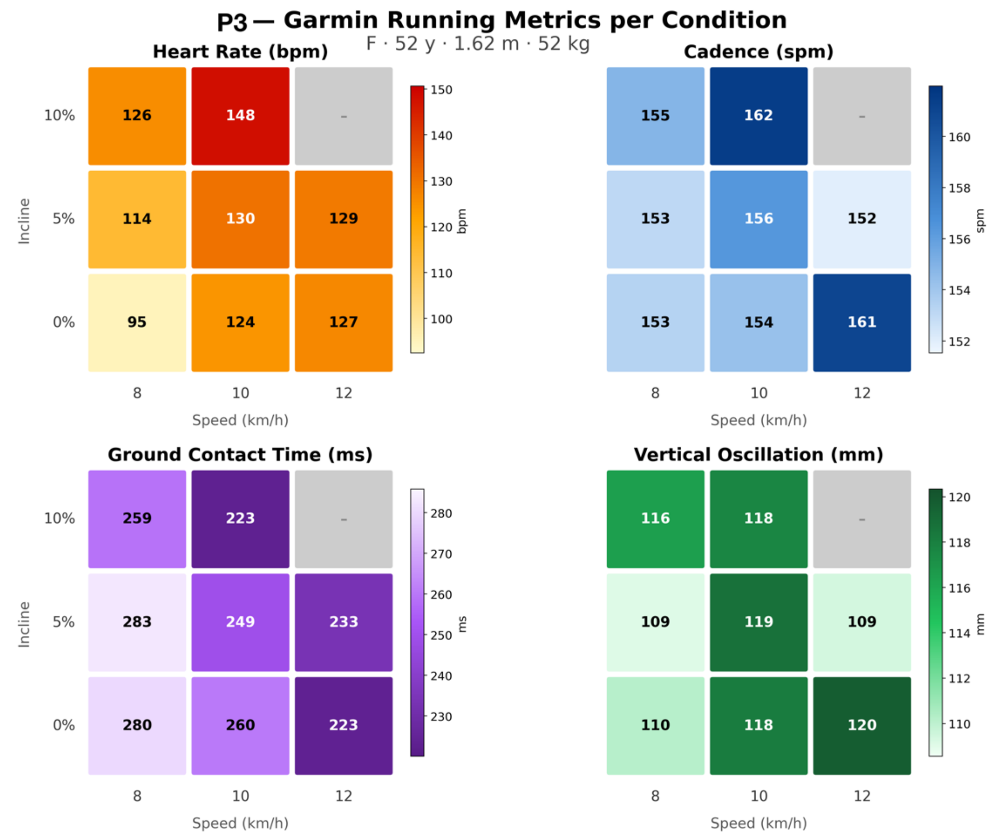


*Figure F.5. Garmin running metrics per condition for P3.*

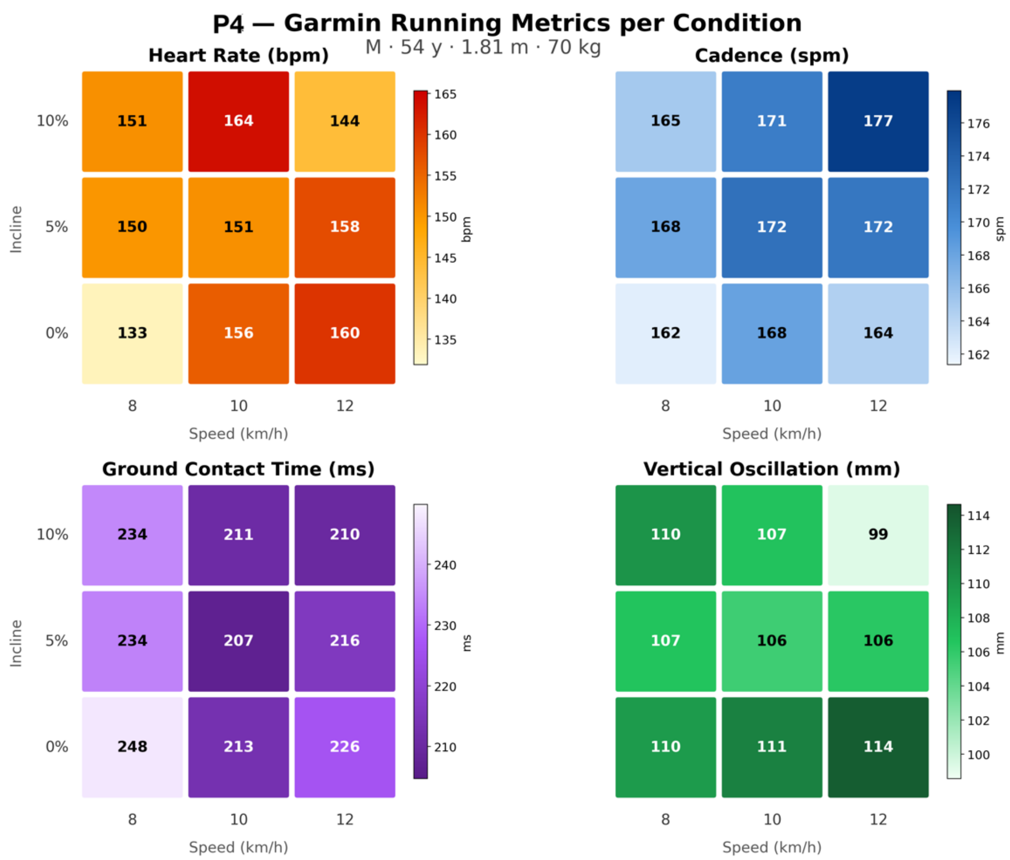


*Figure F.6. Garmin running metrics per condition for P4.*

## Annex G: Interactive Result Dashboards per Participant

An interactive dashboard was developed as part of the collaboration with Myalbatross. The dashboard consolidates the full results for all four participants across all nine running conditions, combining EMG activation maps, joint ROM heatmaps, bilateral symmetry indices, and Garmin running metrics in a single interface. The participant selector at the top of the dashboard allows switching between P1, P2, P3, and P4. The dashboard is designed for use by coaches and trainers to explore individual athlete data without requiring access to the raw data files.

The full interactive version is available as a supplementary digital file: *athlete_dashboard_v2.html*.

The figure below shows a screenshot of a part of the dashboard.

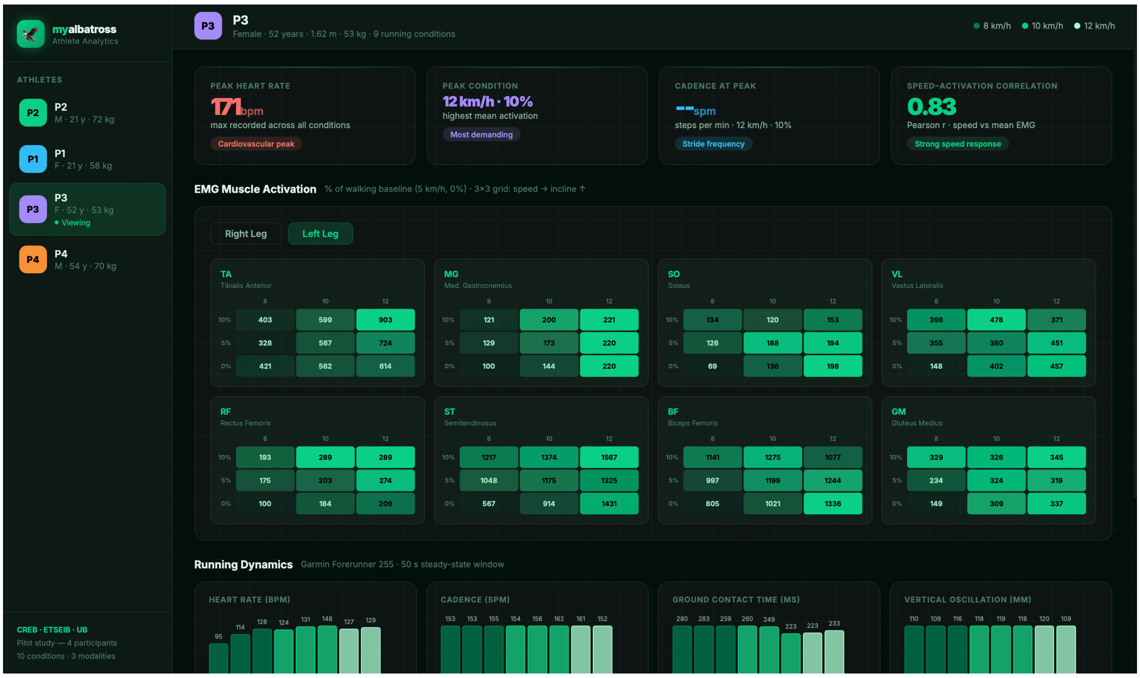


***Figure G.1.*** *Interactive result dashboard. Participant selector visible at the top. Results update dynamically on selection.*